APPENDIX 5
VELOCITY MODELING

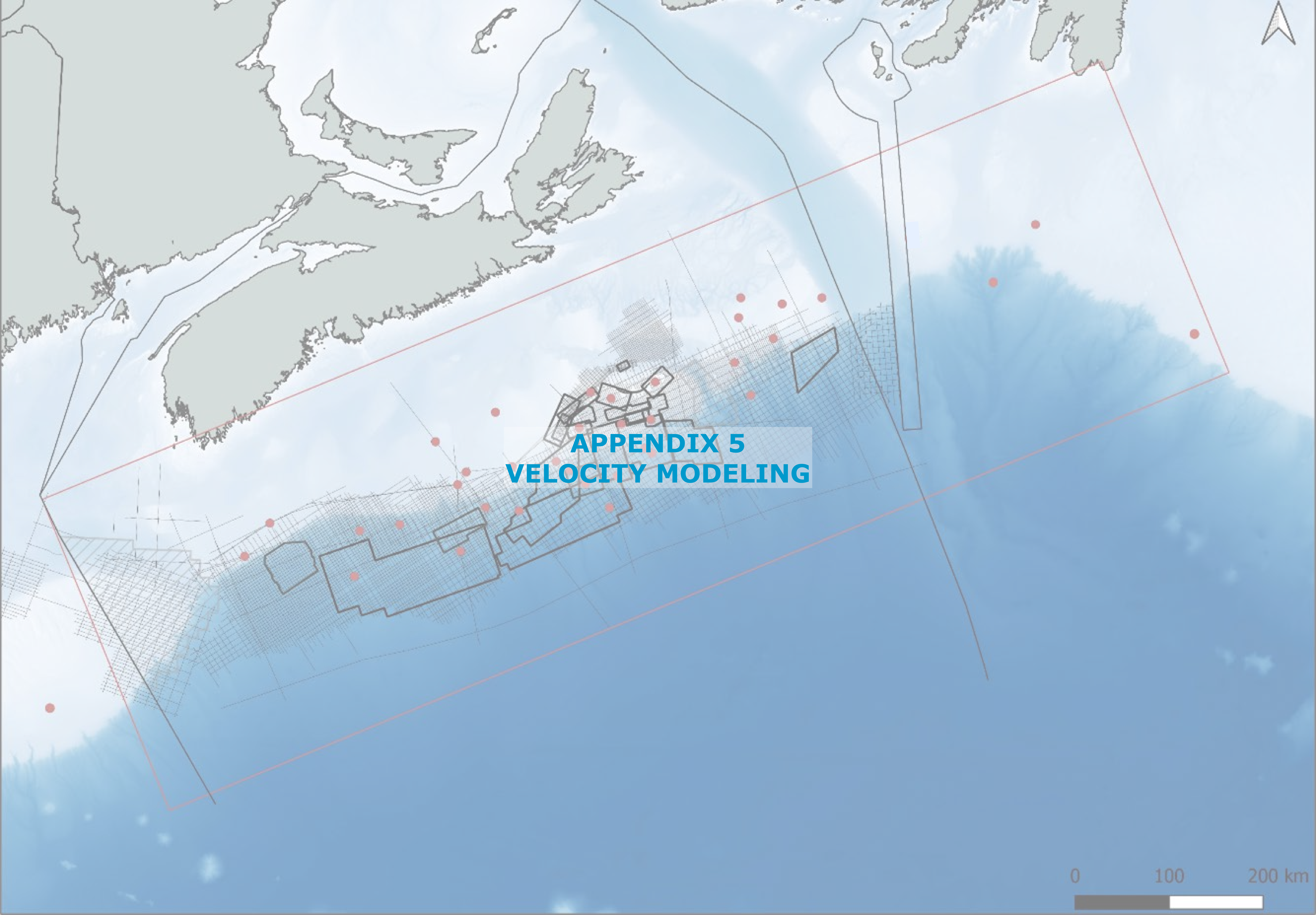

Nova Scotia Offshore Velocity Modeling

2022

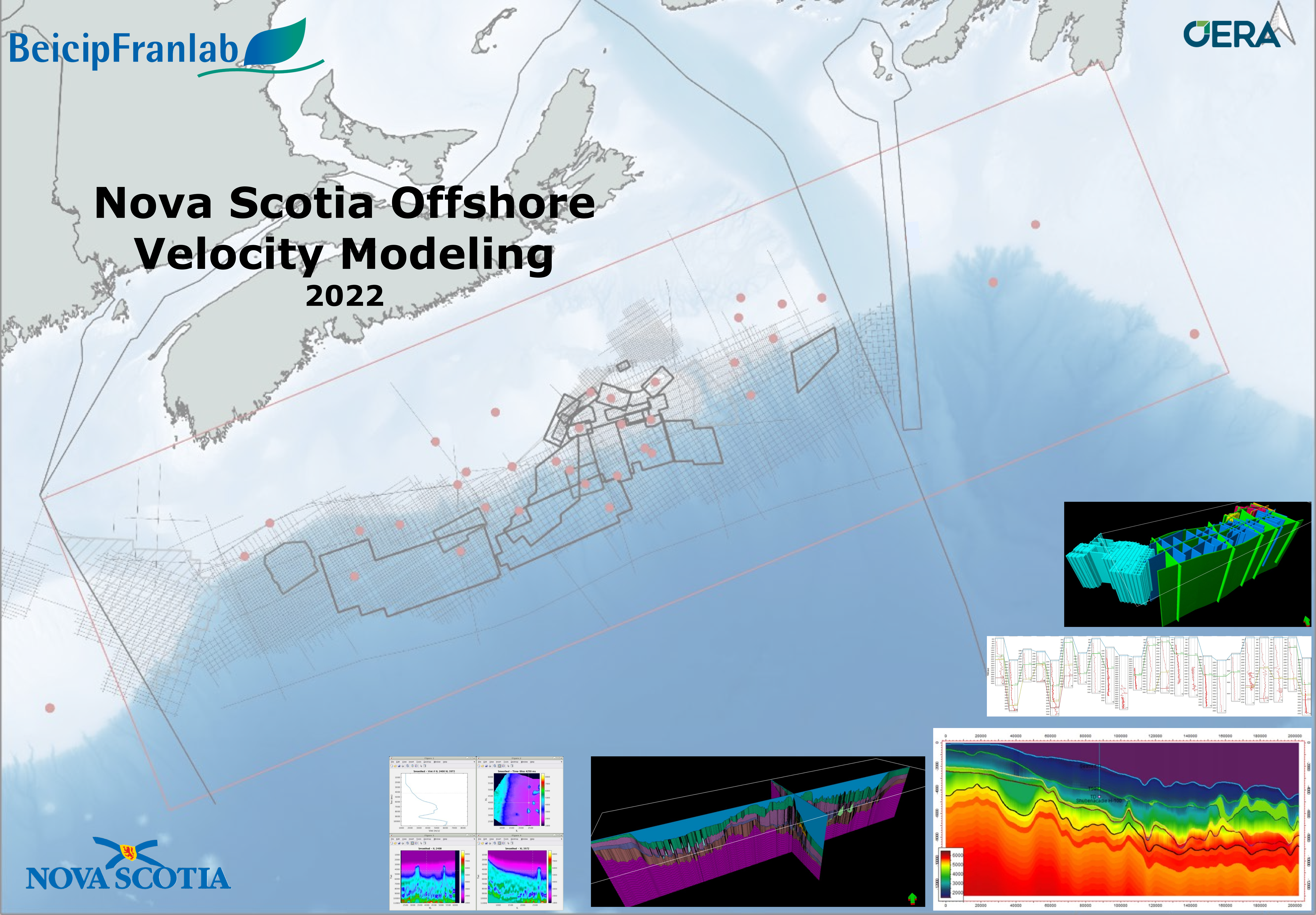

ACKNOWLEDGEMENTS

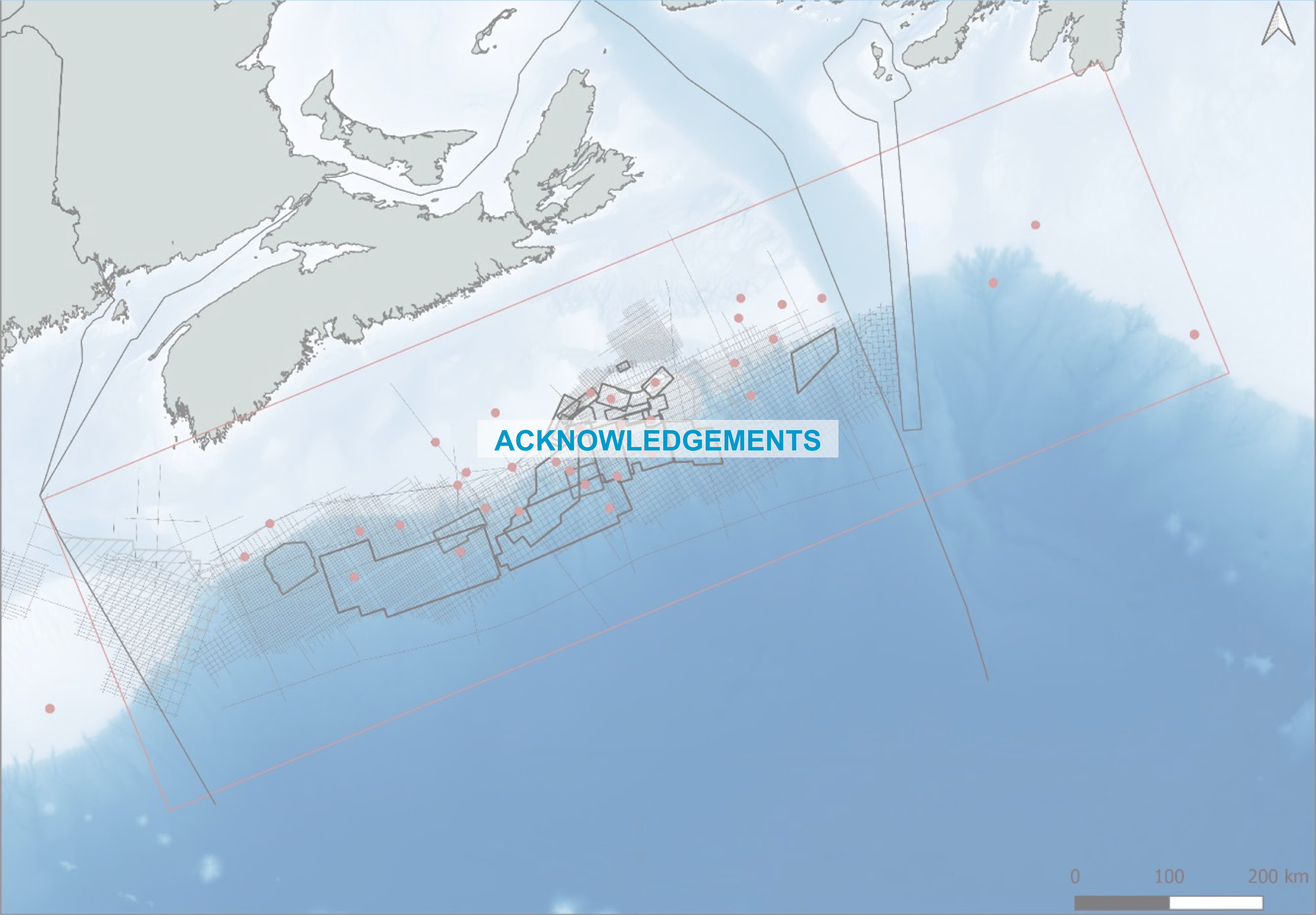

Offshore Nova Scotia Velocity Modeling – CANADA – January 2022

ACKNOWLEDGEMENTS:

This project relies on contributions from many individuals from a variety of disciplines and organizations that are listed below.

Organisation	Contributors
Nova Scotia Department of Natural Resources and Renewables	Fraser Duncan Keppie, Adam MacDonald, Natasha Morrison
OERA	Russell Dmytriw
CNSOPB	Mark Deptuck, Kris Kendell
BeicipFranlab	Ingrid Breda-Dupin, Tomasz Chrest, Laurent Cuilhe

TABLE OF CONTENTS

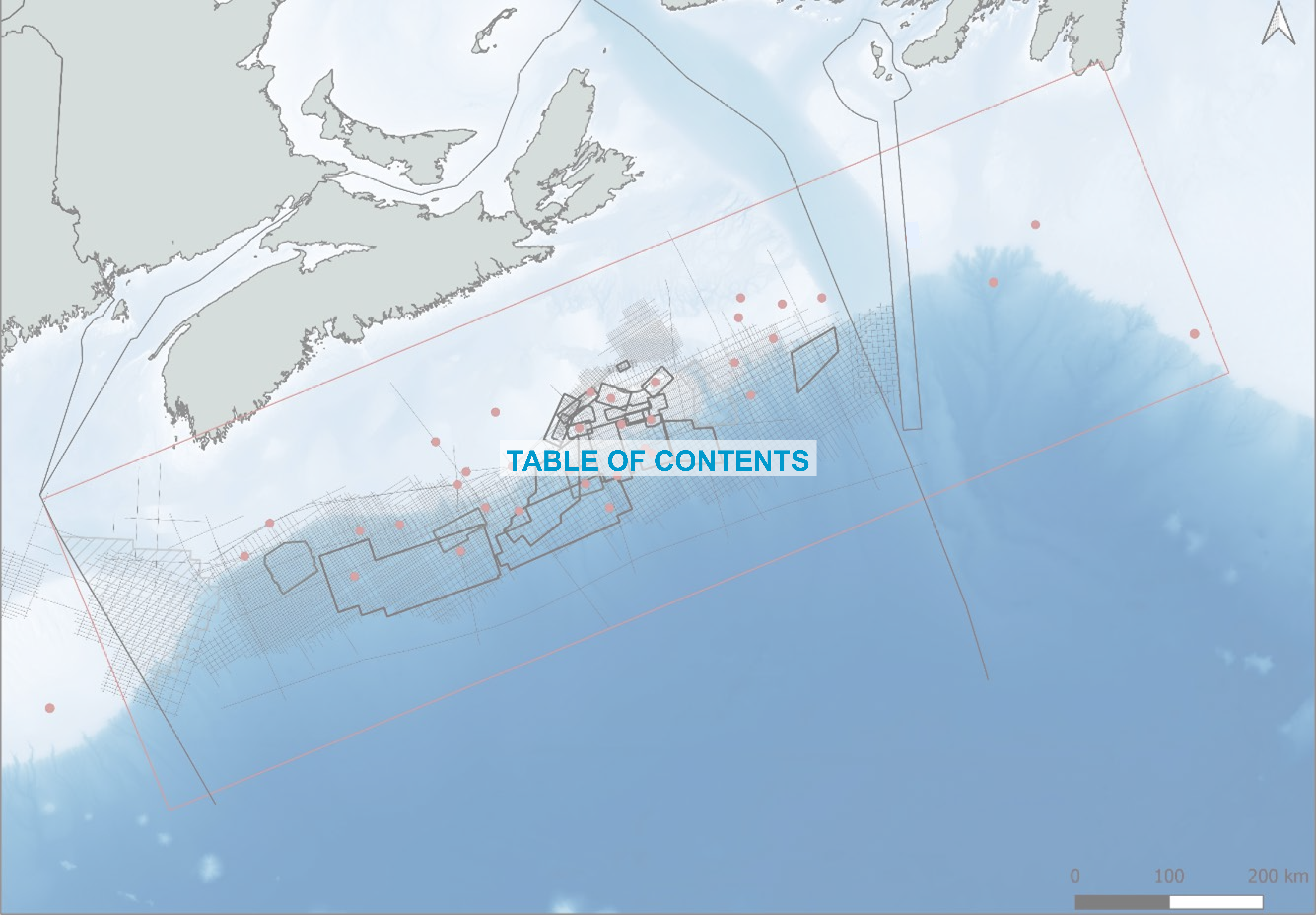

Table of Contents

List of plates

EXECUTIVE SUMMARY

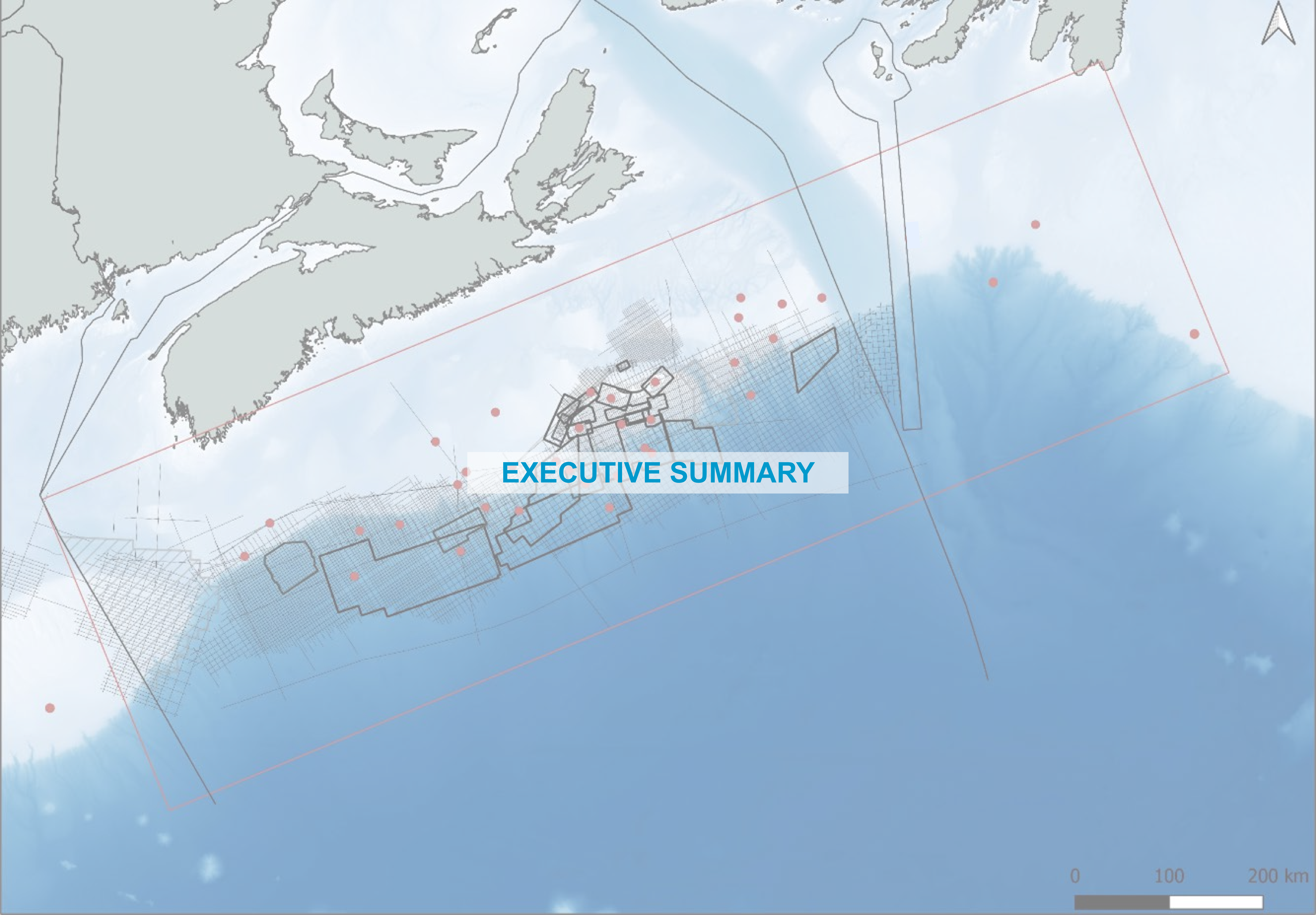

Introduction – Objectives

In past Play Fairway Analysis (PFA) projects 2010-2021, velocity models were variously developed to allow time-to-depth conversion of interpreted seismic. In 2021, OERA / NSDRR (previously NSDEM) find themselves with a collection of past PFA regions of interest with different stages of interpretation and velocity models.

CNSOPB and others have updated interpretations of some horizons in time for different parts of the margin. To make use of these past projects and new updates in the depth domain, OERA / NSDRR are faced with the general challenge of creating and justifying a time-to-depth or velocity model conversion.

This study provides OERA / NSDRR with a regional time-to-depth velocity model that integrates diverse inputs and reconciles inconsistencies in a systematic way to support approximate, yet reasonable depth-converted seismic interpretations with justification in offshore Nova Scotia.

Database

A rectangular area – the AOI – delimits the zone where the velocity model is constructed. It measures 358 x 1224 km along a WSW-ENE main direction (structurally the main N68 'strike' direction), delimiting a 438,000 km² surface, and covers the whole offshore Nova Scotian margin plus a large part of the Laurentian sub-basin belonging to the province of Newfoundland and Labrador.

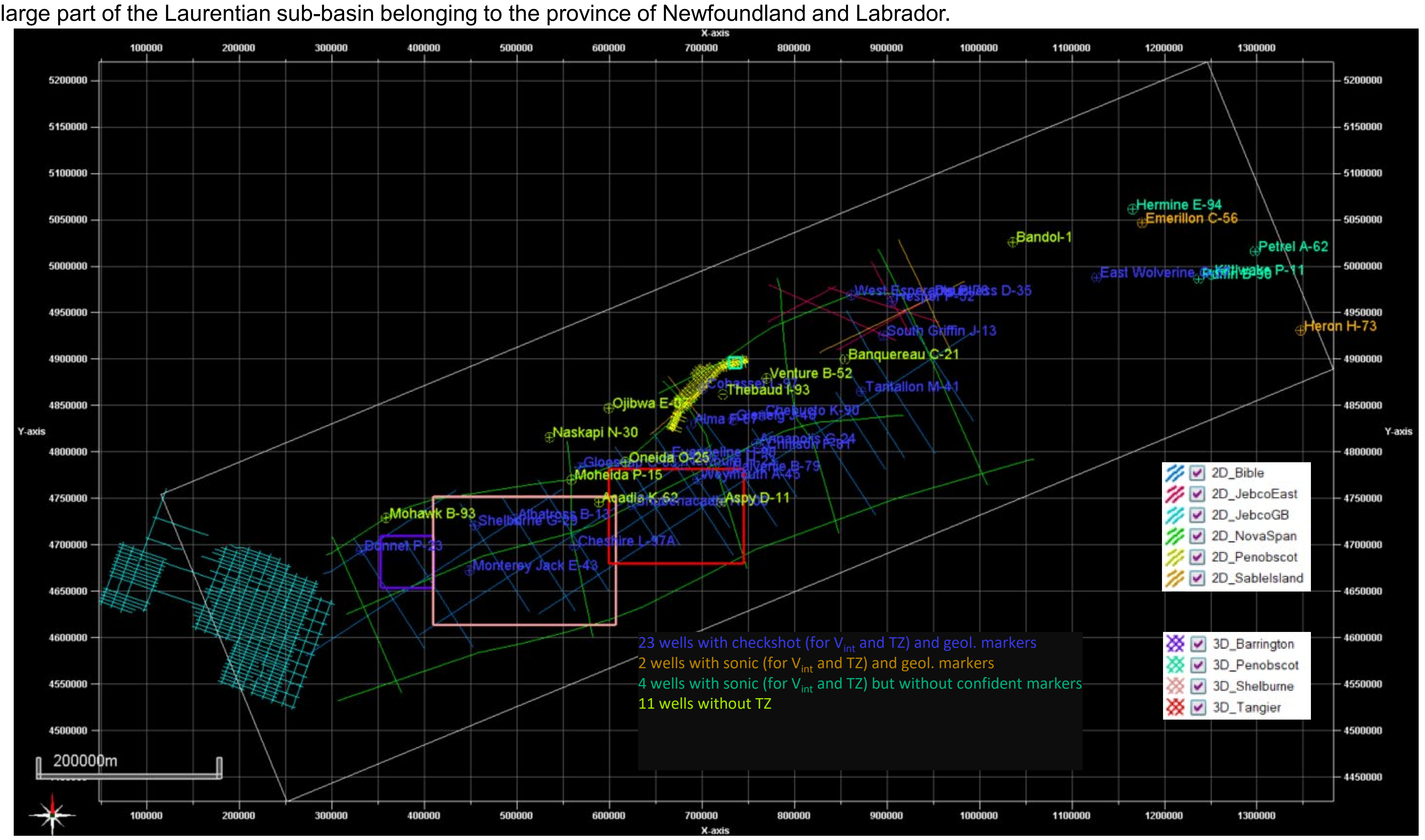

A total of 40 wells are considered, whatsoever about the type of data they include (checkshot or VSP data, sonic log, geological markers).

Seismic processing velocities of any kind are divided into six 2D surveys and four 3D cubes.

The AOI encompass five gridded main horizons. Three sets of salt horizons divide the salt area into diapirs and canopies. They were smartly worked to get extended horizons that do not cross each other.

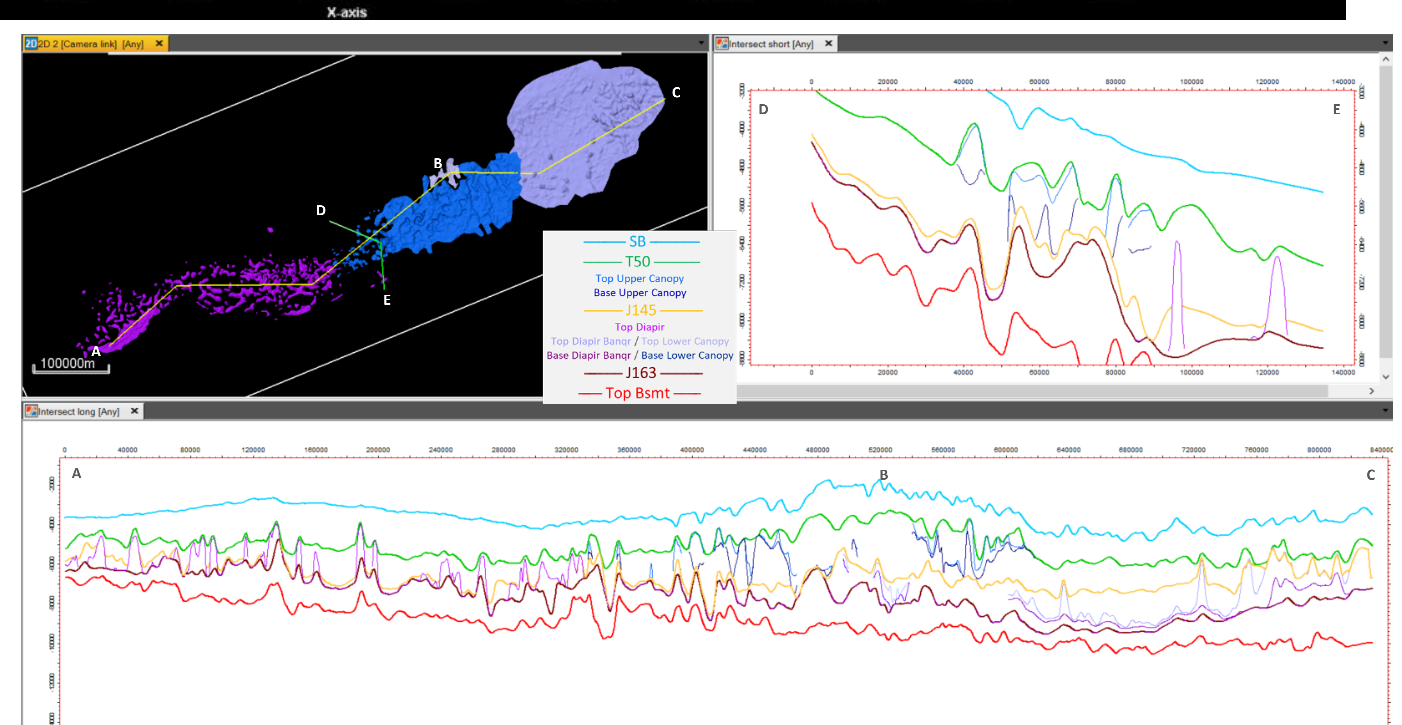

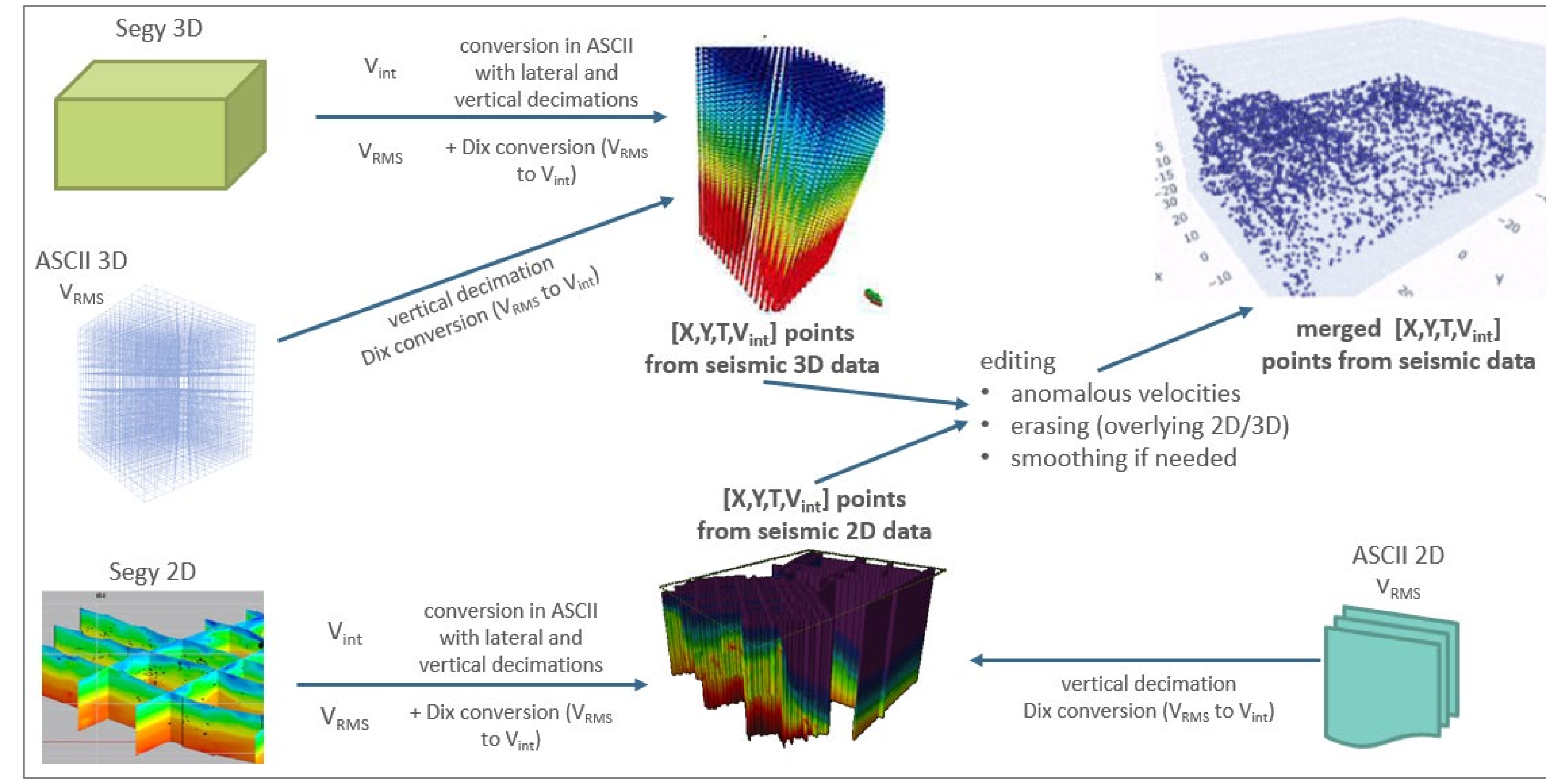

Methodology

Phase 1 (top): Creation of a merged set of [X,Y,T,V_{int}] points from various sources of raw seismic velocities. Different kind of editing (erasing, cropping, smoothing, upscaling) were done before merging.

Phase 2 (bottom): 3D interpolation of seismic velocities through a stratigraphic model built using all the horizons after editing them. Different zones of layering are set between the edited horizons: regular layering in the sedimentary/reservoir zones, constant layer/velocity in the salt and water.

Phase 3 (bottom): Co-kriging of the calibrated well velocities with the seismic velocity cube. Such co-kriging preserves the calibrated TZ laws, consequently no further residual correction would be necessary (the residuals are corrected/estimated previously to the co-kriging).

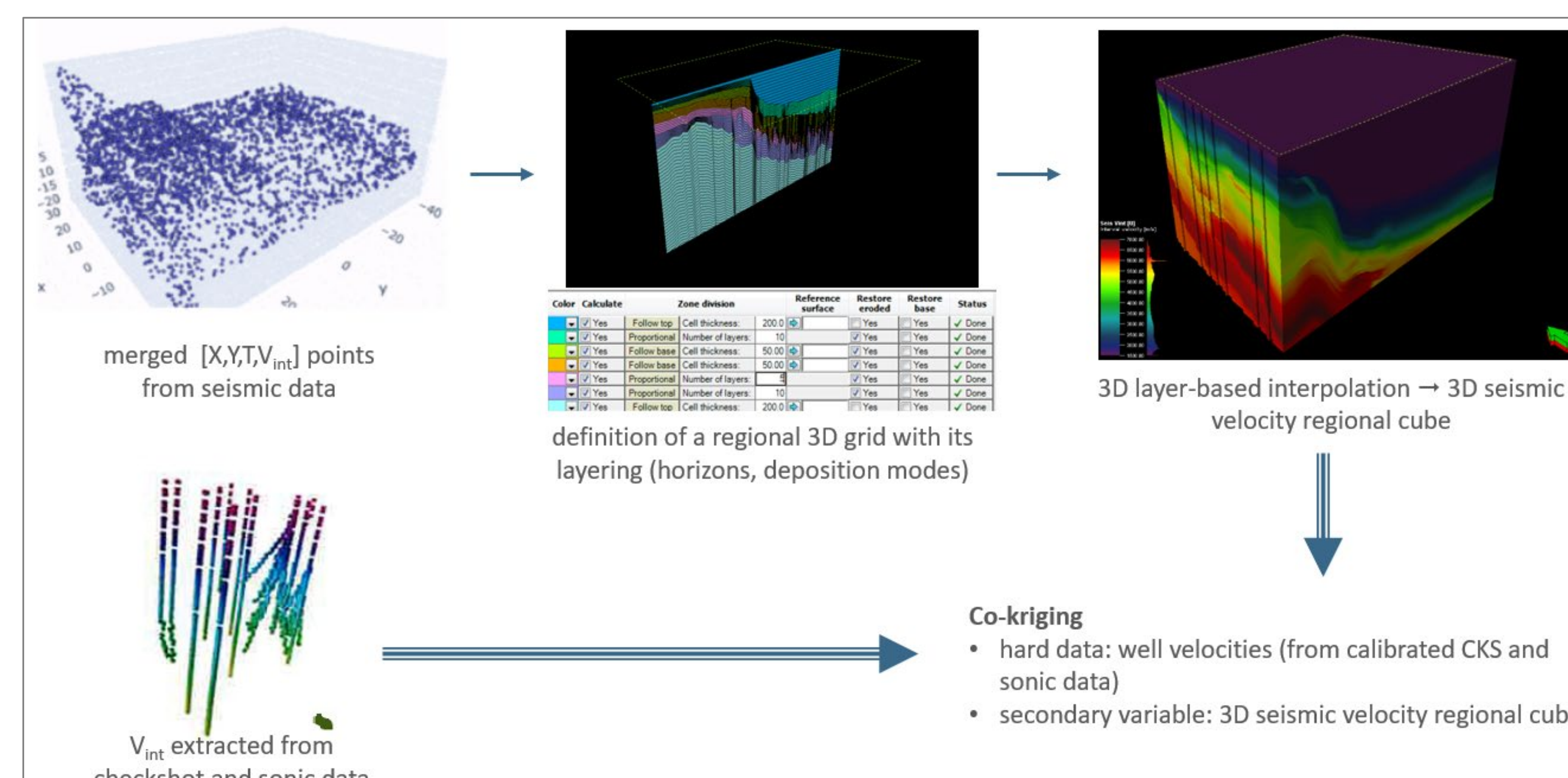

Calibrating the well velocities

Specific workflows were created to set the well velocities to an optimal vertical calibration (from depth to time), whether with the checkshot velocities or the sonic ones. After a first estimation, the TZ calibrations were corrected using the horizons/markers match, without forcing the checkshot velocities (correction done 'at best' with all the relevant markers/horizons couples). Some easternmost wells in the Laurentian sub-basin have too much uncertainties in their markers depth values to be processed with the same recalibration: their digitized sonic logs were set with a simple calibration (TZ from the extrapolated sonic).

Some checkshot velocities were completed – using seismic velocity trends – in the parts where data was missing.

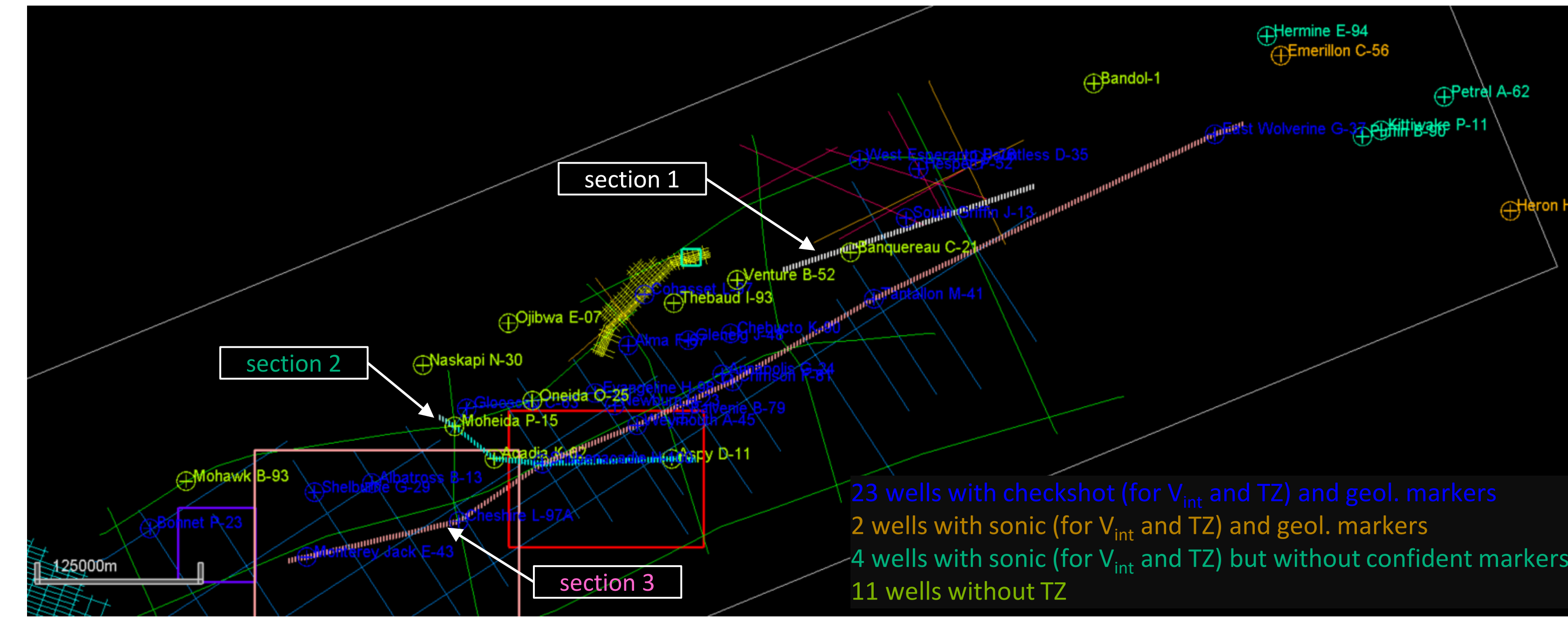

Seismic Velocity interpolation

A single blank 3D TWT grid was created within the AOI with a lateral mesh of 1 x 1 km, and a vertical layering of 50 ms in the reservoir zones, as illustrated here below.

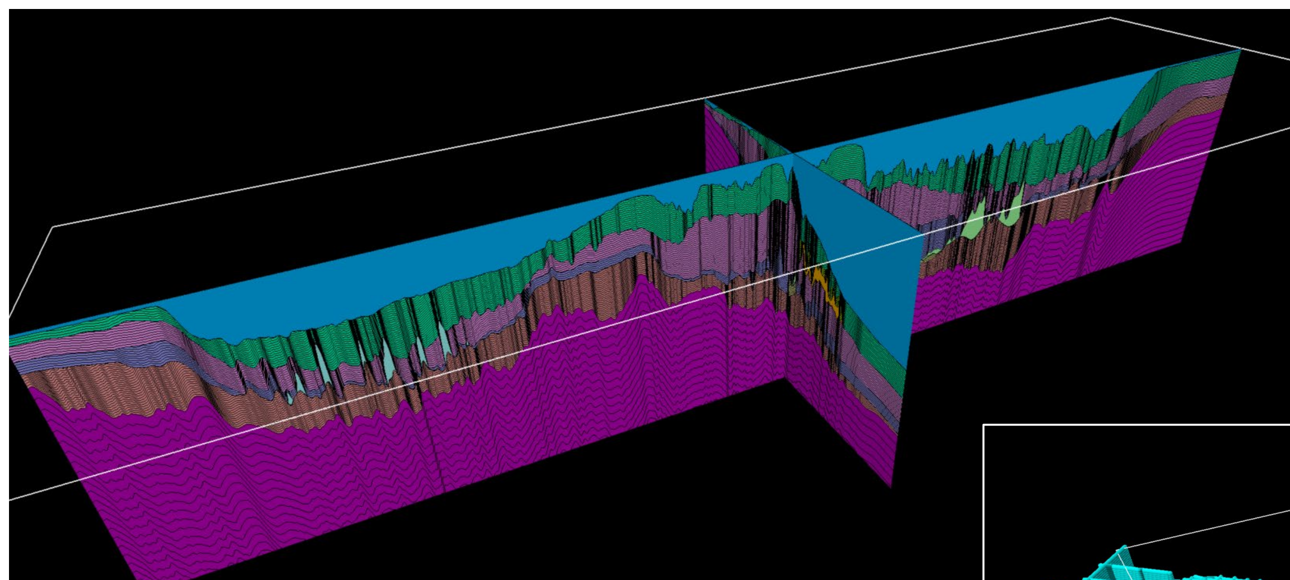

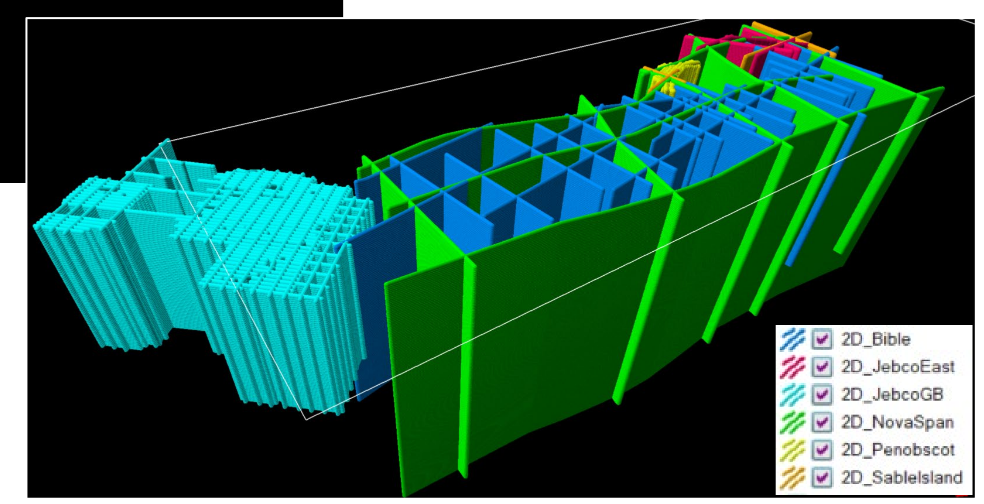

The [X,Y,T,V_{int}] points were upscaled into the grid, as illustrated to the right. It enabled to compute ratio factors between well, 2D and 3D velocities, and adjust the different seismic velocity sources at best, especially between adjacent velocity cubes. An example of ratio factor here below illustrates how the interval velocities were modified in that cube following the depth (TWT here), in order to accommodate the values with other sources.

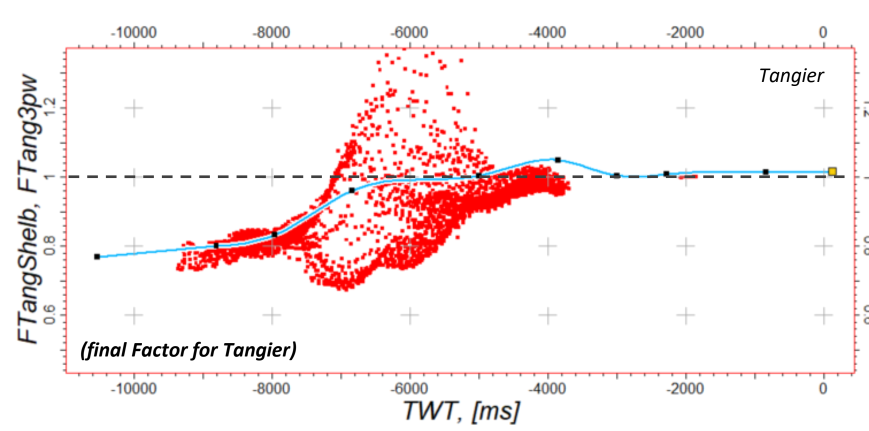

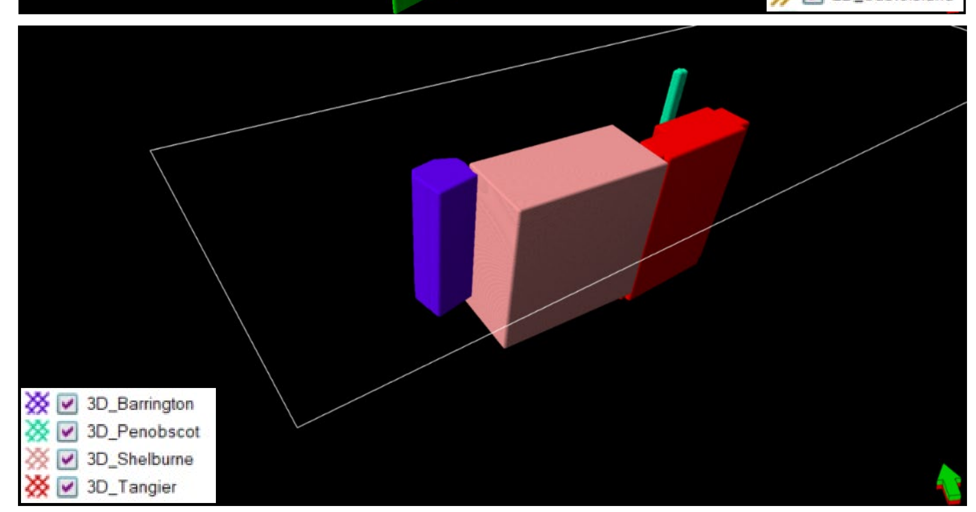

Various editing passes were also needed for 2D and 3D velocities (with the addition of some pseudo-traces to control the extrapolation). A Moving Average interpolator enabled to fill the whole 3D grid, which represents the "trend" for the following co-kriging.

Co-kriging

The calibrated well velocities (hard data) were co-kriged using the seismic velocity property as secondary variable. Constant velocity layers were filled separately. After a first pass, the resulting velocities were extracted at the 11 wells without own TZ, to get their first Depth to Time conversion that was afterwards adjusted with the help of the markers/horizons couples. A second and definitive co-kriging was then run with all the wells. The figures on the right illustrate 3 sections with the co-kriged interval velocity and the resulting average velocity (used for conversions).

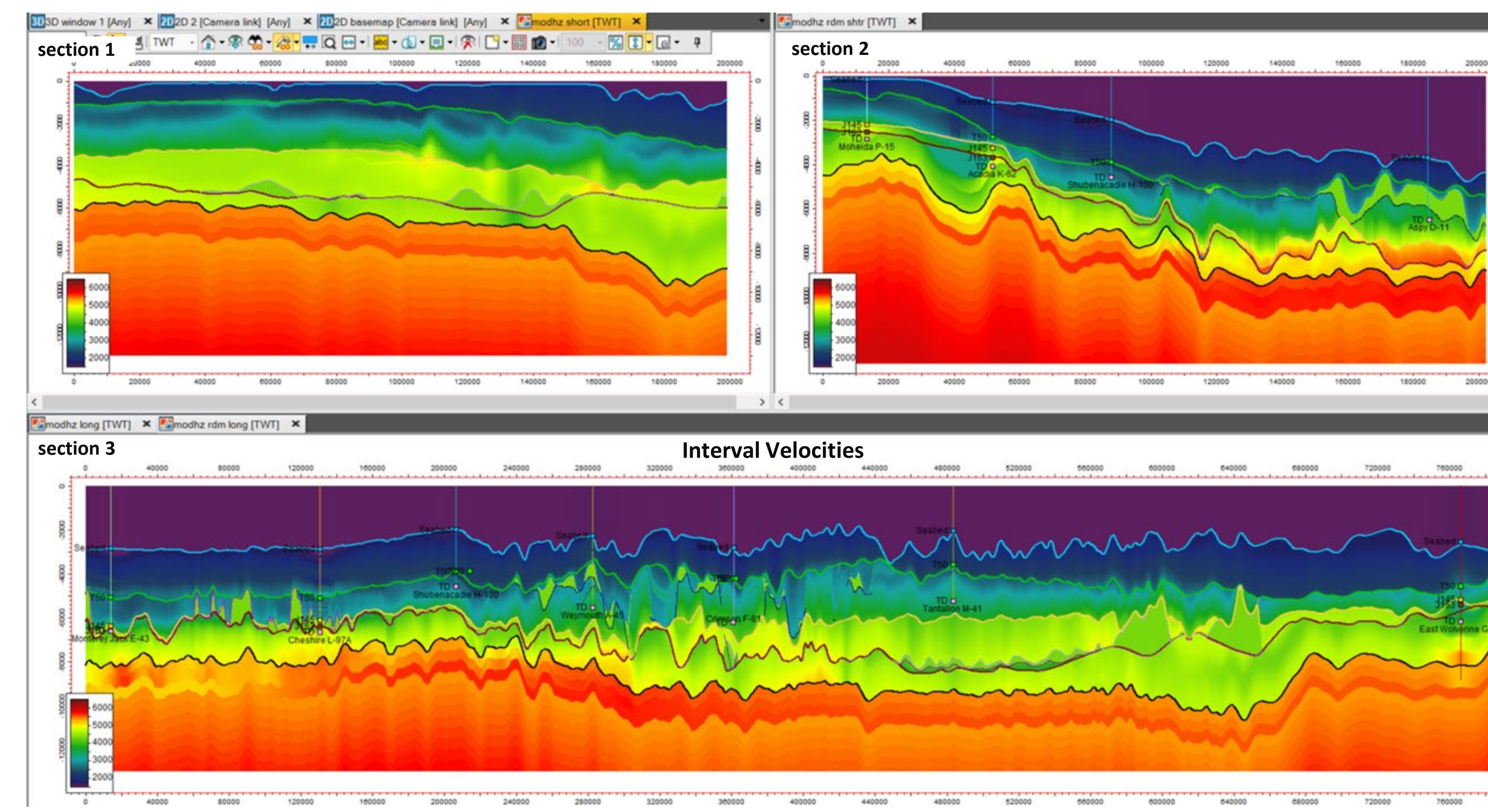

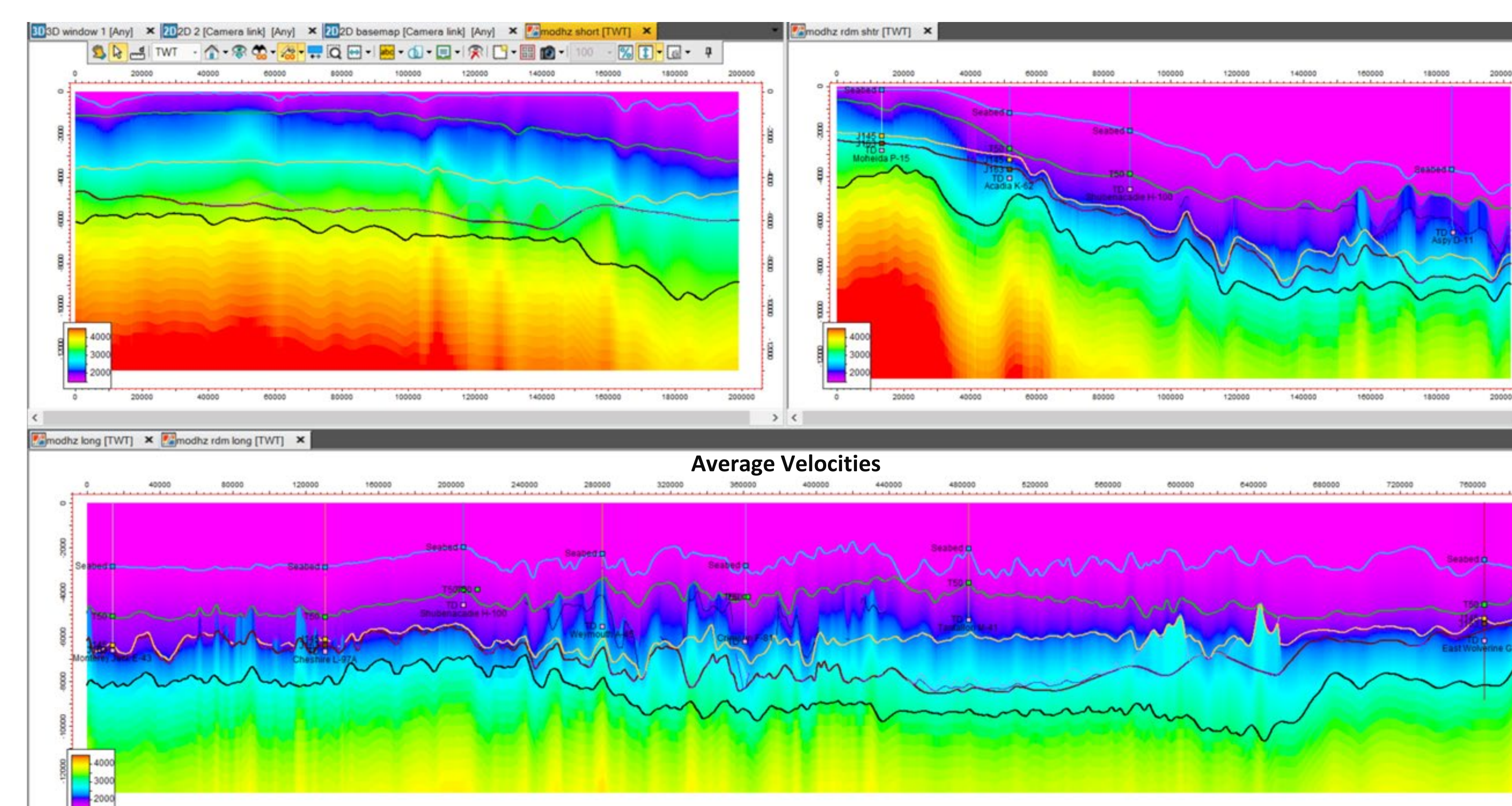

<u>Conclusion</u>

To reach the objectives of the project, all the sources of available velocities (3D and 2D seismic data, checkshot, sonic, constant velocity in the salt) were used. They were worked to their optimal possibility, especially the large adjacent 3D sets were adjusted between them and with the true well velocities. The geological markers and the time horizons were jointly compared to calibrate the raw velocities (checkshot or sonic) at the wells → the final model respects that calibration. Limitations : some 2D seismic velocity sets remain different between themselves in the deep layers (below the total depth of the wells), without the possibility to identify where is the best accuracy ; the Velocity Model is more uncertain far from the wells – especially the 11 ones without own TZ – and in the deeper interval below J145 poorly drilled by the wells and with a low Signal / Noise ratio leading to more uncertain seismic processing velocities ; this Velocity Model does not consider any local geological feature, not identified with the current input data, as a source of local velocity anomaly.

The Average Velocity property is now implemented into a Petrel^{TM} Velocity Model.

CHAPTER 1

DATABASE CONSTRUCTION FOR VELOCITY MODELING

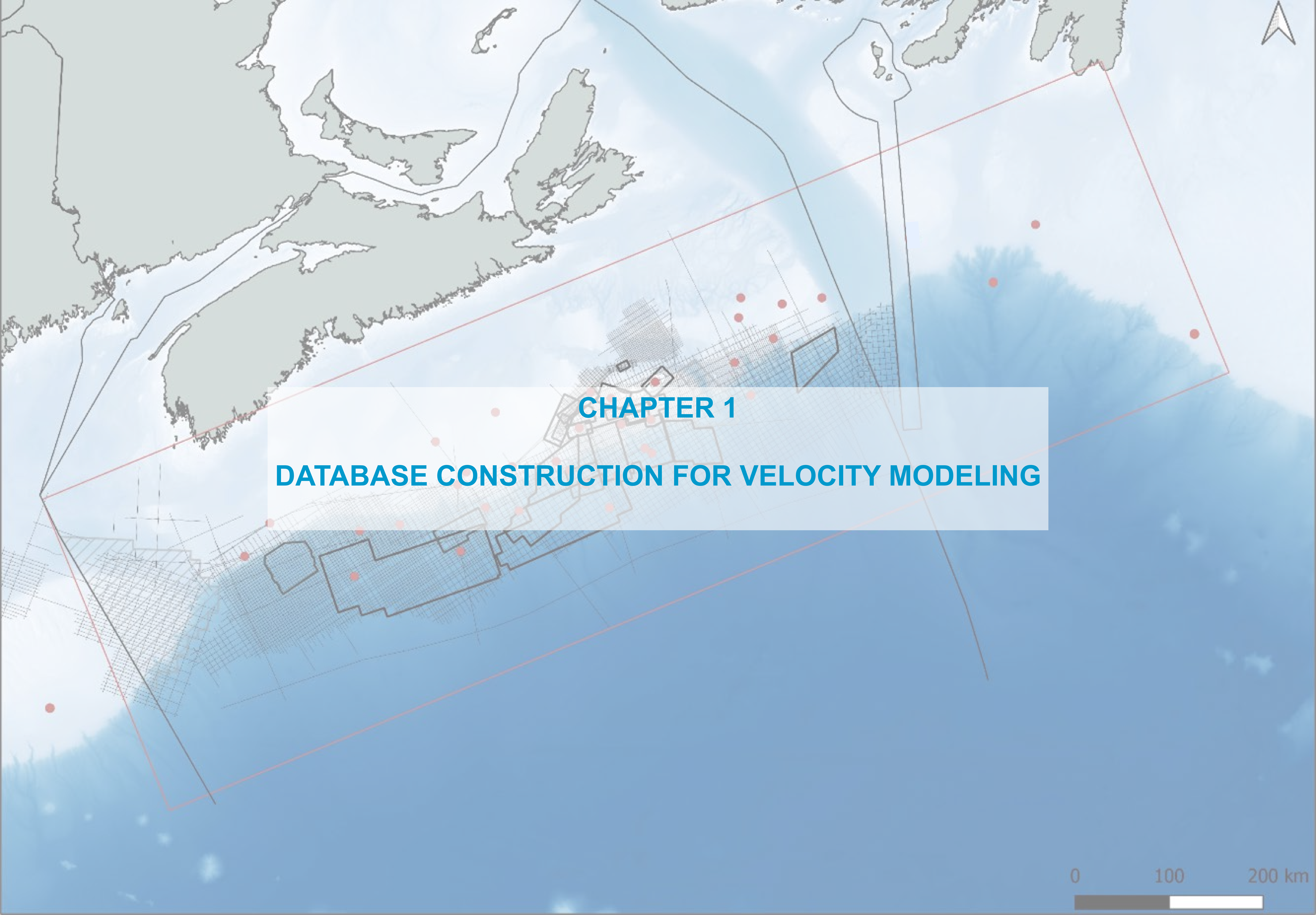

Area of Interest (AOI)

[NB: the geodetical datum used in this project and in the figures is NAD-1927; the cartographic projection is UTM 20N]

A rectangular area (Figure 1) delimits the zone where the velocity model is constructed. It measures 358 x 1224 km along a WSW-ENE main direction (structurally the main N68 'strike' direction), delimiting a 438,000 km² surface, and covers the whole offshore Nova Scotian margin plus a large part of the Laurentian sub-basin mainly located in the province of Newfoundland and Labrador.

The Figure 2 reminds the chronostratigraphic chart and underlines the stratigraphic location of the main time horizons with their names highlighted by red rectangles (see them in PL.1.3).

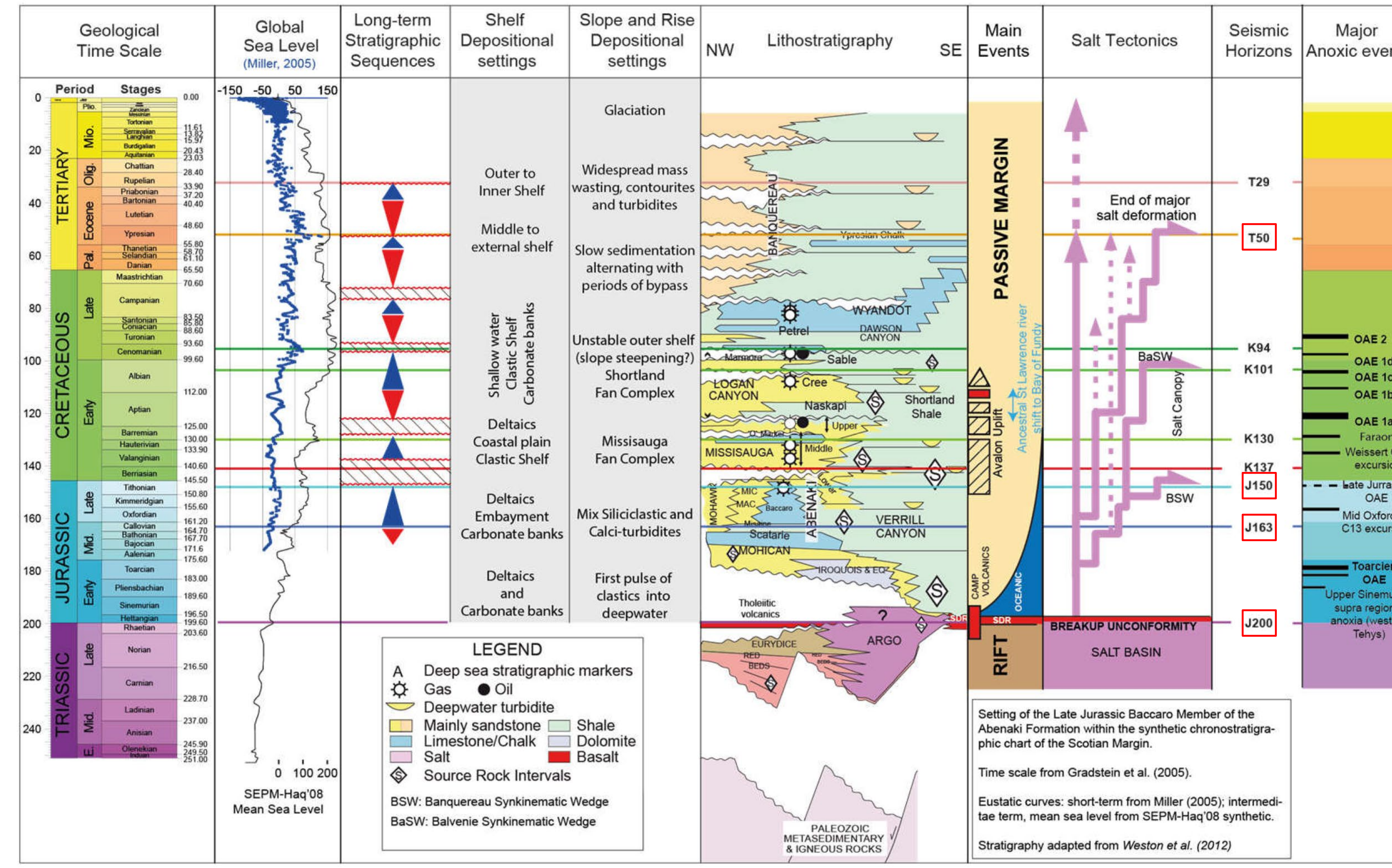

Figure 2: Chronostratigraphic chart of Nova Scotian margin

Wells

A total of 40 wells are taken into account, whatsoever about the type of data they include (checkshot or VSP data, sonic log, geological markers). A detailed list of them is added in PL. 1.2. They may be divided into 4 groups:

- 23 wells with checkshot data and geological markers (in blue in Figure 1)
- 2 wells with sonic log and geological markers (in orange)
- 4 wells with sonic log, with no geological markers except some litho-stratigraphical information (in dark green)
- 11 wells without TZ (Time-to-Depth) data (in light green)

Figure 1: Basemap and AOI (Area Of Interest) limits

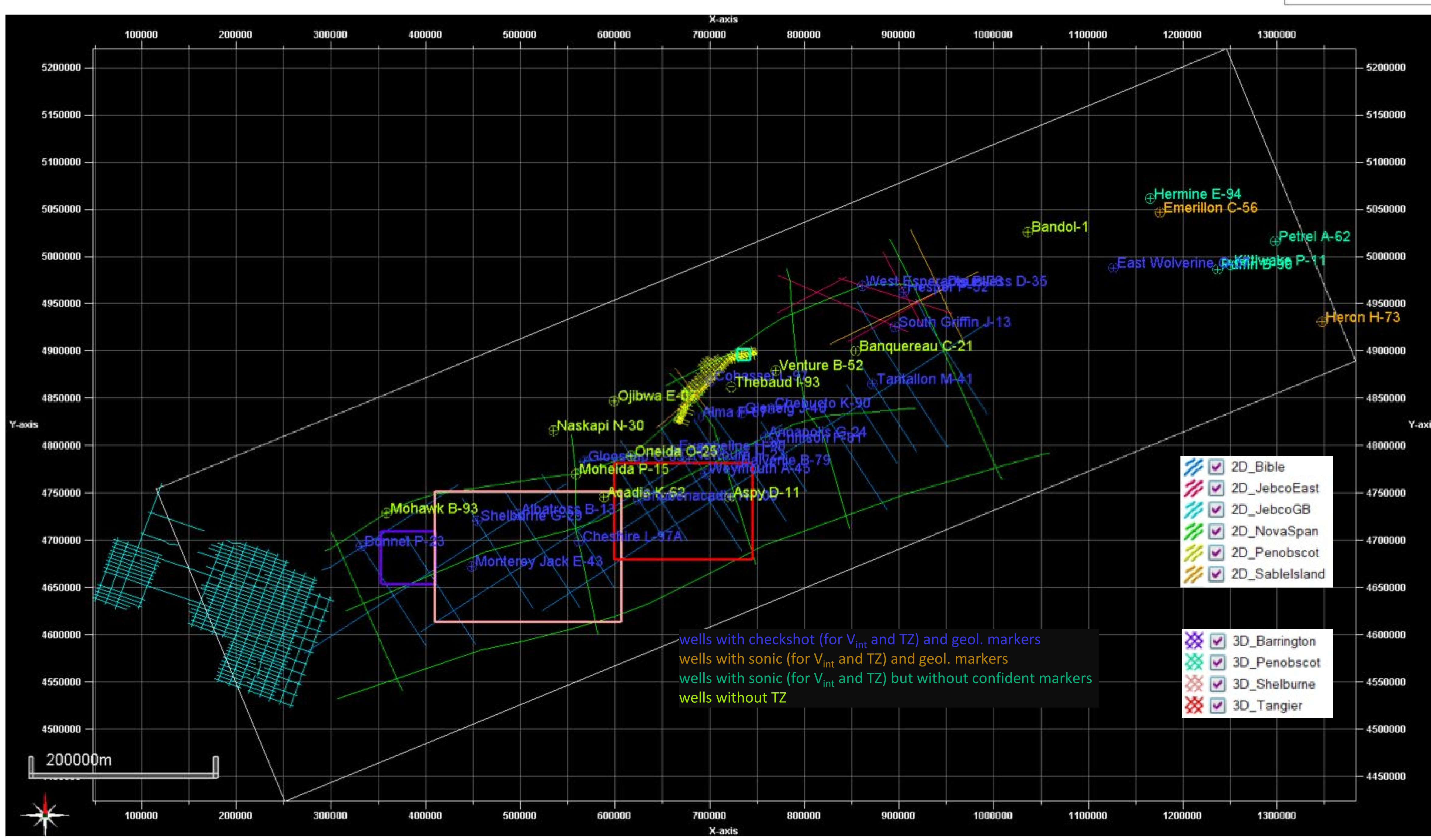

Seismic velocity data

Different types of seismic velocities (more precisely seismic processing velocities) are used, with their respective velocity properties, vertical sampling and file format. A detailed list of them is available in PL. 1.3. They are available into 3D surveys (4 cubes) and 2D surveys (6 sets): their locations are displayed here to the left. In the last eastern quarter of the AOI (Laurentian Basin), no seismic velocity is provided.

Most of the 3D surveys are adjacent and located in the main Shelburne basin:

- Barrington (~ 2300 km²)
- Shelburne (~ 15300 km²)
- Tangier (~ 8300 km²)

The last 3D survey – Penobscot – is much smaller (~ 90 km²) and located to the North of Thebaud I-93 well.

The 6 surveys of 2D lines are better distributed in the whole Nova Scotian margin. A detailed list of them is presented in PL. 1.4. The 6 surveys are:

- Bible: long lines covering the whole Nova Scotian margin
- Jebco East: some lines in the northern area, around West-Esperanto B-78
- Jebco Georges Bank: dense set of lines covering the extreme western part of the AOI
- Nova Span: as Bible set, with a denser coverage
- Penobscot: very dense set of short lines localised in a small area around Cohasset L-97
- Sable Island: few lines (2 in Penobscot survey and 2 in among Jebco East survey)

Figure 1: Well chart

Well	dev'd	deviation	CKS vel.	Sonic log	no TZ	no geol. mark.	X	Y	UTM	RT
40	*18*		*23*	*6*	*11*	*4*				
Acadia K-62		dif.TD 2 m			x		588433	4745831	UTM 20	13
Albatross B-13		vertical	x				496994	4727585	UTM 20	24
Alma F-67	D	dif.TD 11 m	x				688407	4830393	UTM 20	24
Annapolis G-24	D	dif.TD 26 m	x				758531	4808827	UTM 20	36
Aspy D-11	D	dif.TD 206 m			x		720856	4745645	UTM 20	31
Balvenie B-79		vertical	x				729168	4779300	UTM 20	25
Bandol-1		no survey			x		564665	5003662	UTM 21	23
Banquereau C-21		dif.TD 1 m			x		854441	4899949	UTM 20	27
Bonnet P-23	D	dif.TD 10 m	x				331182	4693790	UTM 20	25
Chebucto K-90	D	dif.TD 8 m	x				764910	4839385	UTM 20	23
Cheshire L-97A	D	dif.TD 3 m	x				561754	4699121	UTM 20	32
Cohasset L-97	D	dif.TD 4 m	x				700665	4868393	UTM 20	33
Crimson F-81	D	dif.TD 68 m	x				766226	4803559	UTM 20	21
Dauntless D-35		no survey	x				947661	4968885	UTM 20	31
East Wolverine G-37	D	dif.TD 5 m	x				651698	4959297	UTM 21	32
Emerillon C-56	D	dif.TD 5 m		x			1175776	5046818	UTM 20	30
Evangeline H-98	D	dif.TD 11 m	x				663802	4794849	UTM 20	21
Glenelg J-48	D	dif.TD 13 m	x				733404	4834320	UTM 20	24
Glooscap C-63	D	dif.TD 15 m	x				567773	4783412	UTM 20	23
Hermine E-94		no survey		x		x	695812	5029266	UTM 21	26
Heron H-73		no survey		x			385591	4877173	UTM 22	26
Hesper P-52	D	dif.TD 3 m	x				905198	4962293	UTM 20	41
Kittiwake P-11		no survey		x		x	299537	4950343	UTM 22	26
Mohawk B-93		no survey			x		358193	4729045	UTM 20	31
Moheida P-15		no survey			x		558704	4769952	UTM 20	30
Monterey Jack E-43		dif.TD 1 m	x				448404	4672464	UTM 20	32
Naskapi N-30		vertical			x		535021	4815742	UTM 20	26
Newburn H-23	D	dif.TD 88 m	x				678317	4785626	UTM 20	24
Ojibwa E-07		no survey			x		599015	4847058	UTM 20	30
Oneida O-25		vertical			x		616903	4789243	UTM 20	26
Petrel A-62		no survey		x		x	349521	4968029	UTM 22	30
Puffin B-90		no survey		x		x	285289	4947815	UTM 22	30
Shelburne G-29		no survey	x				454159	4720817	UTM 20	25
Shubenacadie H-100		dif.TD 1 m	x				624365	4742186	UTM 20	24
South Griffin J-13		dif.TD 1 m	x				895795	4925546	UTM 20	40
Tantallon M-41		dif.TD 2 m	x				871906	4865251	UTM 20	24
Thebaud I-93	D	dif.TD 7 m			x		722474	4861934	UTM 20	37
Venture B-52		dif.TD 2 m			x		769669	4879374	UTM 20	34
West Esperanto B-78	D	dif.TD 3 m	x				861040	4968862	UTM 20	23
Weymouth A-45	D	dif.TD 20 m	x				695037	4770820	UTM 20	25

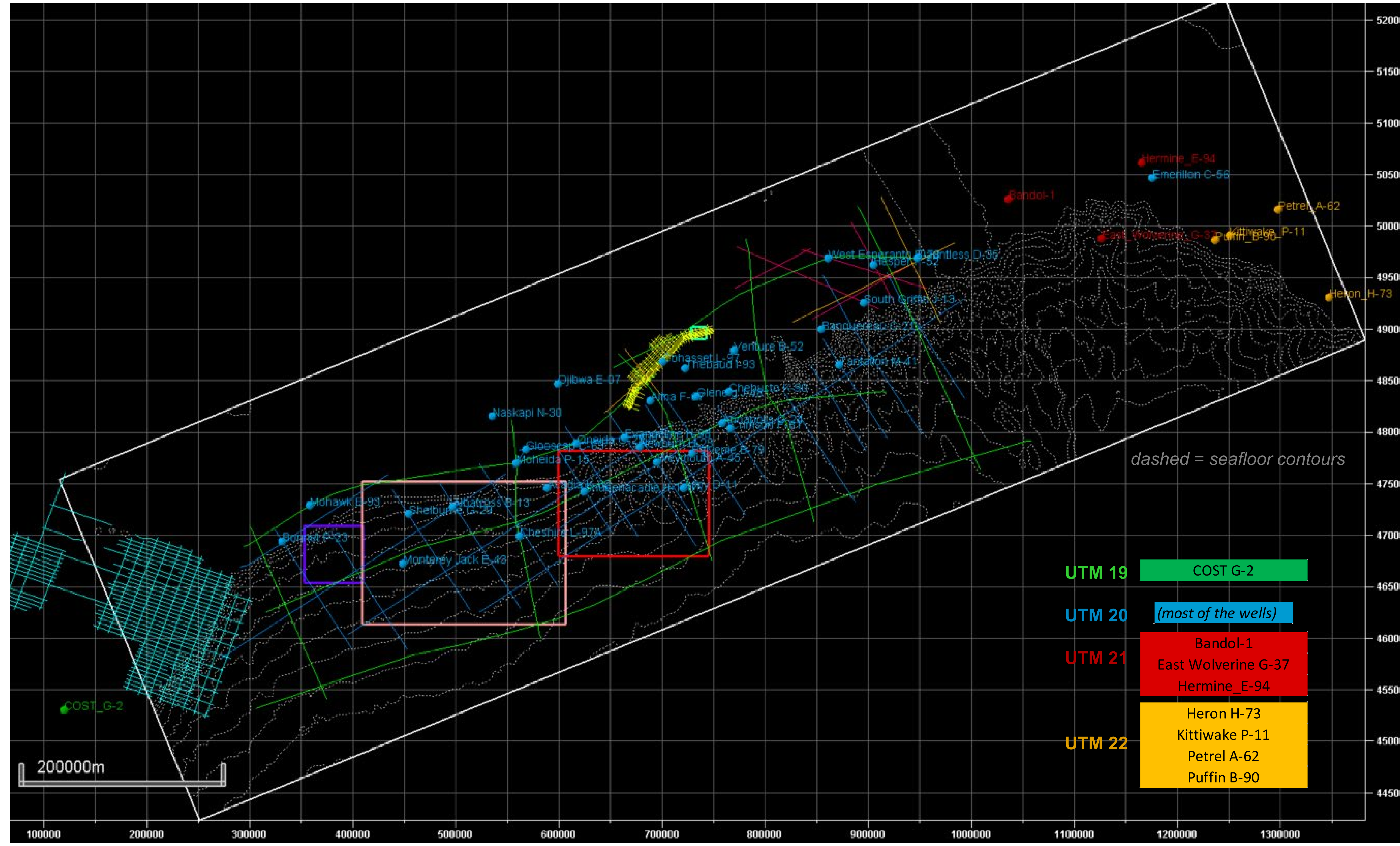

Figure 2: Well basemap according to the original coordinate zones

Figure 3: Velocities from checkshot data

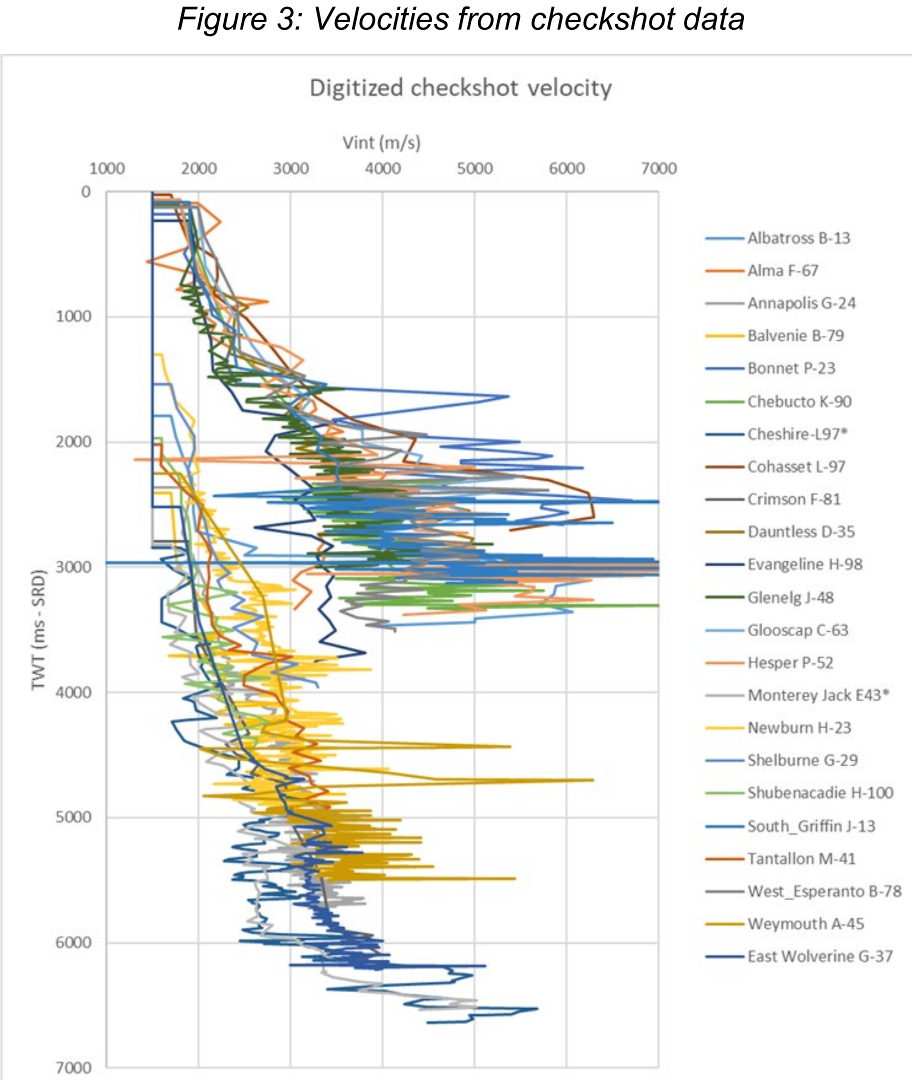

Figure 4: Velocities from sonic log

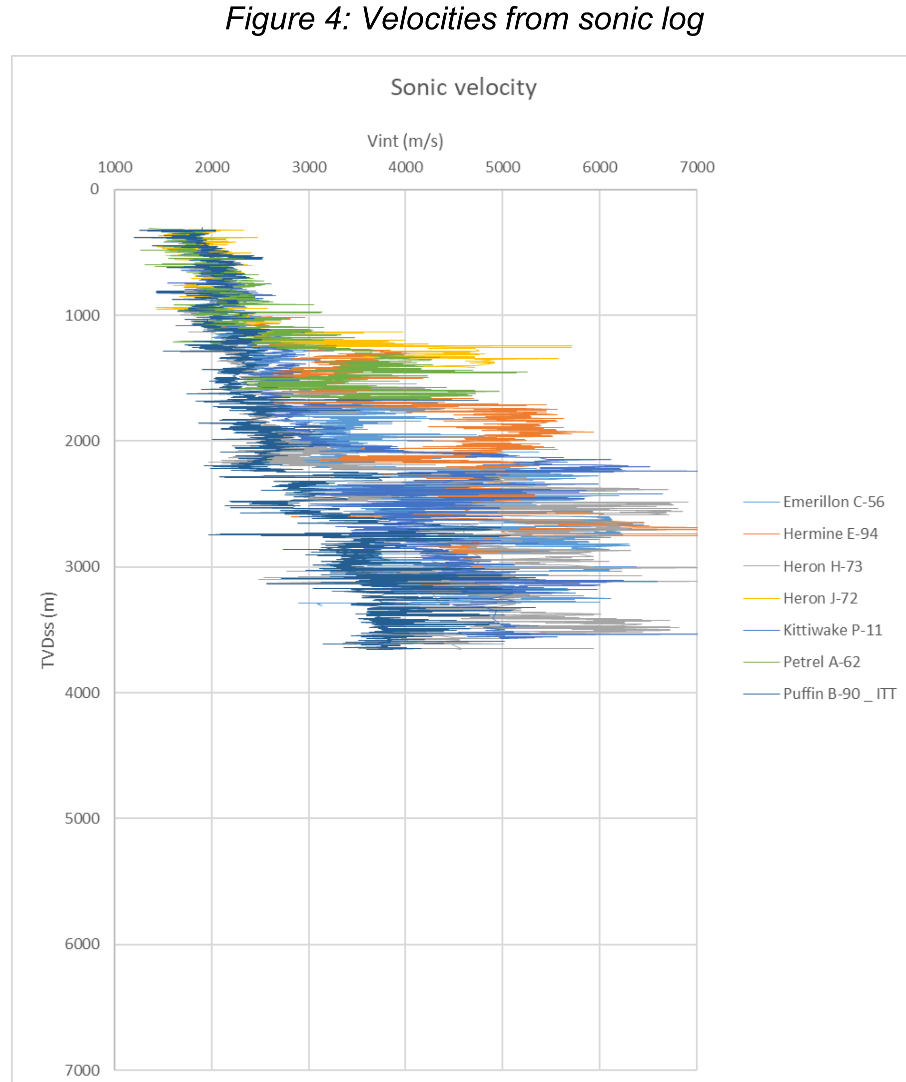

Wells

40 wells are available. Few of them are much deviated (Fig.1): only those whose depth difference TVD vs. MD at Terminal Depth is more than 3 m are considered as deviated with their deviation survey loaded into software. The provided coordinates are mainly UTM 20N (blue in Fig.2); the wells in the Laurentian sub-basin are provided in UTM21N or -22N.

Velocity and TZ sources

As a priority, the interval velocities at the wells were extracted from checkshot data when they are available (23 wells – Fig.3). As second source, the interval velocity is converted from the sonic log (6 wells – Fig.4).

Well Time-to-Depth relationships (TZ) were based on these same items (checkshot and sonic) after calibration (see PL. 2.4).

The 11 last wells have no velocity data ("no TZ" tick). They were used as tertiary control to adjust the final pass of velocity co-kriging (see PL. 3.1).

Well velocities

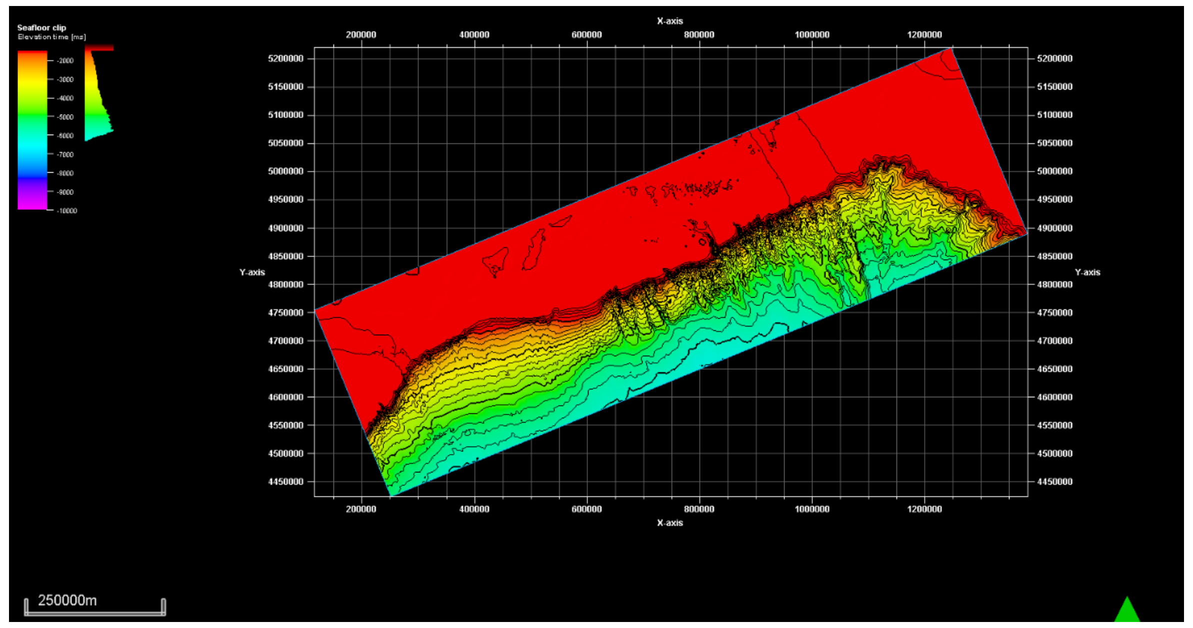

Seafloor

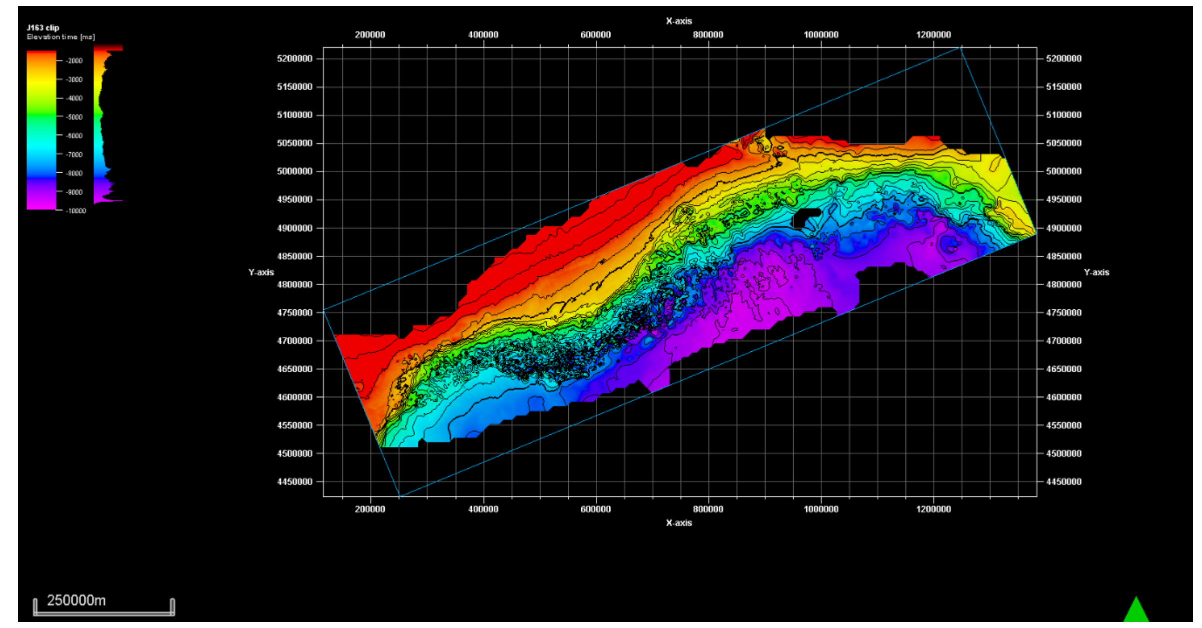

J163

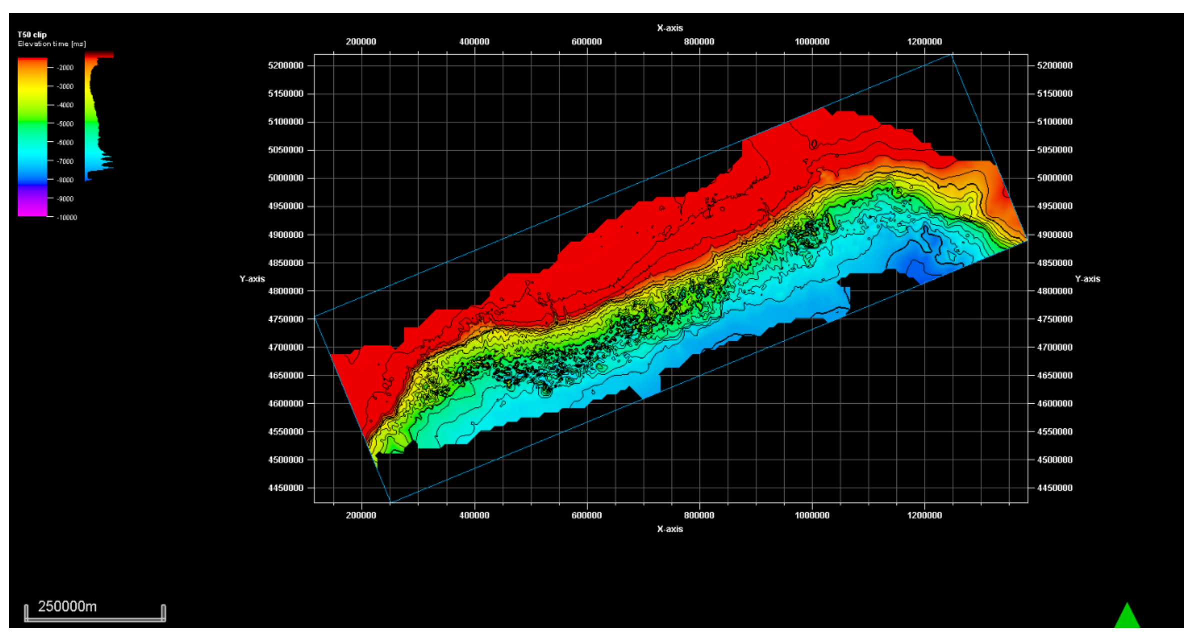

T50

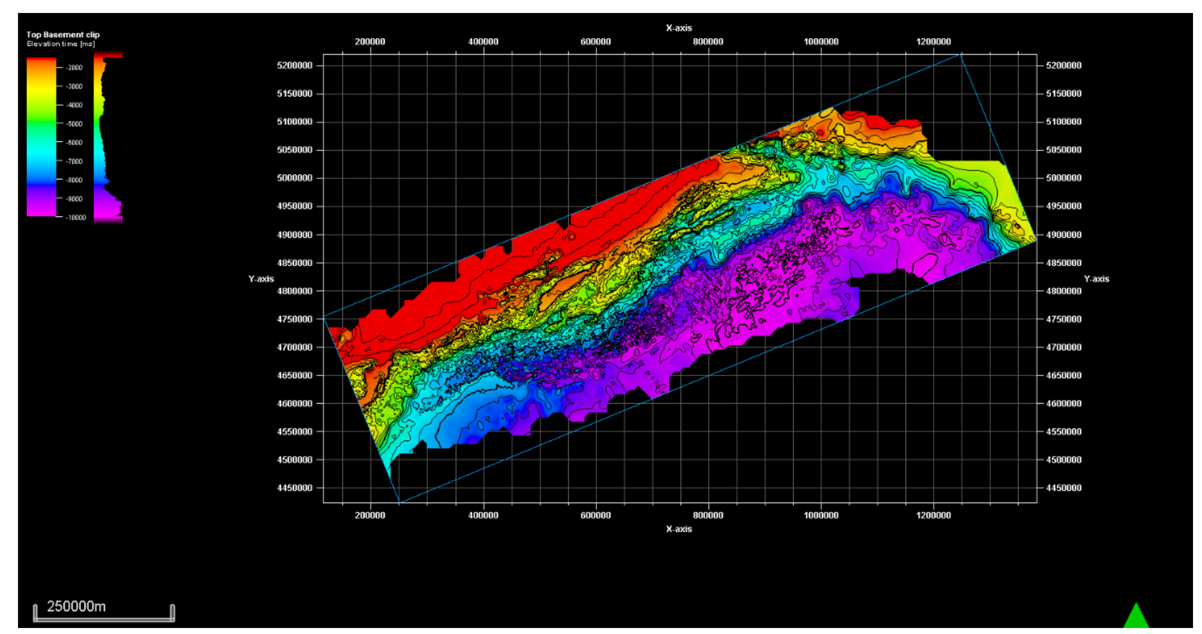

Top Basement

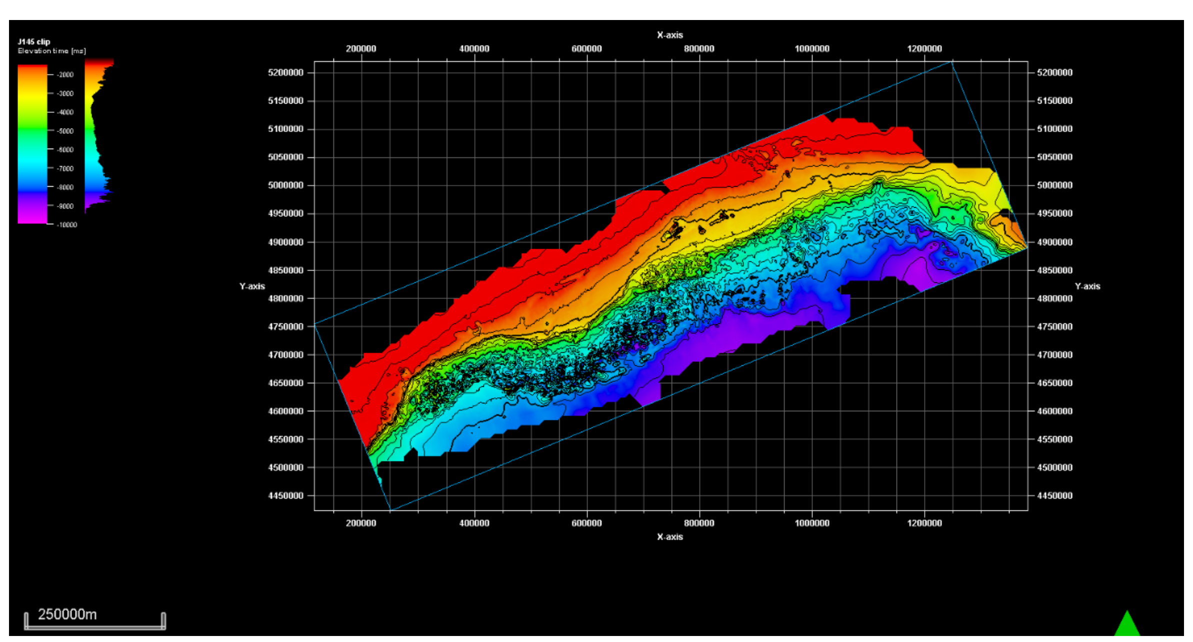

J145

Main horizons

5 main gridded horizons were provided in TWT, and cover most of the AOI. They will be used to guide the velocity interpolation:

- Seafloor: totally gridded (200 x 200 m) in the AOI
- T50: gridded (200 x 200 m) without any gap
- J145: gridded (200 x 200 m) without any gap
- J163: gridded (200 x 200 m) with small gaps (1300 km^2)
- Top Basement: gridded (200 x 200 m) without any gap

Salt

5 salt grids were provided in TWT (50 x 50m), representing 3 sets of salt structures (diapirs and canopies):

- “Top Salt diapirs west Scotian Slope”: top salt representing the local western salt diapirs emerging from Late Jurassic layers along one third of the AOI length. Its base salt is supposed to be joined at J163
- “Top & Base Sable Canopy Salt”: top and base of central salt canopy mainly developed between T50 and J145
- “Top & Base Salt Banquereau Wedge”: top and base of eastern diapir/canopy complex in the area of Sable Island , mainly developed between J145 and J163

A global strategy of horizon editing is exposed in PL. 1.8.

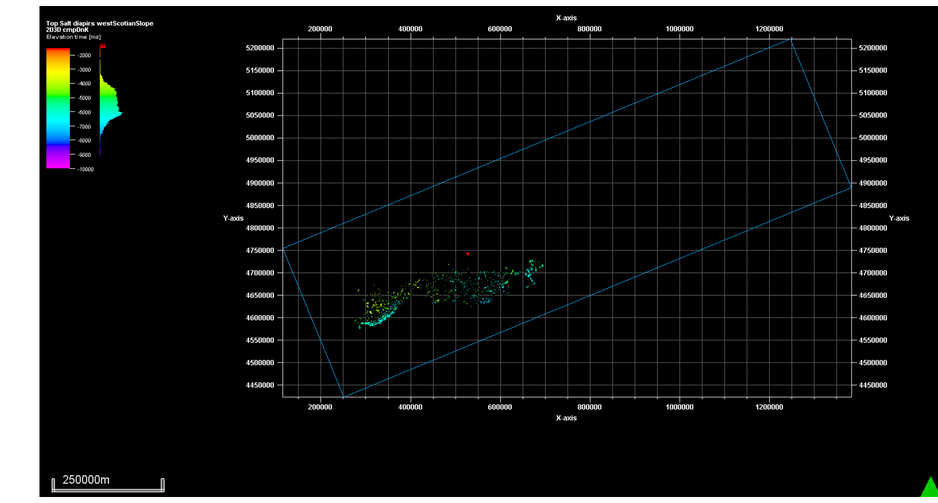

Top Salt diapirs “west Scotian Slope”

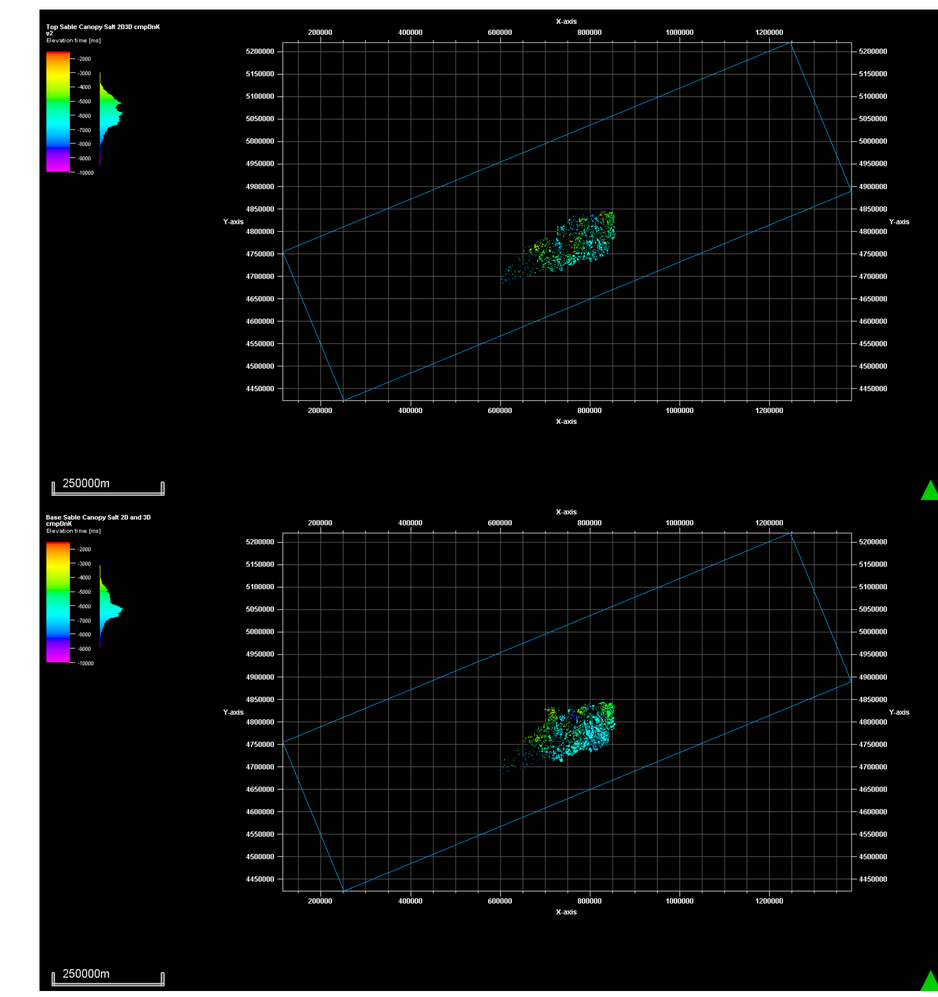

Top & Base Sable Canopy Salt

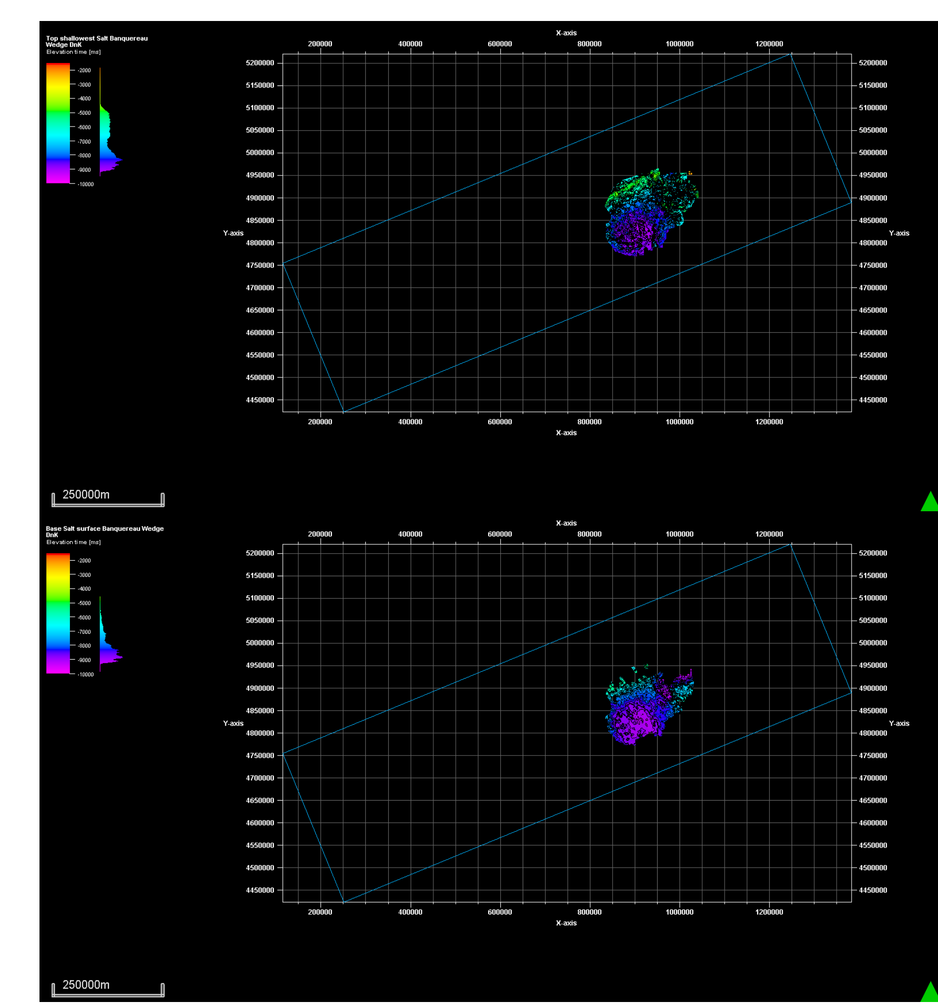

Top & Base Salt Banquereau Wedge

Database Construction for Velocity Modeling

3D

V_{RMS}

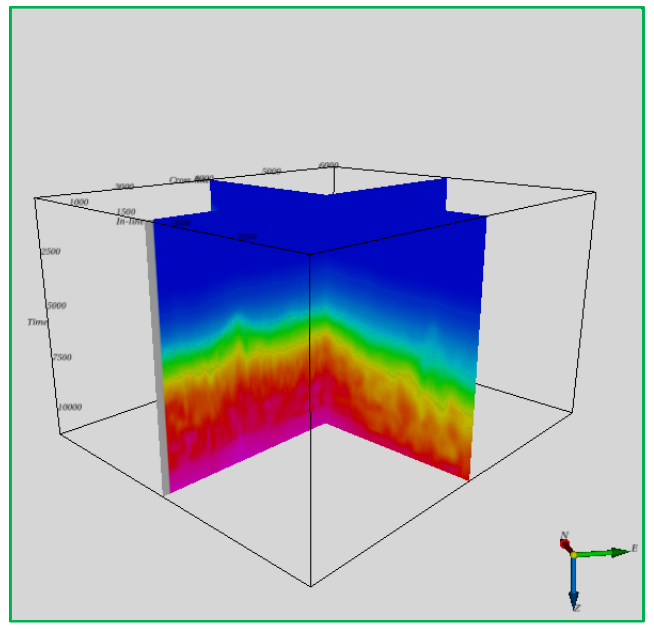

Barrington

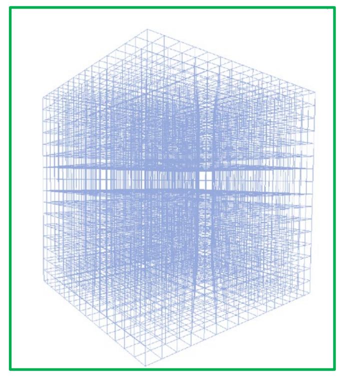

Penobscot
(1 ASCII file of velocity traces)

V_{int}

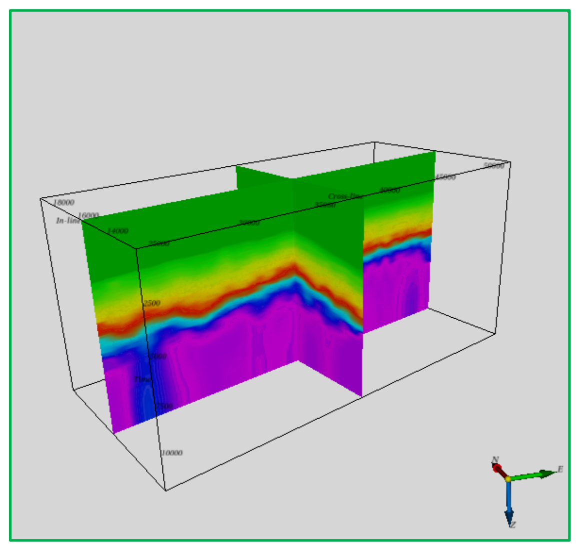

Shelburne

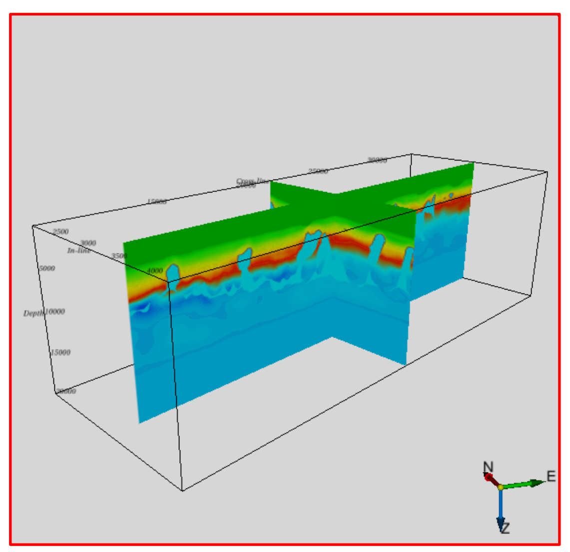

Tangier

2D

Bible

RE2067-100_stack_vel_vol_Time_22-Nov-11_15_57.segy
RE560A-100_stack_vel_vol_Time_22-Nov-11_15_57.segy
RE560-100_stack_vel_vol_Time_22-Nov-11_15_57.segy
RE764-100_stack_vel_vol_Time_22-Nov-11_15_57.segy
RE660-100_stack_vel_vol_Time_22-Nov-11_15_57.segy
RE892-100_stack_vel_vol_Time_22-Nov-11_15_57.segy
RE688-100_stack_vel_vol_Time_22-Nov-11_15_57.segy
RE924-100_stack_vel_vol_Time_22-Nov-11_15_57.segy
RE181A-100_stack_vel_vol_Time_22-Nov-11_15_57.segy
RE844-100_stack_vel_vol_Time_22-Nov-11_15_57.segy
RE584-100_stack_vel_vol_Time_22-Nov-11_15_57.segy
RE2068-100_stack_vel_vol_Time_22-Nov-11_15_57.segy
RE256-100_stack_vel_vol_Time_22-Nov-11_15_57.segy
RE352-100_stack_vel_vol_Time_22-Nov-11_15_57.segy
RE196-109_stack_vel_vol_Time_22-Nov-11_15_57.segy
RE464-100_stack_vel_vol_Time_22-Nov-11_15_57.segy
RE1036-100_stack_vel_vol_Time_22-Nov-11_15_57.segy
RE716-100_stack_vel_vol_Time_22-Nov-11_15_57.segy
RE408-100_stack_vel_vol_Time_22-Nov-11_15_57.segy
RE245-100_stack_vel_vol_Time_22-Nov-11_15_57.segy
RE644-100_stack_vel_vol_Time_22-Nov-11_15_57.segy
RE397-109_stack_vel_vol_Time_22-Nov-11_15_57.segy
RE964-100_stack_vel_vol_Time_22-Nov-11_15_57.segy
RE181-100_stack_vel_vol_Time_22-Nov-11_15_57.segy
RE213-100_stack_vel_vol_Time_22-Nov-11_15_57.segy
RE245A-100_stack_vel_vol_Time_22-Nov-11_15_57.segy
RE181B-100_stack_vel_vol_Time_22-Nov-11_15_57.segy
RE309-100_stack_vel_vol_Time_22-Nov-11_15_57.segy

Nova Span

1100_PSTM_FINAL_VEL_Time_22-Nov-11_15_57.segy
1400A_PSTM_FINAL_VEL_Time_22-Nov-11_15_57.segy
1600_PSTM_FINAL_VEL_Time_22-Nov-11_15_57.segy
1800_PSTM_FINAL_VEL_Time_22-Nov-11_15_57.segy
2000_PSTM_FINAL_VEL_Time_22-Nov-11_15_57.segy
5100_PSTM_FINAL_VEL_Time_22-Nov-11_15_57.segy
5300_PSTM_FINAL_VEL_Time_22-Nov-11_15_57.segy
5400_PSTM_FINAL_VEL_Time_22-Nov-11_15_57.segy
5420_PSTM_FINAL_VEL_Time_22-Nov-11_15_57.segy

Penobscot
(64 ASCII files of velocity traces)

1A_PSTM_vels_ASCII
1B_PSTM_vels_ASCII
2A_PSTM_vels_ASCII
2B_PSTM_vels_ASCII
2C_PSTM_vels_ASCII
3A_PSTM_vels_ASCII
3B_PSTM_vels_ASCII
3C_PSTM_vels_ASCII
4A_PSTM_vels_ASCII
4B_PSTM_vels_ASCII
4C_PSTM_vels_ASCII
5A_PSTM_vels_ASCII
5B_PSTM_vels_ASCII
5C_PSTM_vels_ASCII
6A_PSTM_vels_ASCII
6B_PSTM_vels_ASCII
6C_PSTM_vels_ASCII
7A_PSTM_vels_ASCII
7B_PSTM_vels_ASCII
7C_PSTM_vels_ASCII
8A_PSTM_vels_ASCII
8B_PSTM_vels_ASCII
8C_PSTM_vels_ASCII
9_PSTM_vels_ASCII
10A_PSTM_vels_ASCII
11_PSTM_vels_ASCII
12_PSTM_vels_ASCII
13_PSTM_vels_ASCII
14_PSTM_vels_ASCII
15_PSTM_vels_ASCII
16_PSTM_vels_ASCII
17_PSTM_vels_ASCII
18_PSTM_vels_ASCII
19_PSTM_vels_ASCII
20_PSTM_vels_ASCII
21_PSTM_vels_ASCII
22_PSTM_vels_ASCII
23_PSTM_vels_ASCII
24_PSTM_vels_ASCII
25_PSTM_vels_ASCII
26_PSTM_vels_ASCII
27_PSTM_vels_ASCII
28_PSTM_vels_ASCII
29_PSTM_vels_ASCII
30_PSTM_vels_ASCII
31_PSTM_vels_ASCII
32_PSTM_vels_ASCII
33_PSTM_vels_ASCII
34_PSTM_vels_ASCII
35_PSTM_vels_ASCII
36_PSTM_vels_ASCII
37_PSTM_vels_ASCII
38_PSTM_vels_ASCII
39_PSTM_vels_ASCII
40_PSTM_vels_ASCII
41_PSTM_vels_ASCII
42_PSTM_vels_ASCII
43_PSTM_vels_ASCII
44_PSTM_vels_ASCII
45_PSTM_vels_ASCII
46_PSTM_vels_ASCII
47_PSTM_vels_ASCII
48_PSTM_vels_ASCII
49_PSTM_vels_ASCII

Jebco Georges Bank

JGM96_intvel.segy
JGM98A_intvel.segy
JGM98B_intvel.segy
JGM100_intvel.segy
JGM102_intvel.segy
JGM104A_intvel.segy
JGM104B_intvel.segy
JGM106A_intvel.segy
JGM106B_intvel.segy
JGM106C_intvel.segy
JGM108_intvel.segy
JGM110_intvel.segy
JGM110A_intvel.segy
JGM112_intvel.segy
JGM114_intvel.segy
JGM114A_intvel.segy
JGM116_intvel.segy
JGM118_intvel.segy
JGM128F_intvel.segy
JGM128FA_intvel.segy
JGM132_intvel.segy
JGM132A_intvel.segy
JGM134_intvel.segy
JGM136F_intvel.segy
JGM208_intvel.segy
JGM208A_intvel.segy
JGM208F_intvel.segy
JGM209_intvel.segy
JGM210_intvel.segy
JGM211_intvel.segy
JGM212_intvel.segy
JGM213_intvel.segy
JGM214A_intvel.segy
JGM214B_intvel.segy
JGM214C_intvel.segy
JGM215_intvel.segy
JGM215E_intvel.segy
JGM216A_intvel.segy
JGM216B_intvel.segy
JGM216C_intvel.segy
JGM217A_intvel.segy
JGM217B_intvel.segy
JGM218_intvel.segy
JGM218A_intvel.segy
JGM218F_intvel.segy
JGM219_intvel.segy
JGM219F_intvel.segy
JGM220_intvel.segy
JGM220F_intvel.segy
JGM221A_intvel.segy
JGM221B_intvel.segy
JGM221C_intvel.segy
JGM221D_intvel.segy
JGM221E_intvel.segy
JGM222_intvel.segy
JGM222A_intvel.segy
JGM222F_intvel.segy
JGM223A_intvel.segy
JGM223B_intvel.segy
JGM223F_intvel.segy
JGM224_intvel.segy
JGM224E_intvel.segy
JGM224F_intvel.segy
JGM225_intvel.segy
JGM225F_intvel.segy
JGM226A_intvel.segy
JGM226B_intvel.segy
JGM226F_intvel.segy
JGM227_intvel.segy
JGM227E_intvel.segy
JGM227F_intvel.segy
JGM228_intvel.segy
JGM229_intvel.segy
JGM230A_intvel.segy
JGM230B_intvel.segy
JGM231_intvel.segy
JGM231F_intvel.segy
JGM232A_intvel.segy
JGM232B_intvel.segy
JGM232F_intvel.segy
JGM233A_intvel.segy
JGM233B_intvel.segy
JGM233E_intvel.segy
JGM233F_intvel.segy
JGM234A_intvel.segy
JGM234B_intvel.segy
JGM235_intvel.segy
JGM235A_intvel.segy
JGM235F_intvel.segy
JGM236A_intvel.segy
JGM236B_intvel.segy
JGM237A_intvel.segy
JGM237B_intvel.segy
JGM238A_intvel.segy
JGM238B_intvel.segy
JGM239A_intvel.segy
JGM239B_intvel.segy
JGM239C_intvel.segy
JGM240_intvel.segy
JGM241A_intvel.segy
JGM241B_intvel.segy
JGM242_intvel.segy
JGM243A_intvel.segy
JGM243B_intvel.segy
JGM244A_intvel.segy
JGM244B_intvel.segy
JGM245A_intvel.segy
JGM245B_intvel.segy

Jebco East

JEBCO_2013_Depth_Mig_Velocity_Interval_J05_05.SGY
JEBCO_2013_Depth_Mig_Velocity_Interval_J08_08.SGY
JEBCO_2013_Depth_Mig_Velocity_Interval_J09_09.SGY
JEBCO_2013_Depth_Mig_Velocity_Interval_J11_11.SGY
JEBCO_2013_Depth_Mig_Velocity_Interval_J13_13.SGY

Sable Island

Sable_Island_2013_Depth_Mig_Velocity_Interval_L187.SGY
Sable_Island_2013_Depth_Mig_Velocity_Interval_L369.SGY
Sable_Island_2013_Depth_Mig_Velocity_Interval_L405.SGY
Sable_Island_2013_Depth_Mig_Velocity_Interval_L613.SGY

Seismic velocity data

The [processing] seismic velocities are provided trough many kinds of data:

- files: Seg-Y (by default) and some ASCII files
- type: RMS velocities (V_{RMS}) or Interval velocities (V_{int})
- dimension: TWT (green contours here above) or Zss (red contours)

Different processing steps are necessary to recompute them into a single data format: 3D V_{int} pointsets (i.e. [X,Y,T,V_{int}] points)

Seismic velocities

Database Construction for Velocity Modeling

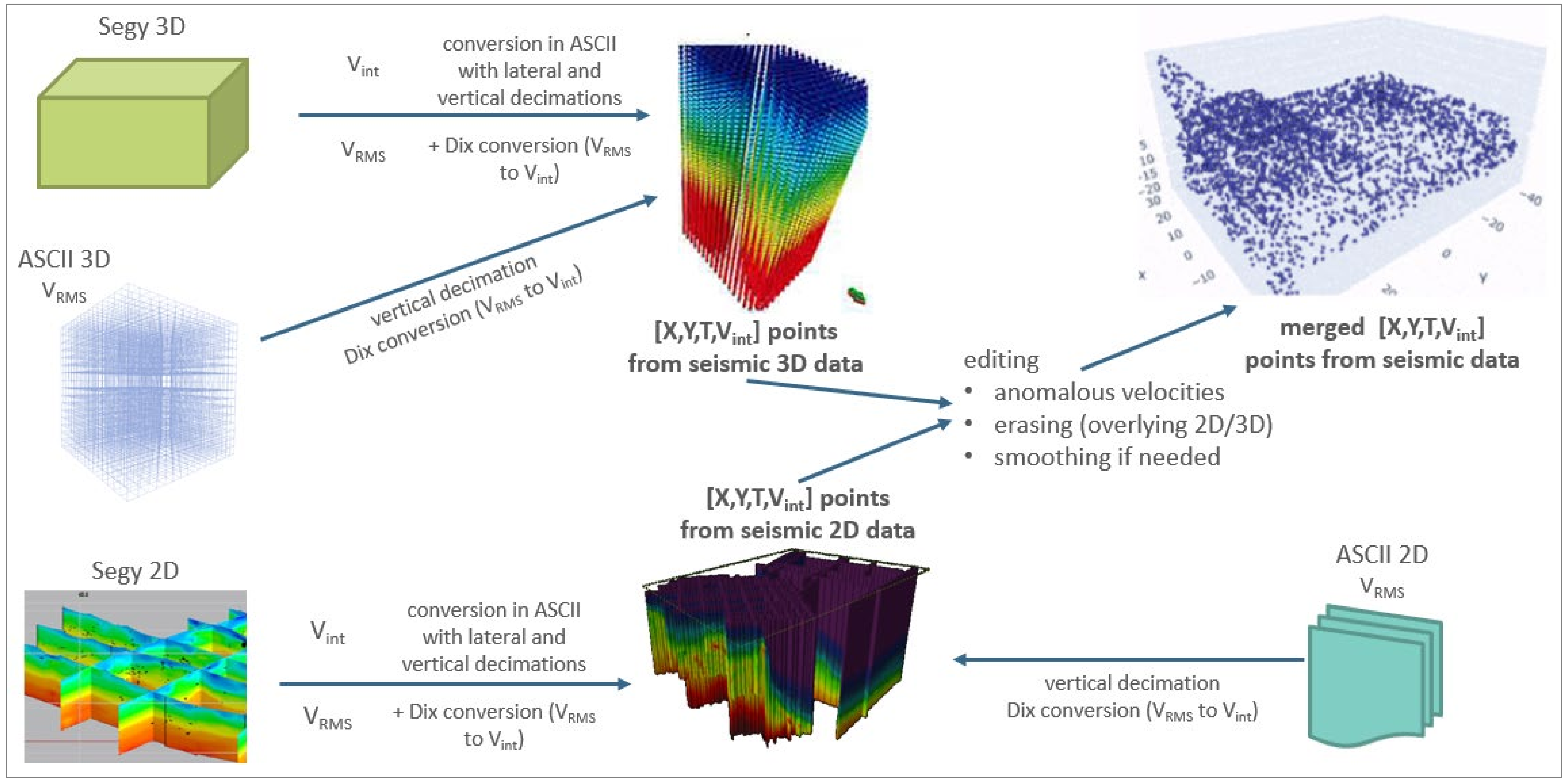

Phase 1: Creation of a merged set of [X,Y,T,V_{int}] points from raw seismic velocities

All the different sets of data were individually transformed into interval velocities via various programming scripts (run in *Matlab*^{TM}):

- via Dix conversions if quadratic velocities (RMS)
- directly taken as V_{int} when they were available; when both quadratic and interval velocities were available, the former ones were favored (indeed the corresponding interval velocities presented either a blocky shape – see PL. 1.7 with Jebco Georges Bank example – or a "quantum effect", i.e. when Dix conversion was applied on the Segy format without upscaling these quadratic velocities that were oversampled, resulting a very limited range of interval velocities)

The editing of anomalous velocities was done in a first step before the merging: removing obviously wrong velocities, cropping, smoothing, upscaling them to regular 100-ms intervals (see PL. 1.6 and -.7). Actually, supplementary stages of editing were deemed necessary and applied before the final version of the seismic velocities interpolation (see PL. 2.5 to -.7)

Concerning the seismic velocities available in depth instead of TWT, scripts were also created to make them convert from Zss to TWT by their own values (once differentiated, a velocity may also be seen as TZ law).

Phase 2: 3D interpolation of seismic velocities through a stratigraphic model

A stratigraphic model is built using all the horizons (main ones and salt) after editing them (adjustment to remove the crossing zones, smoothing, recreation of separated diapir/canopy structures), deep enough to handle all the seismic data.

Different zones of layering are set between the edited horizons: regular layering in the sedimentary/reservoir zones, constant layer/velocity in the salt and water, broad layering in the basement unknown velocity zone.

A global interpolation of the seismic velocities is then performed along the stratigraphy to get a complete 3D seismic velocity regional cube.

Phase 3: Co-kriging of the calibrated well velocities with the seismic velocity cube

Once calibrated to the horizons, markers and in accordance with the checkshot times, the well velocities can be co-kriged in the same stratigraphic model, using as secondary variable the 3D seismic velocity regional cube.

Such co-kriging preserves the calibrated TZ laws, consequently further residual correction would not be necessary (the residuals are corrected/estimated previously to the co-kriging).

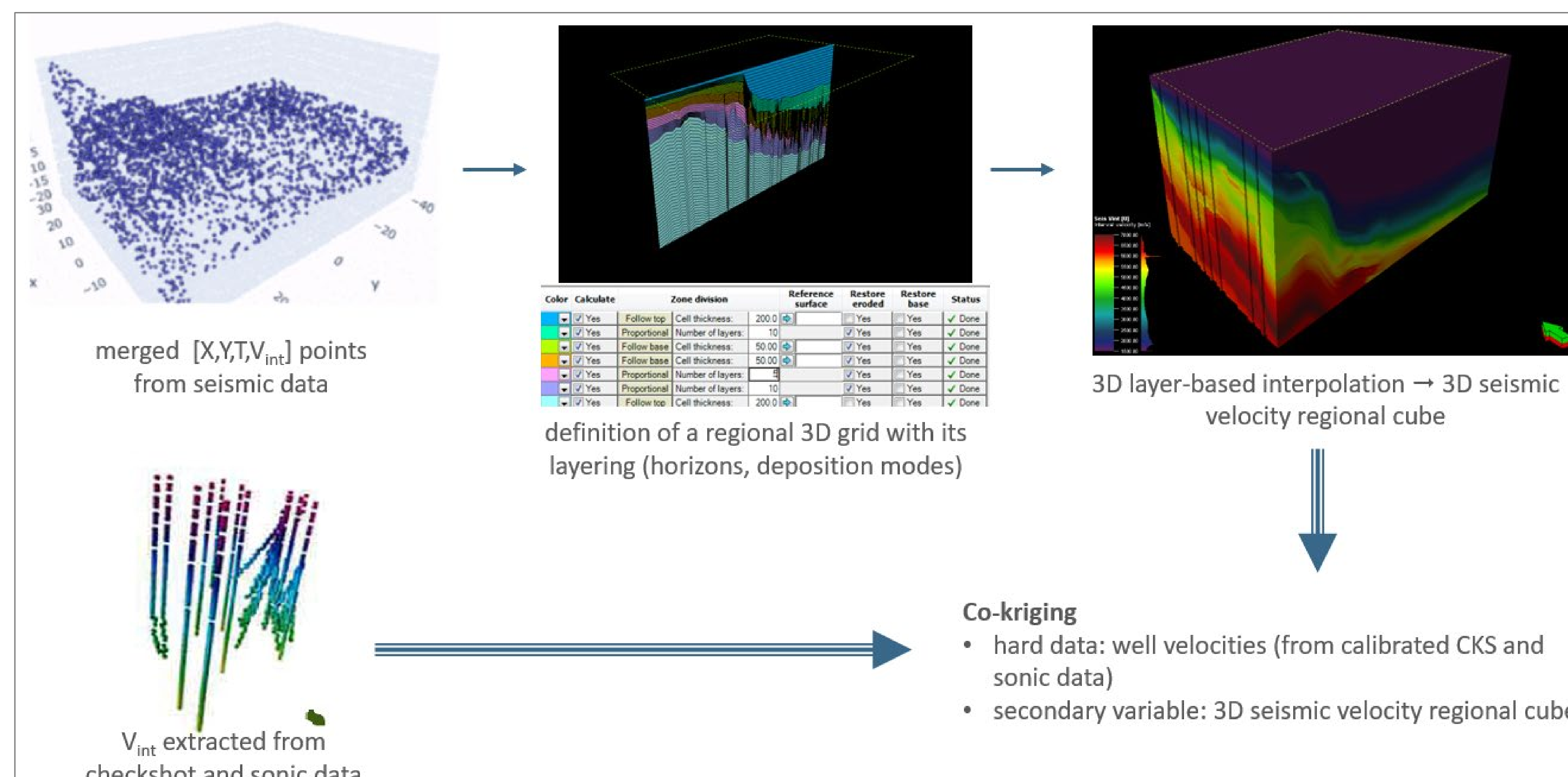

Barrington

Penobscot

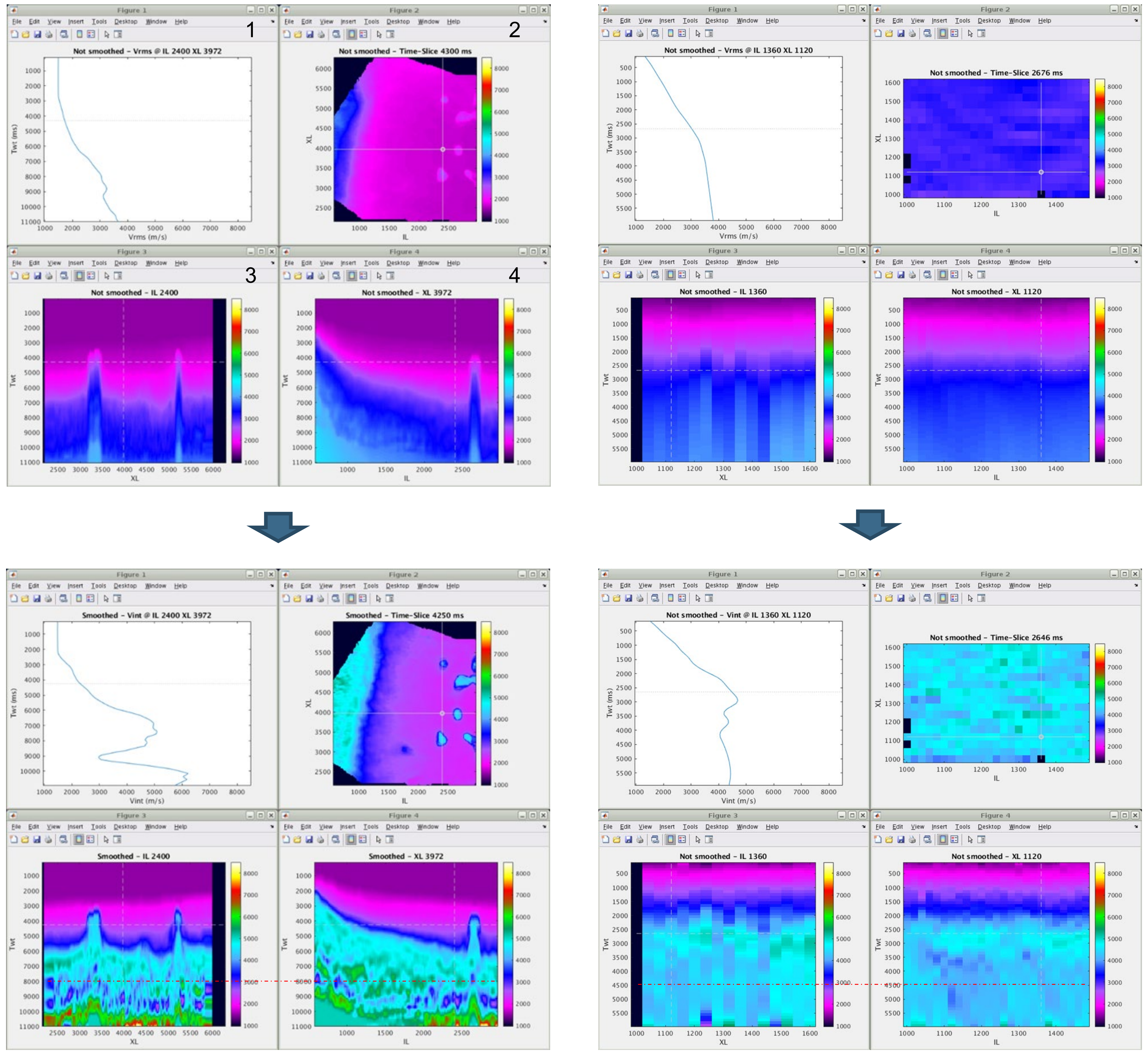

Conversion from V_{RMS} (above) to V_{int} (below) with vertical smoothing and time clipping (red line) (1- trace, 2- timeslice, 3- IL section, 4- XL section)

Different cases

The four 3D sets of seismic velocities were processed through *Matlab*[TM] scripts especially dedicated/written to handle them.

Shelburne

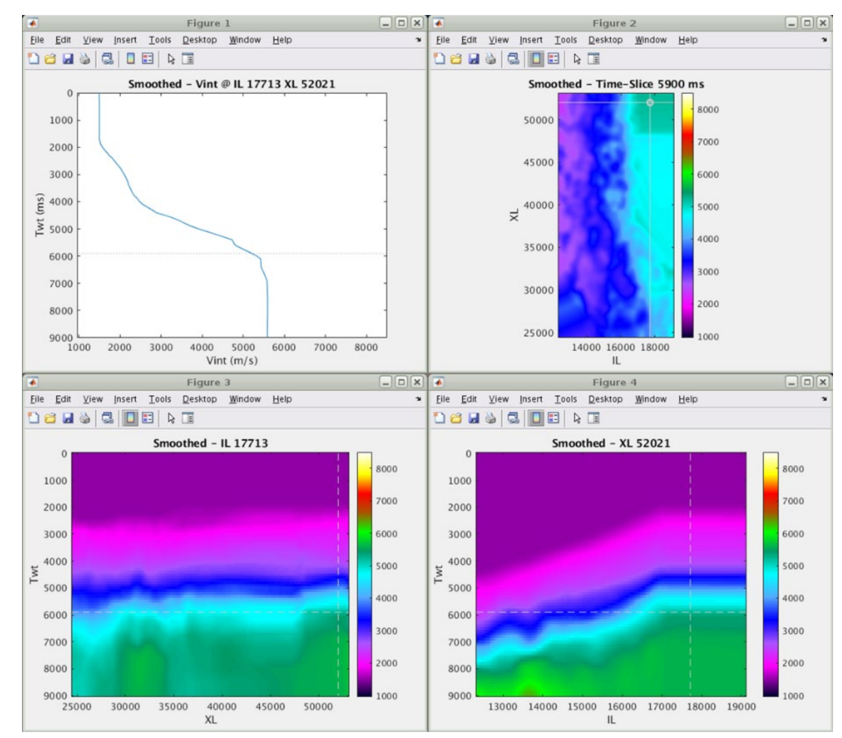

Extraction of V_{int} with vertical smoothing and no time clipping

Tangier

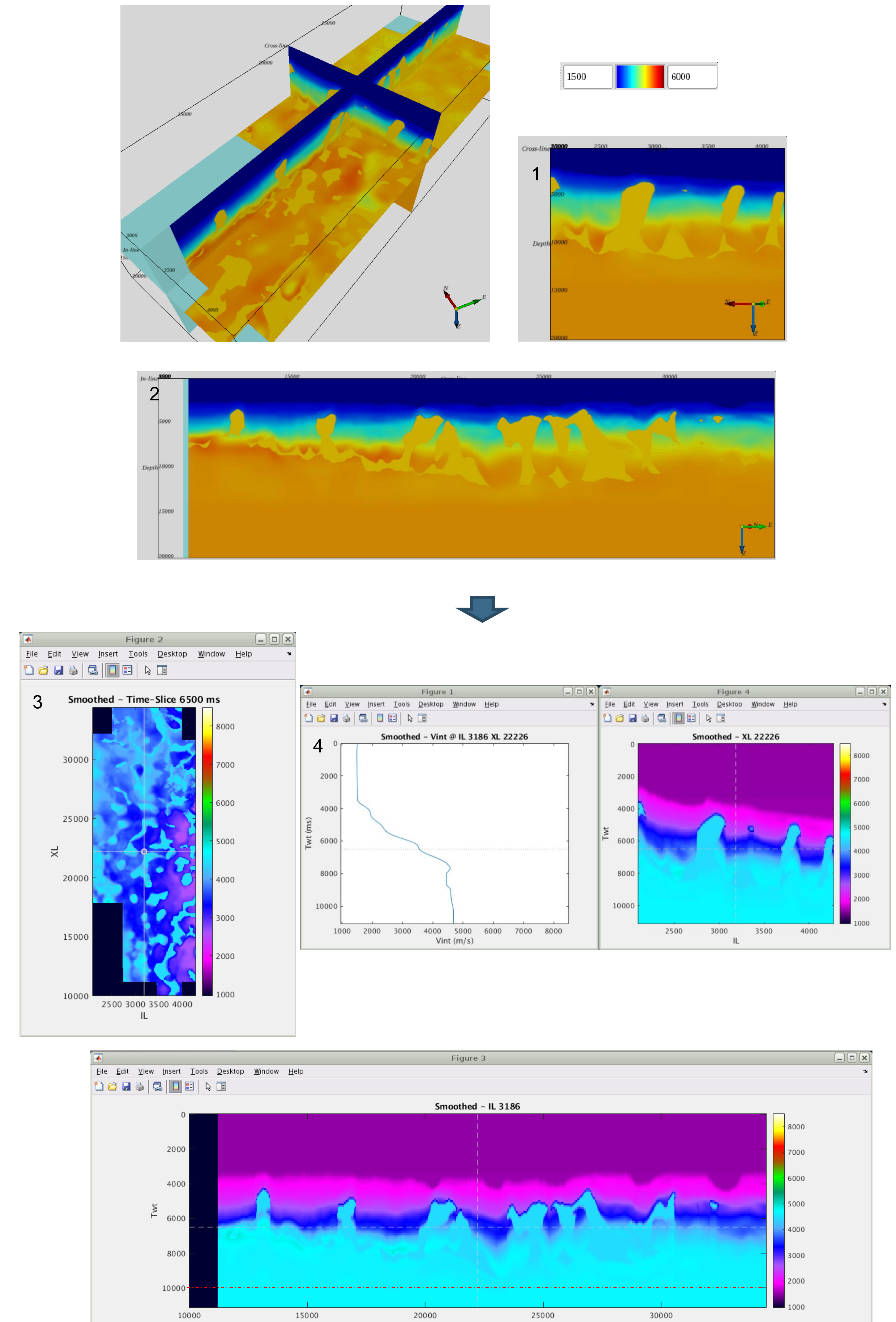

Conversion from Zss (above) to TWT (below) of original V_{int} with slight vertical smoothing and time clipping (red line) (1- XL, 2- IL, 3- timeslice, 4- trace)

3D workflow

The scripts enabled to visualize trough random sections the degree of the “original smoothing” after an upscaling to 100-ms samples and a lateral decimation of 200 m.

The irregular/odd variations of velocities in the deep layers, deemed as not natural, or totally constant ending parts (in Tangier) were clipped along a constant time line (displayed in red).

Database Construction for Velocity Modeling

Bible

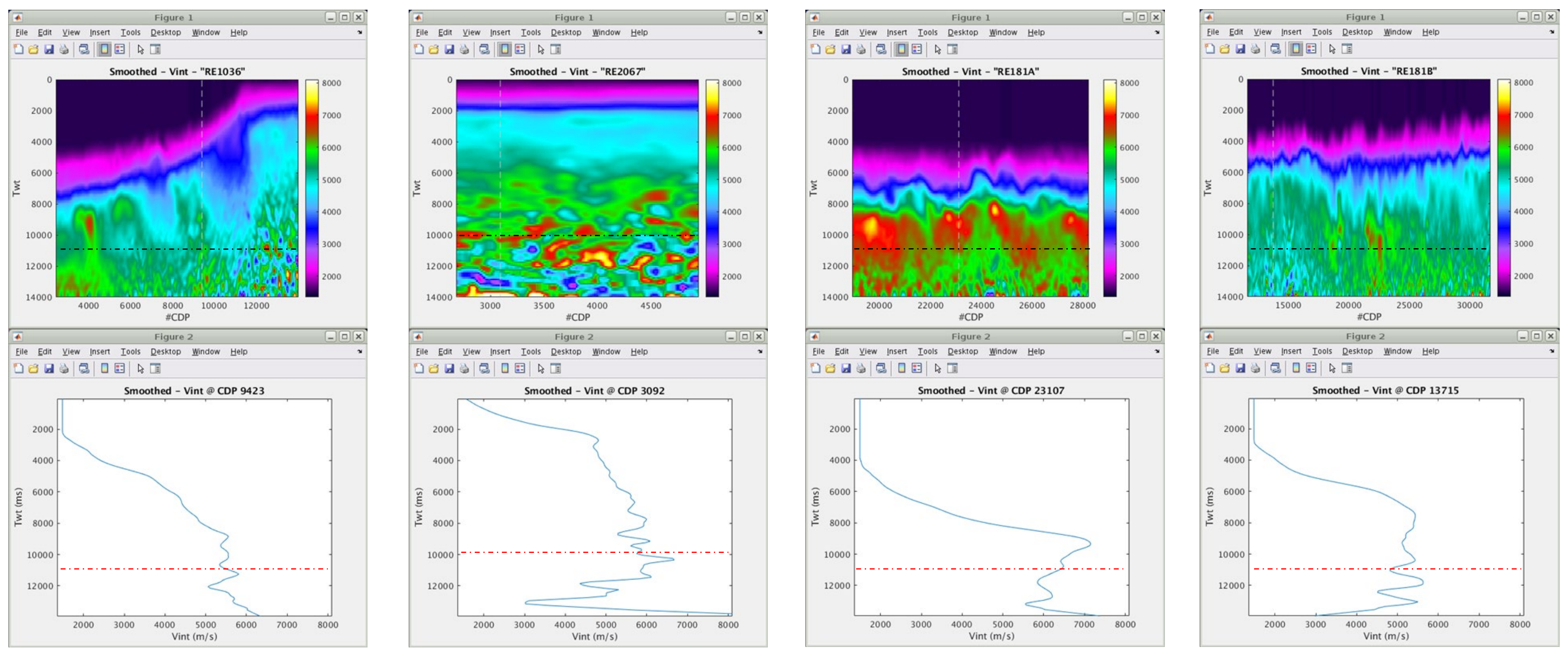

Nova Span

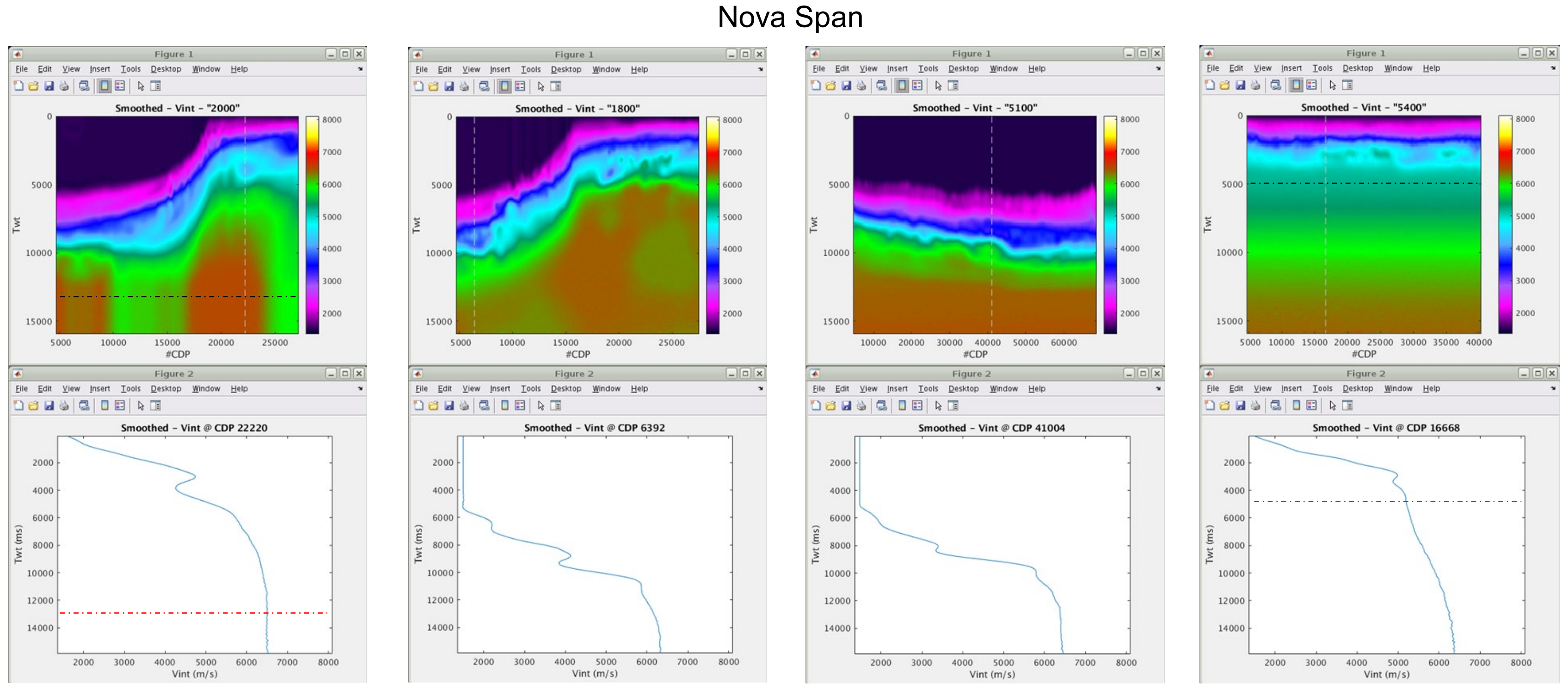

Examples of lines converted from V_{RMS} to V_{int} with vertical smoothing and time clipping

2D workflow

The same kind of scripts as for 3D were used for the 2D lines: conversion from V_{RMS} into V_{int} if not already available, vertical smoothing and time clipping if needed. The lateral decimation is the same taken as for 3D (200 m).

Sections enable to visually check the relative quality of each set, to perform the necessary edition.

In some sets, different versions of data were available (type of processing velocities); the best one was always selected.

Two surveys have velocities in Zss, (see here below) and were firstly converted into TWT through their own velocities values before smoothing and clipping.

NB: the Sable Island lines UTM zone – written in the Seg-Y headers – were corrected into the good one (from UTM 21N to 20N).

Jebco Georges Bank

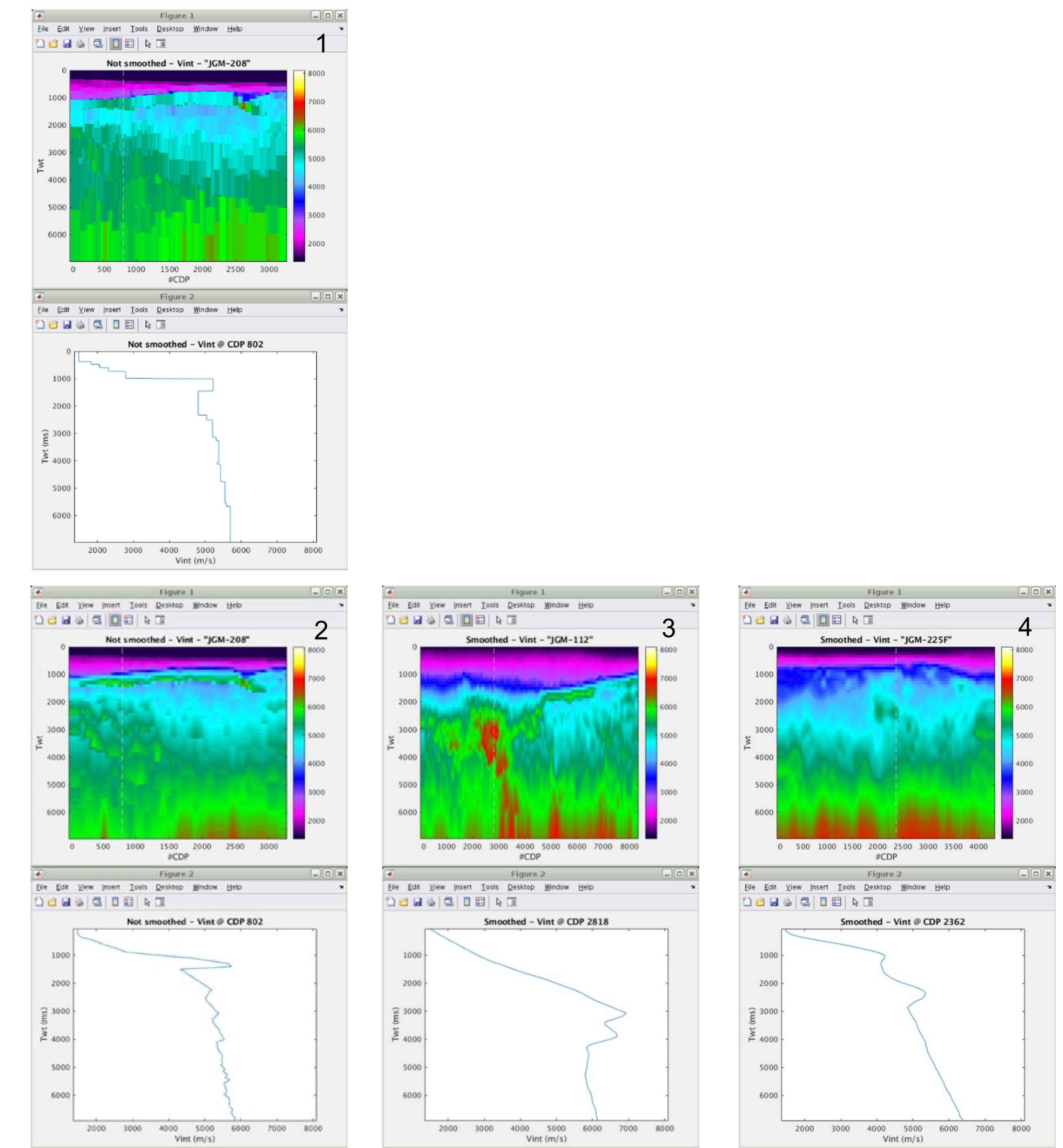

Selection of one velocity version (V_{RMS} converted to V_{int} – 2) instead of another version (already in Vint – 1) that presented blocky samples (not usable)
Vertical smoothing and no time clipping of the selected version (2 to 4)

Penobscot

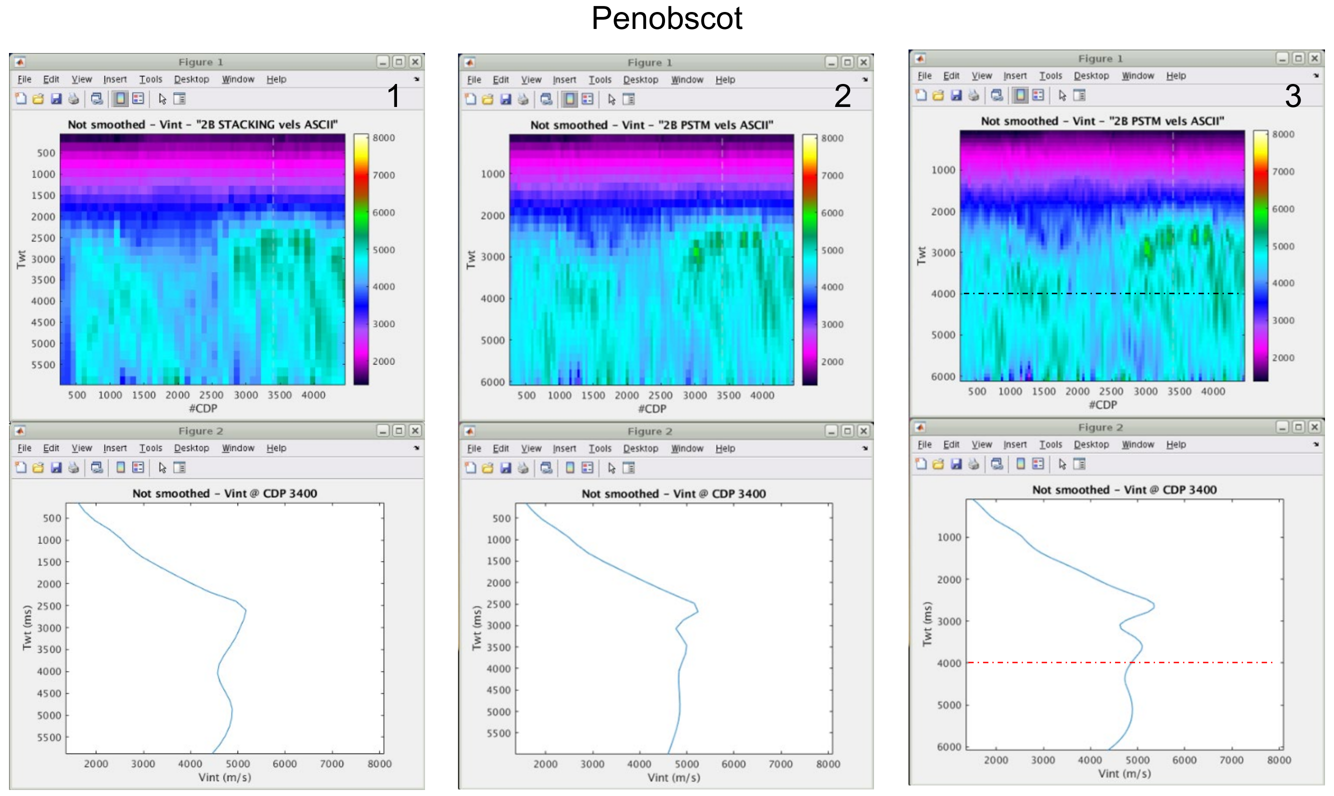

Selection of one velocity version (PSTM – 2) instead of another (STACKING – 1)
Vertical smoothing and time clipping of the selected version (3)

Sable Island

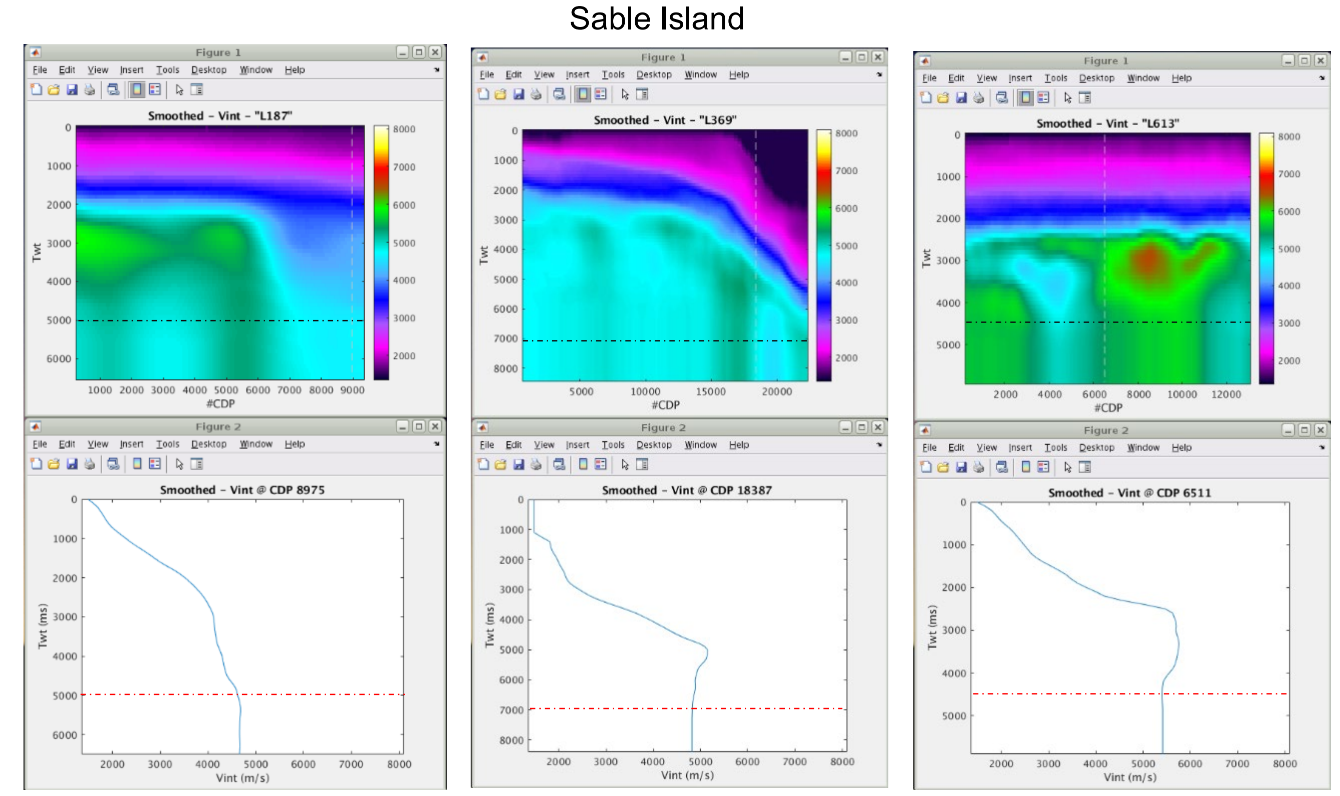

Jebco East

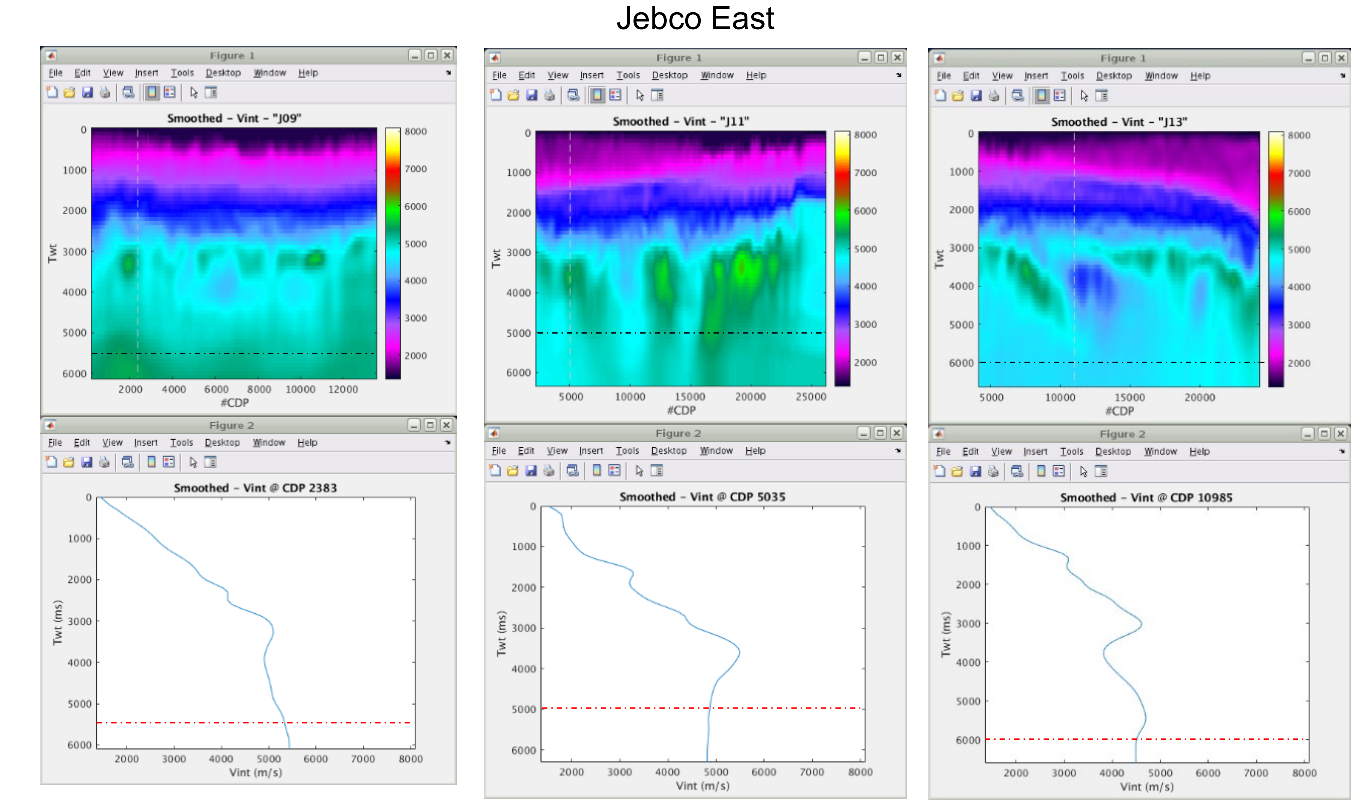

Examples of V_{int} lines converted from Zss to TWT with vertical smoothing and time clipping

Preparing seismic velocity – 2D

Overall strategy of editing

1. Make consistent the 5 main horizons
2. Work on the salt the 3 salt packs (western diapirs, “Sable” central canopies, “Banquereau” eastern diapirs) to recreate, isolate and sort all the 10 horizons in a suitable order (with no internal crossing)

Objectives/ Preliminary constraints

- Full-gridding for all the available horizons in the whole AOI
- No crossing between any horizon → create a sequential layering by adjusting them in space (filling via gridding) and vertically (cropping if crossing: J145 lowered to T50, then J163 lowered to J145, then Top Basement lowered to J163)
- Simulating the salt diapirs piercing the overlying horizons → horizons wrapping the diapirs

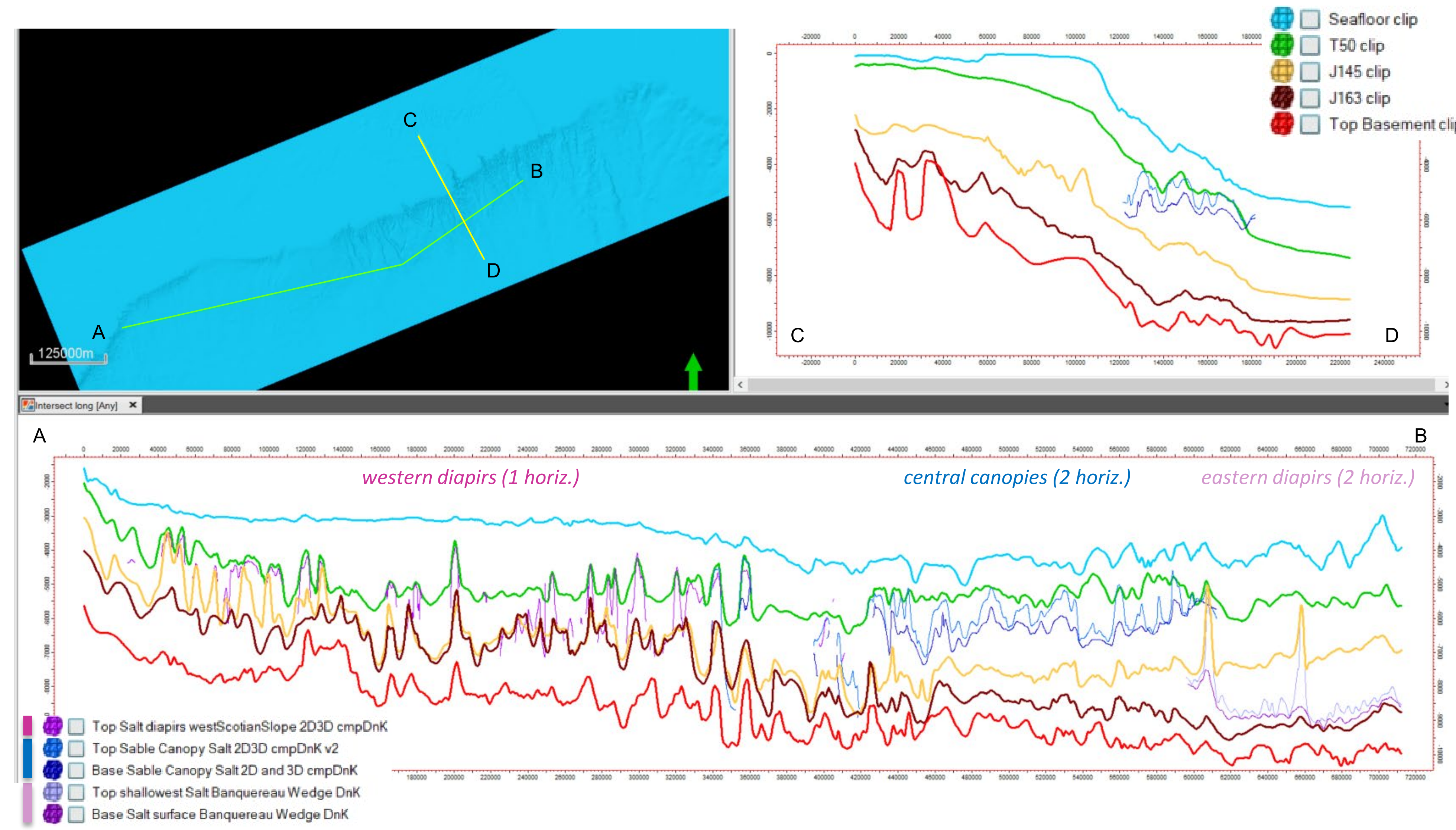

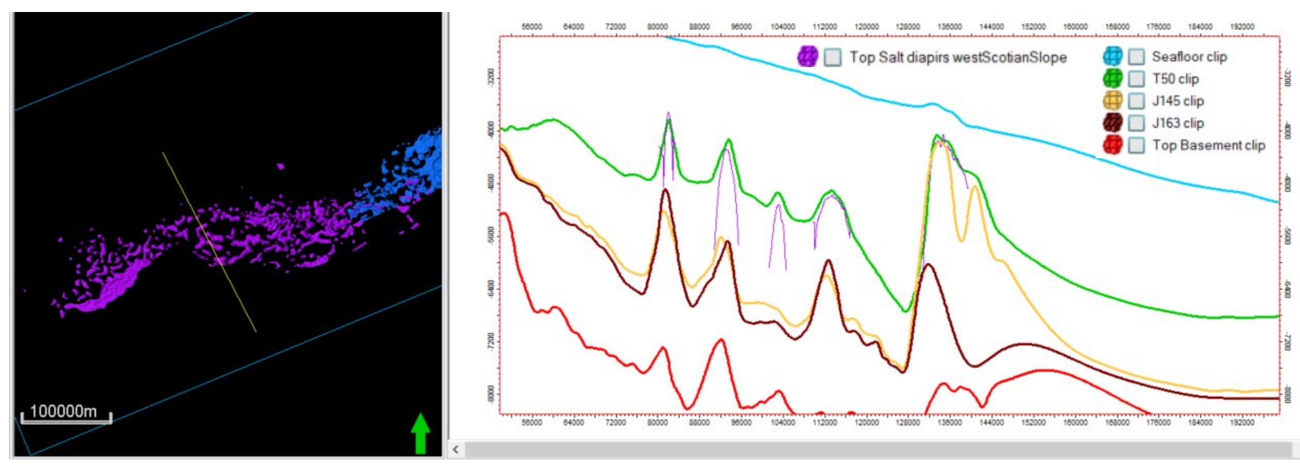

General rules

1. Slight smoothing the salt horizons
2. Top salt clipped with T50
3. Its edges merged with J163 (verticalization of the flanks)

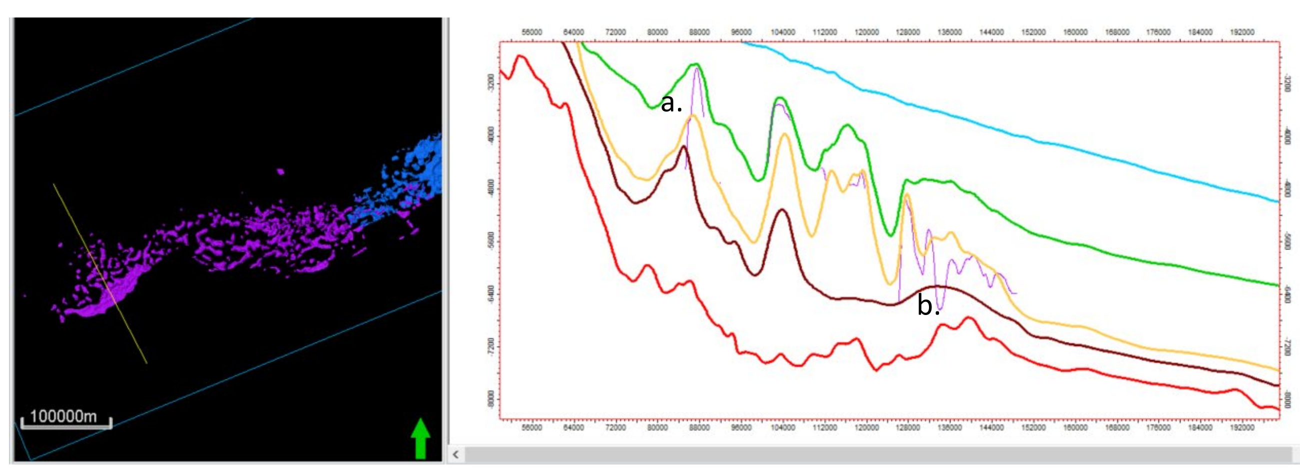

Specific rules for western diapirs

a. J145 will be pierced by top diapir (i.e. top J145 set at top diapir)

b. Top diapir stopped at J163

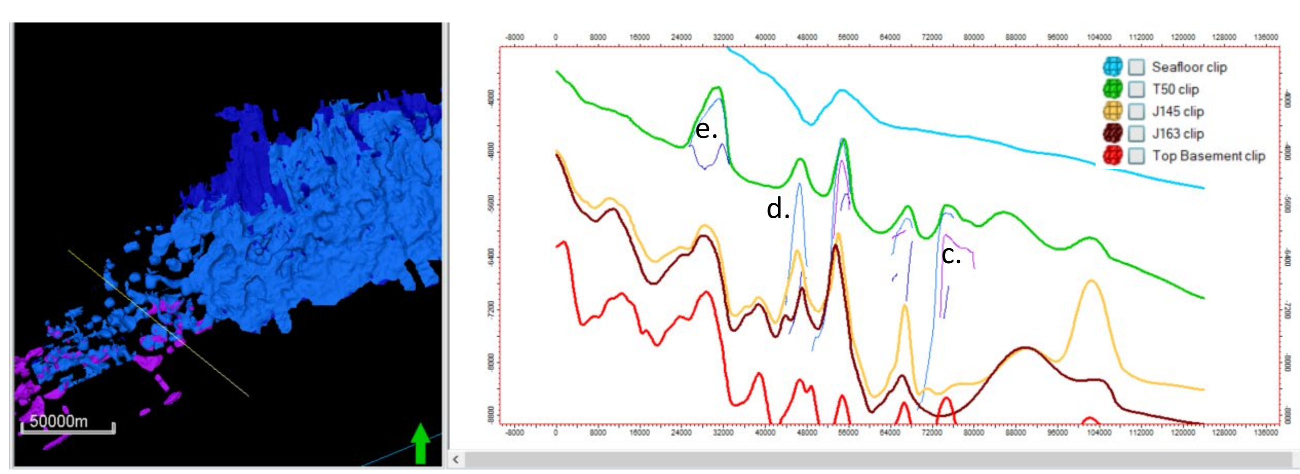

Specific rules for diapir area

c. When both exist, top diapir pierced by top canopy (i.e. top diapir extended shallower) ;

d. Within diapir area, top canopy set as top diapir (merged to it, same rules)

e. In the canopy area, see below

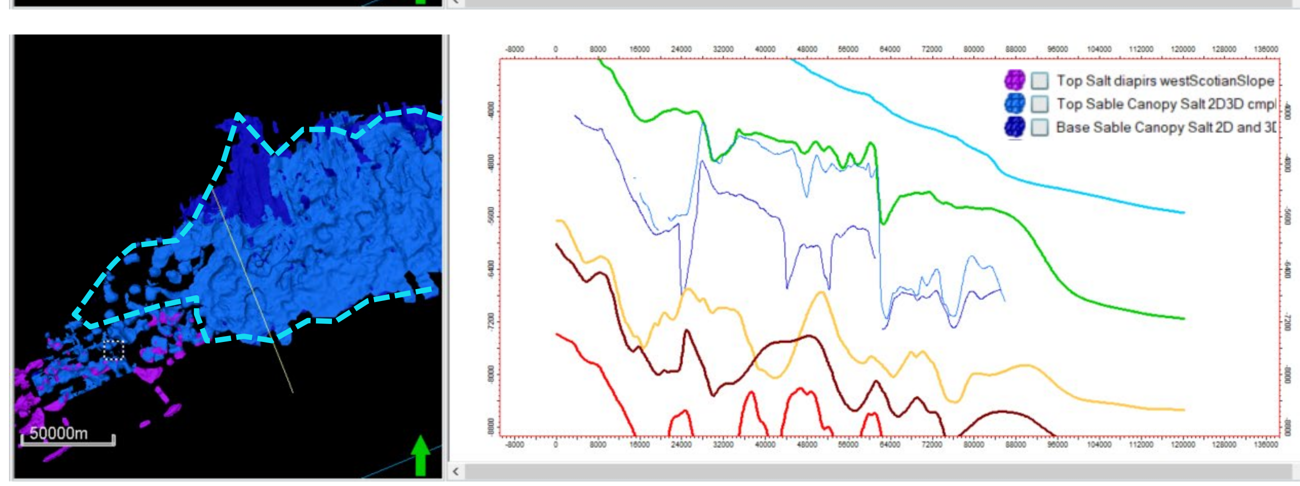

Specific rules for canopy

1. Define a boundary where the isolated canopy will exist → extend top and base canopy to it (gridding)
2. Consider the canopy as in internal layer between T50 and J163 → thickness set to 0+ out of the boundary

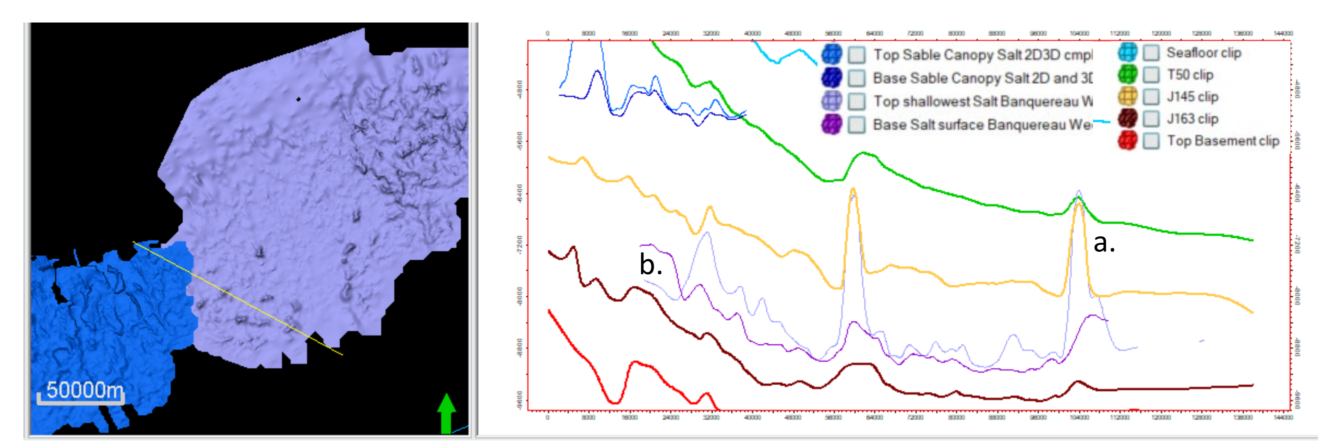

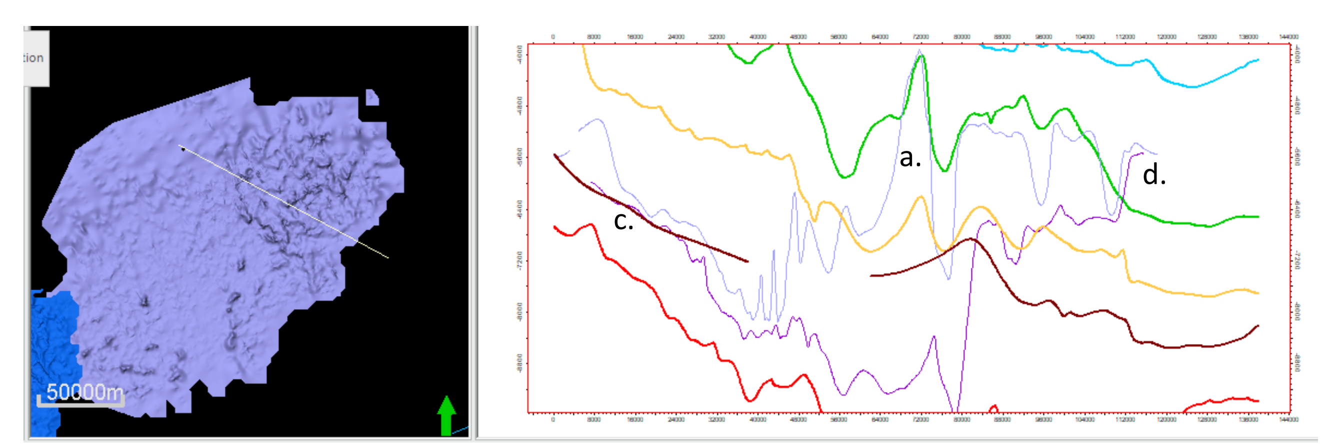

Specific rules for eastern diapirs

Same as for central Canopy (common limits for top and base; considered as new internal layer between J145 and J163):

a. J145 will be pierced by top Banquereau salt diapir (i.e. top J145 set at top diapir)

b. Base clipped by the Top

c. Top and Base salt stopped at J163

d. Top and Base clipped by T50

Whole AOI

The 5 main horizons were gridded and adjusted as previously mentioned (cropping strategy: "the shallower, the more confident", i.e. the 5 horizons are cropped from base to top of the 3D grid). To insert the next salt horizons without any crossing, a space of 5 ms was left between each main horizon (see Figure 1).

SB
(5)
T50
(5)
J145
(5)
J163
(5)
Top Bsmt

Figure 1: Sequential horizon order – first pass

Banquereau (eastern area)

After gridding and adjusting the 5 main horizons, two editing phases were run in Banquereau diapir area:

- J145 was set above top and base Banquereau diapir (J145 wrapping the top)
- Base Sable canopy was set above top Banquereau diapir (NB: there is no intersection between top Sable canopy and Banquereau salt horizons)

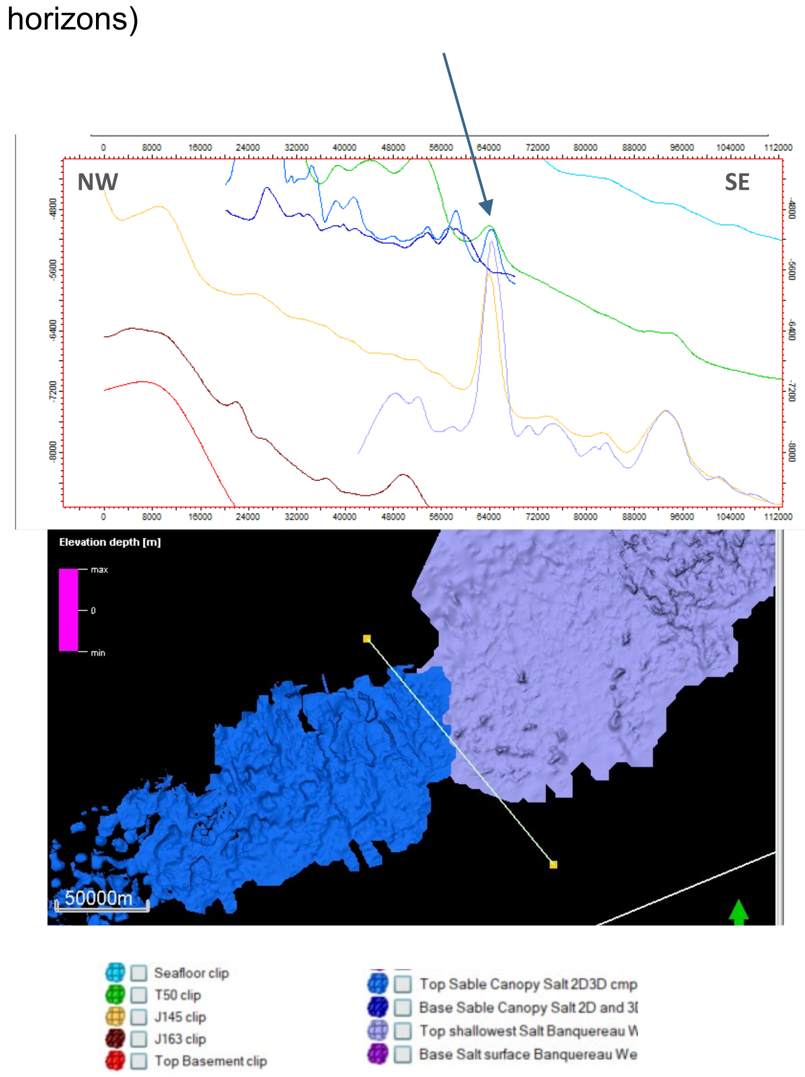

T50
(3)
Top Canopy
(1)
Base Canopy
(1)
J145
(3)
Top Diapir Banqr
(1)
Base Diapir Banqr
(1)
J163

Figure 2: Sequential horizon order – second pass

A second stratigraphic order is consequently defined (Figure 2 – NB: between parenthesis = minimal space in ms TWT between subsequent horizons to prevent any crossing)

Central canopy

The Sable canopy system can be divided into three subgroups (Figure 3):

A. Upper Canopy: a continuous canopy zone defined by top and base salt horizon and located in the [T50; J145] interval

B. Lower Canopy: the extension of Upper Canopy in the [J145; J163] interval

C. Isolated parts of Upper Canopy, equivalent of diapir structures as defined by the eastern Shelburne diapirs

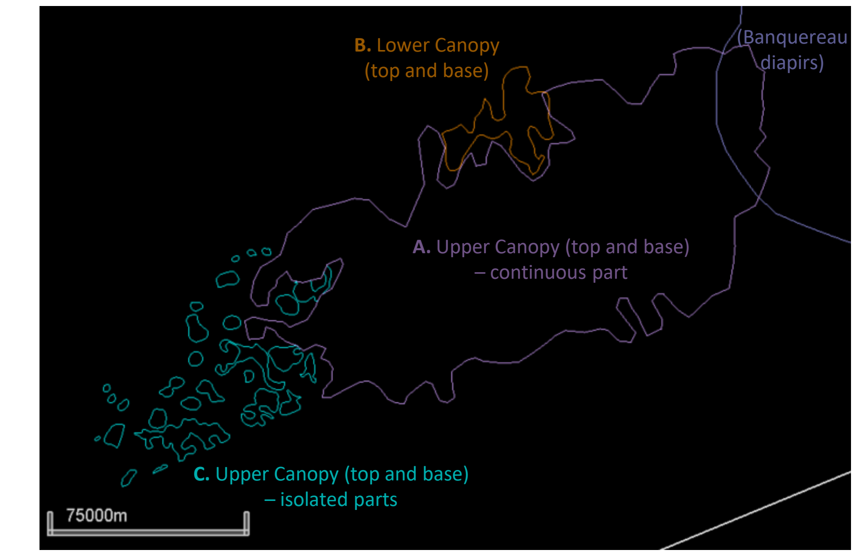

Figure 3: Sable canopy system defined by 3 subgroups

Time thickness maps of top/base canopy vs. J145 enable to draw the polygons that will cut the continuous canopy into its 2 Upper and Lower continuous levels (Figure 4):

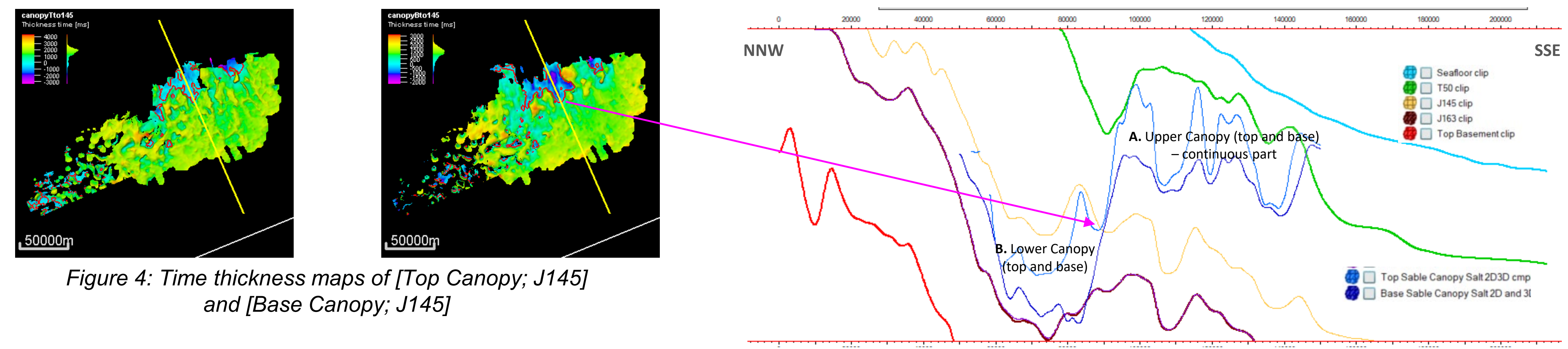

Figure 4: Time thickness maps of [Top Canopy; J145] and [Base Canopy; J145]

In the central continuous part, small parts of the canopy are located below J145 (see blue zones delimiting by red contours in Figure 5): they are negligible and will be clipped.

In the western part of the Sable canopy complex, the isolated salt parts are mostly present above J163. The very deep parts of the canopy that are defined below J163 will be clipped (Figure 6); and as J145 is very close to J163 in this area (see same Figure), the isolated parts will be thus clipped to be preserved above the yellow J145 horizon.

NB: in the westernmost part of Sable salt horizons, the remaining parts of top Canopy will be merged with Shelburne diapirs (see PL. 1.10).

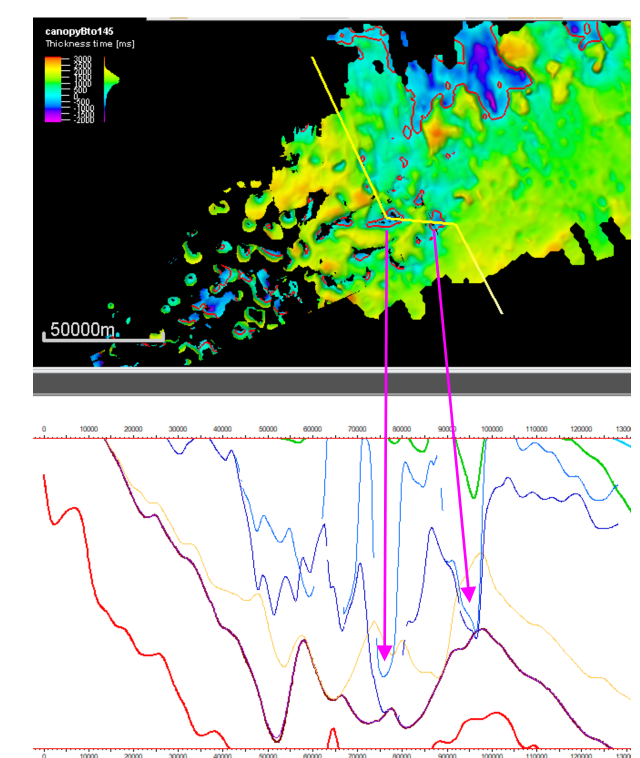

Figure 5: Transect across the continuous part

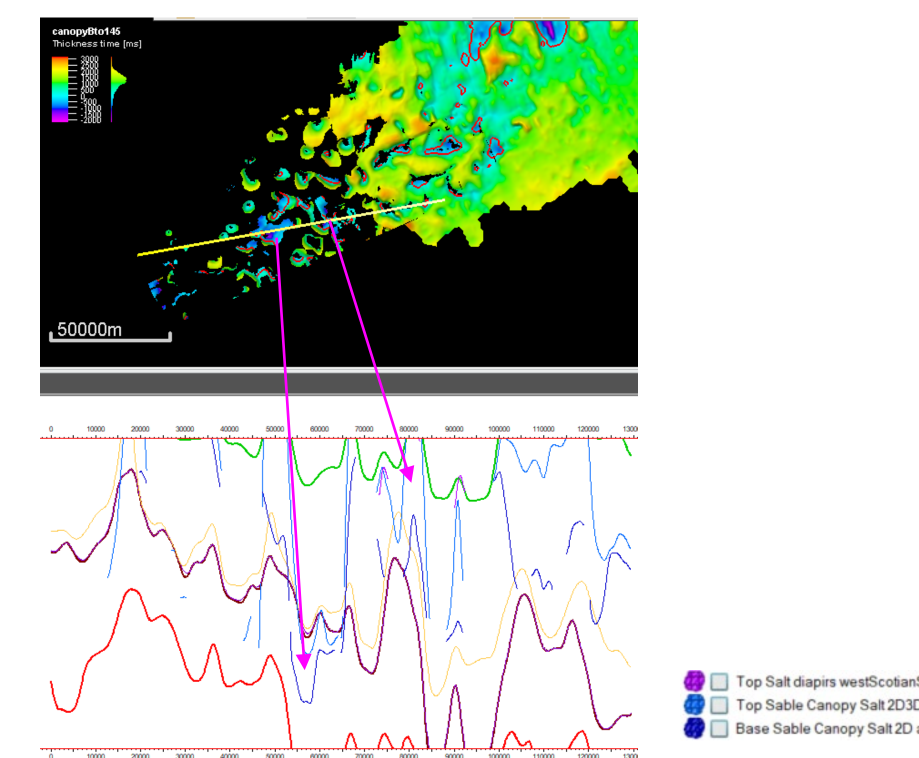

Figure 6: Transect across the isolated parts

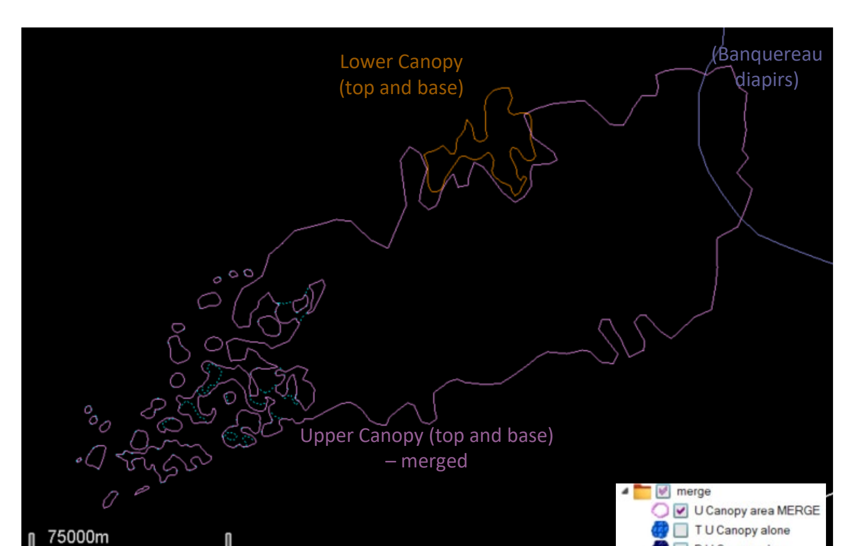

Figure 7: Sable canopy system defined by 3 subgroups

A second pass of editing enables to merge some near isolated parts to the main continuous canopy (cf. Figure 7 with Figure 6). These merging polygons were extended/checked in accordance with the western Shelburne diapirs that were joined to the canopy in these common areas.

Lastly, to simplify the number of horizons, the Lower Canopy top and base were merged with Banquereau salt horizon (both sets located in the same interval and never overlaid by each other). It generates the sequential order as displayed in Figure 8.

T50
(3)
Top Upper Canopy
(1)
Base Upper Canopy
(1)
J145
(3)
Top Diapir Banqr / Top Lower Canopy
(1)
Base Diapir Banqr / Base Lower Canopy
(1)
J163

Figure 8: Sequential horizon order – third pass

Western (Shelburne) diapirs

Sequential editing phases were run between the remaining western zones of top Upper Canopy and top western/Shelburne Diapir:

1. Top western Diapir is pierced by the residual top Canopy, i.e. the next merging will keep the most upper salt
2. Remaining top Canopy merged with top western Diapir, giving a "top Diapir". Figure 1 shows the where the merging in done – the small dark red polygons show the internal excluding areas where the salt does not exist within a salt ring.
3. J145 pierced by top Diapir (wrapping it)

Once merged top Diapir is defined, its base is set as J163. A new sequential order is then defined (Figure 2).

Two sections here below illustrate the final horizon reconstruction (NB: the salt horizons are displayed without their lateral extension up to AOI borders).

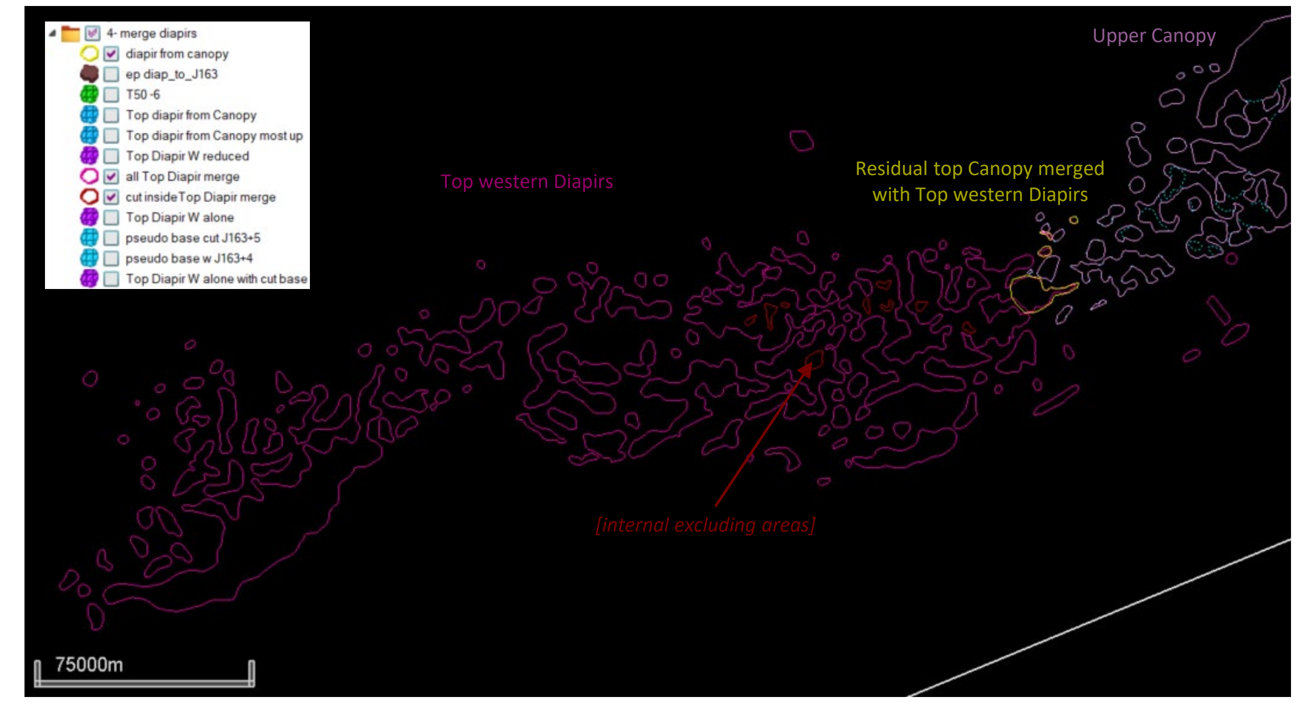

Figure 1: Merging area in the diapir complex

T50
(3)
Top Upper Canopy
(1)
Base Upper Canopy
(1)
J145
(1)
Top Diapir (merge)
(2)
Top Diapir Banqr / Top Lower Canopy
(1)
Base Diapir Banqr / Base Lower Canopy
(1)
J163

Figure 2: Sequential horizon order – forth pass

SB
T50
Top Upper Canopy
Base Upper Canopy
J145
Top Diapir
Top Diapir Banqr / Top Lower Canopy
Base Diapir Banqr / Base Lower Canopy
J163
Top Bsmt

Final sequential horizon order

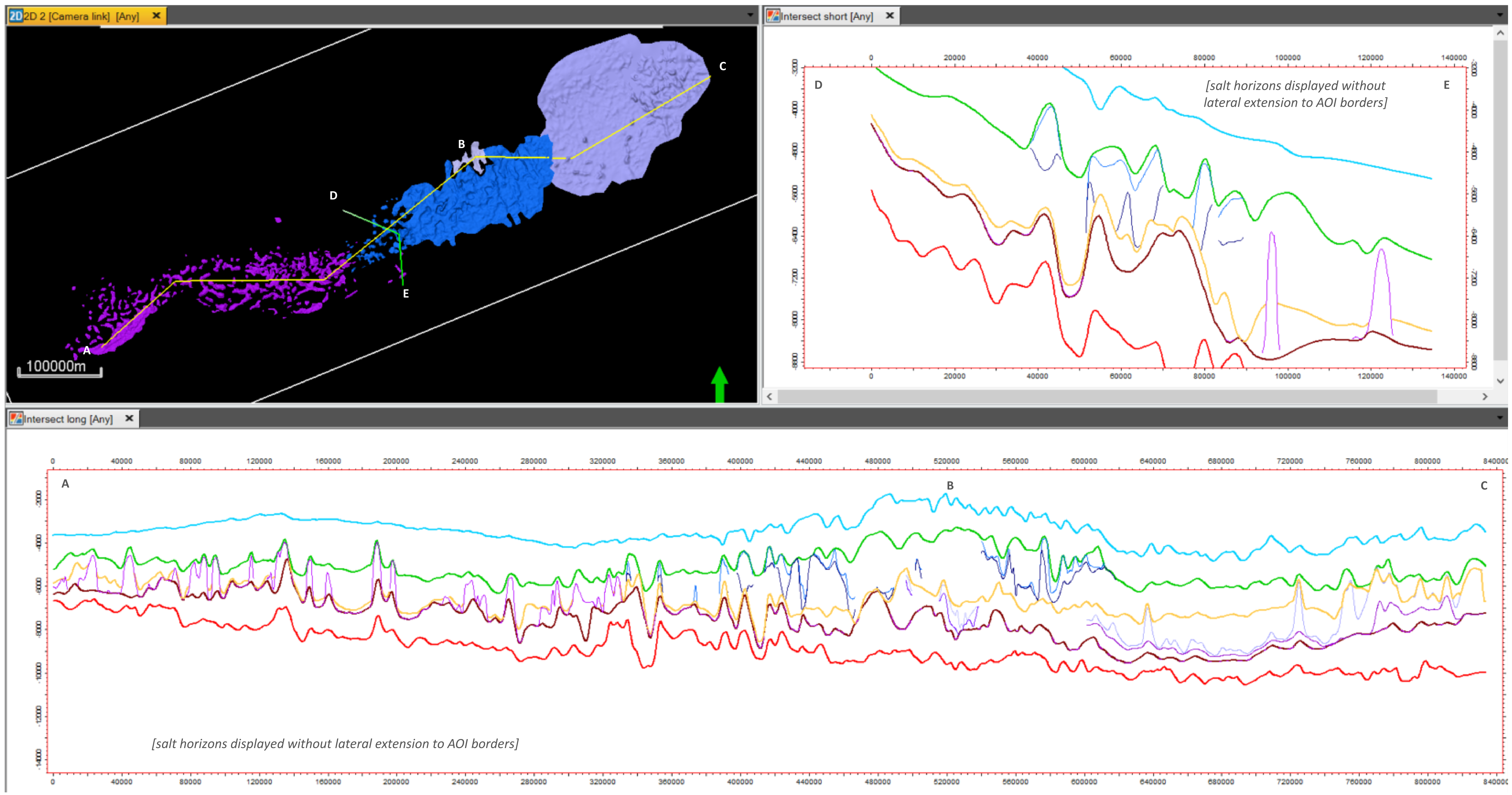

Final horizons

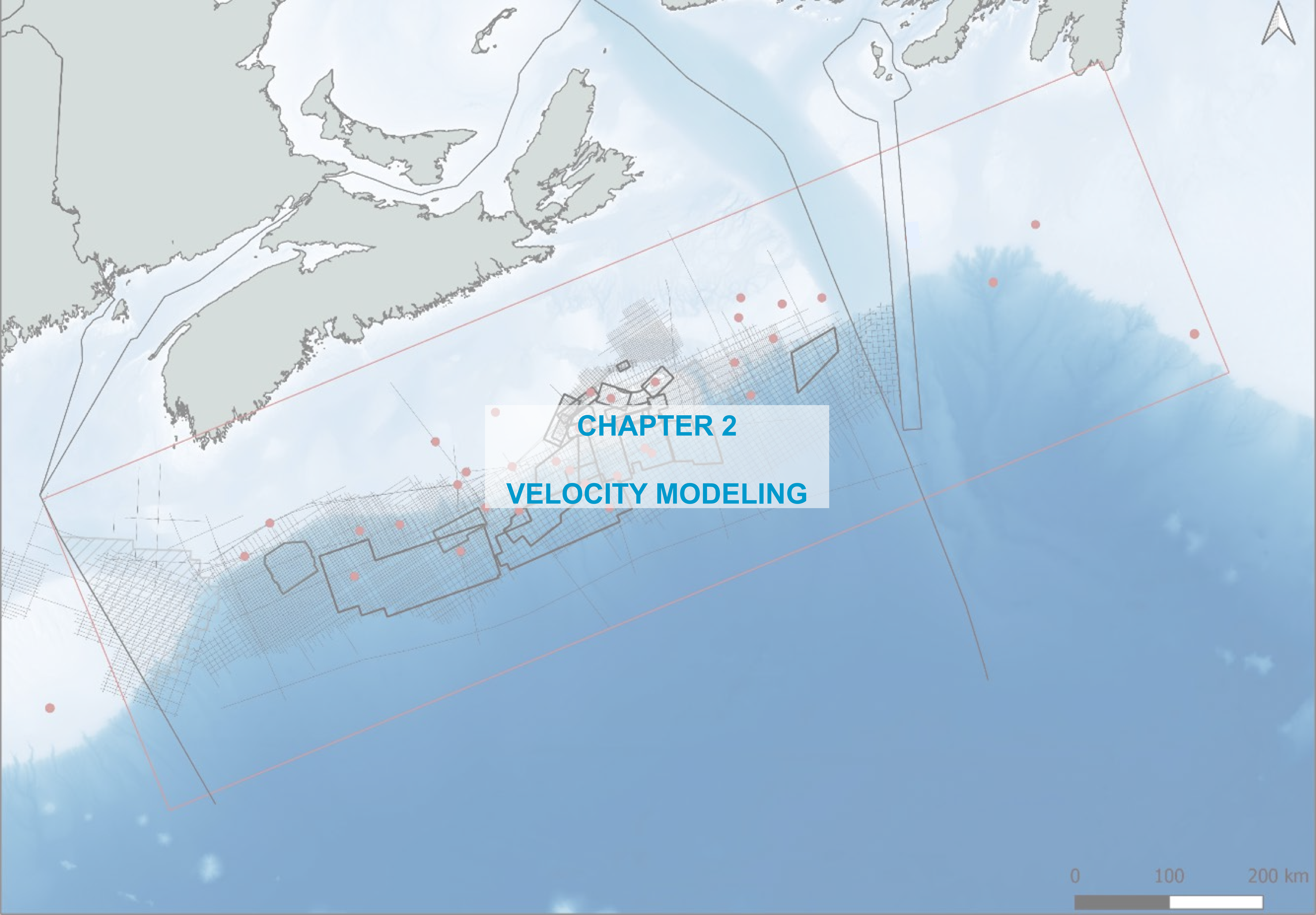

CHAPTER 2

VELOCITY MODELING

Making the skeleton

A blank 3D TWT grid was created using a *Simple Grid* process:

- Top defined at 0 ms TWT (MSL), base defined at 13 s
- Lateral limits set at AOI (same corner points and rotation): 358 km x 1224 km (438,000 km^2)
- Lateral mesh set at 1 km (good compromise between smoothing and stratigraphic precision) – see Figure 1
- Zoning done with 10 horizons as defined in Figure 2: 11 zones are created from MSL to 13 s
- Layering done every 50 ms (Figure 3), except for:
  - water and salt zone: 1 layer with constant velocity (resp. 1500 and 4300 m/s)
  - in [Top Basement; +13 s] zone: 500-ms intervals

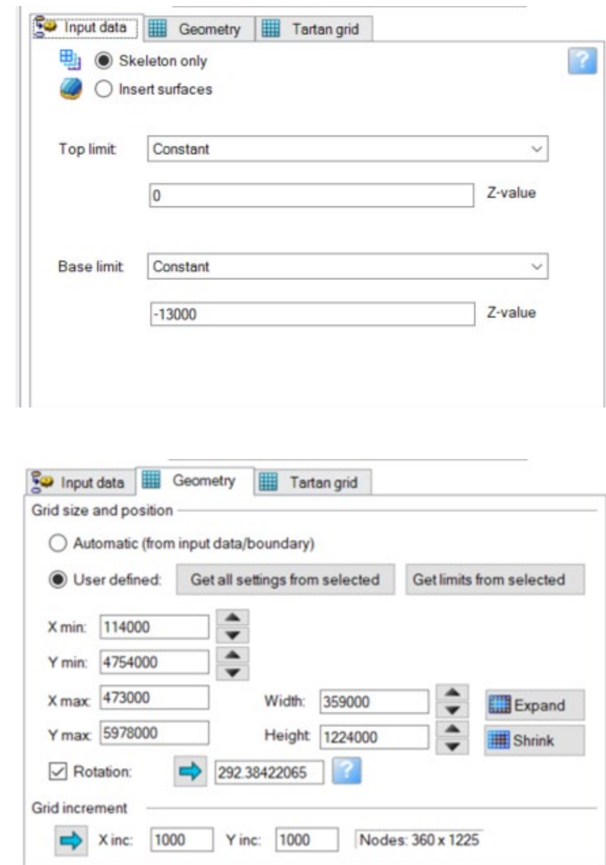

Figure 1: Lateral settings of the modeling grid

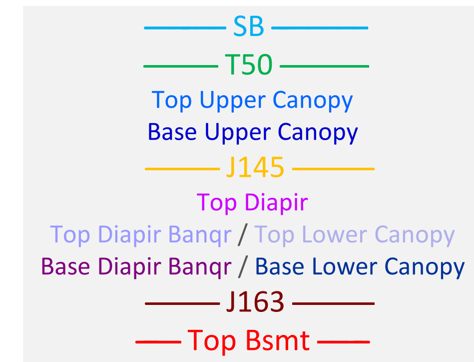

Figure 2: The 10 horizons

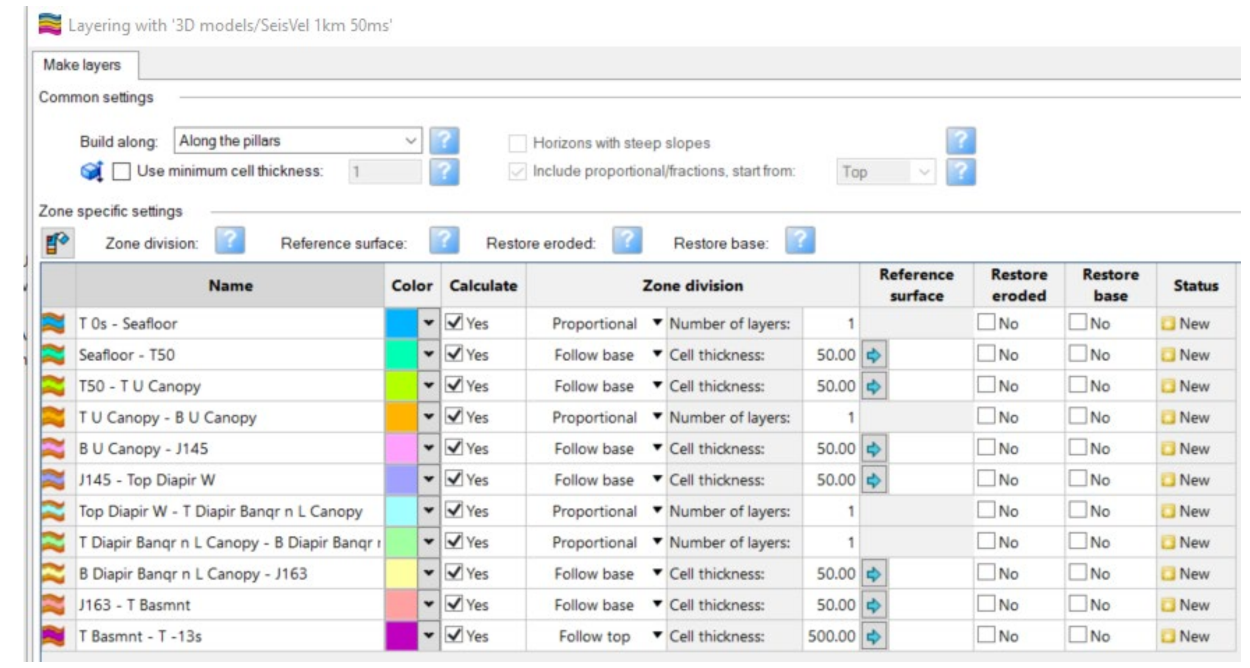

Figure 3: Zoning and layering

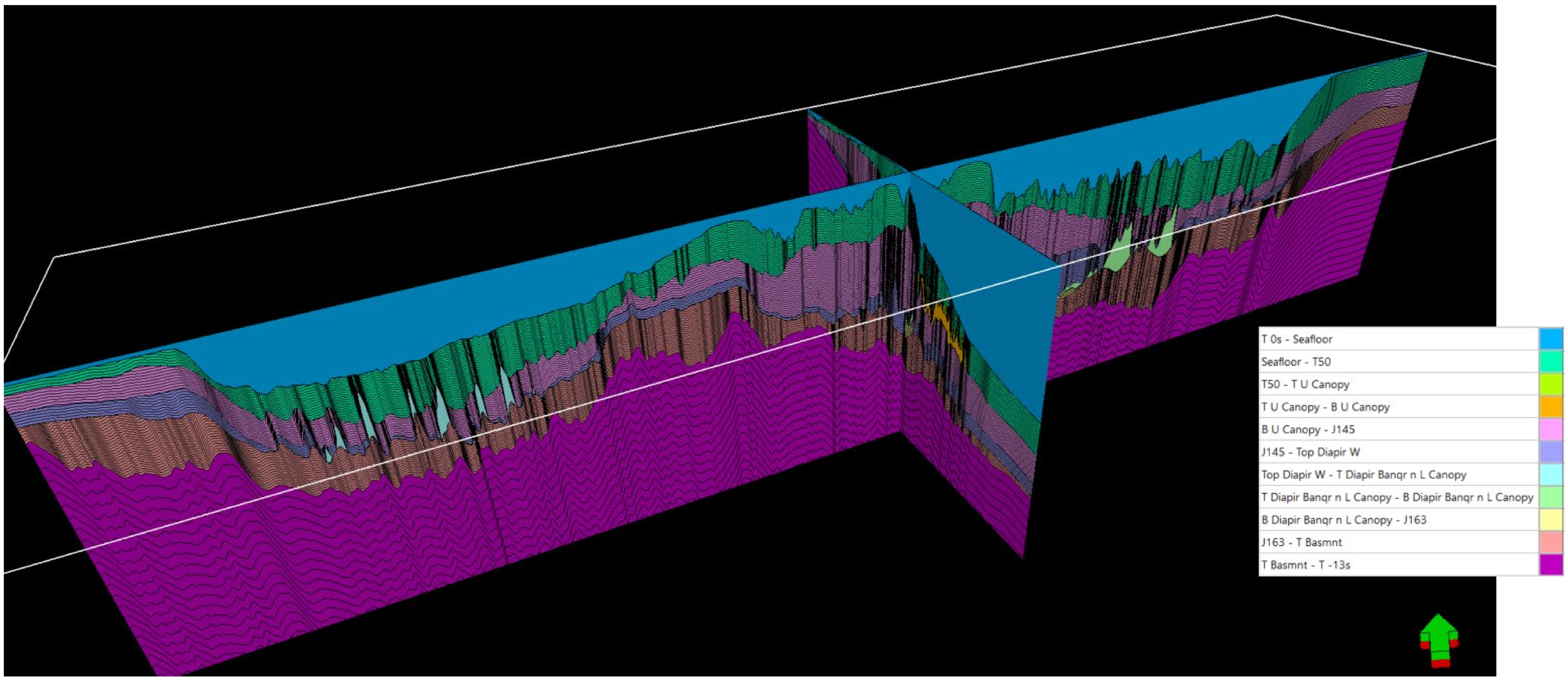

Wells with only sonic logs

To convert the well data (trajectory, markers, logs) from depth to time (TZ) for the 6 wells with only sonic log available as velocity data (Figure 1), different phases were applied.

A preparation workflow was first run in *EasyTrace™*:

- V_{int} computation in m MD from DT (green curve in Figure 2) with small editions if needed
- 1m-regularization
- Smoothing (red curve)
- 20m-regularization (blue curve) up to Seafloor

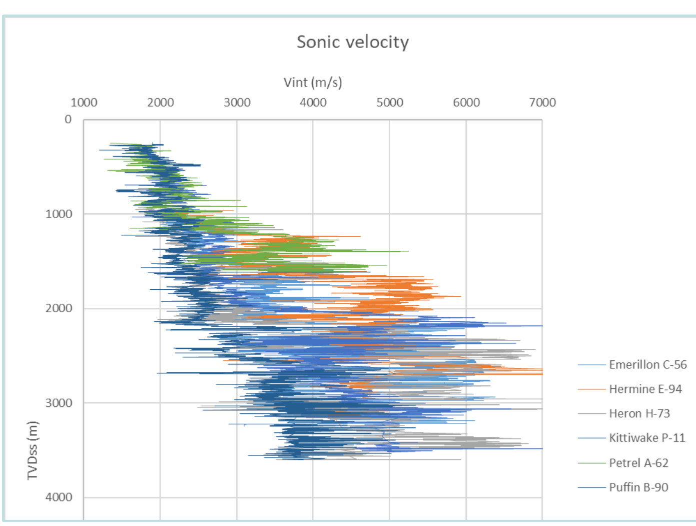

Figure 1: Sonic logs

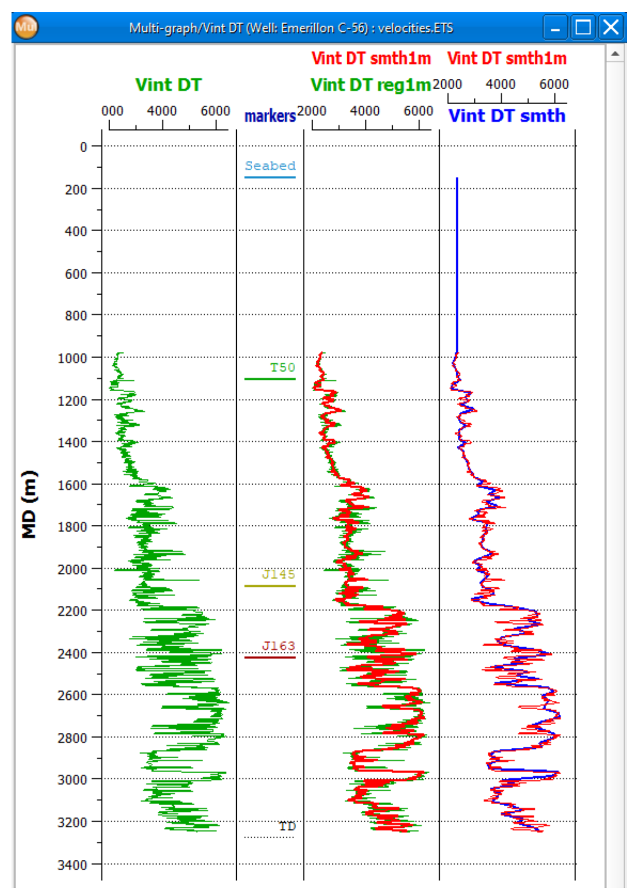

Figure 2: Preparation run for one well

Figure 3 displays the reprocessed sonic logs that can be used for the next phase: their calibration to the horizons to estimate the shallowest velocities not available in the sonic log (see methodology on the right side).

Besides, 4 wells out of the 6 ones do not have geological markers but only bio- and litho-stratigraphic information at different depths defined during various versions/vintages of interpretation. An attempt of setting the main horizons depths was done for those wells (see Figure 4).

Figure 3: Sonic logs prepared for the 6 wells

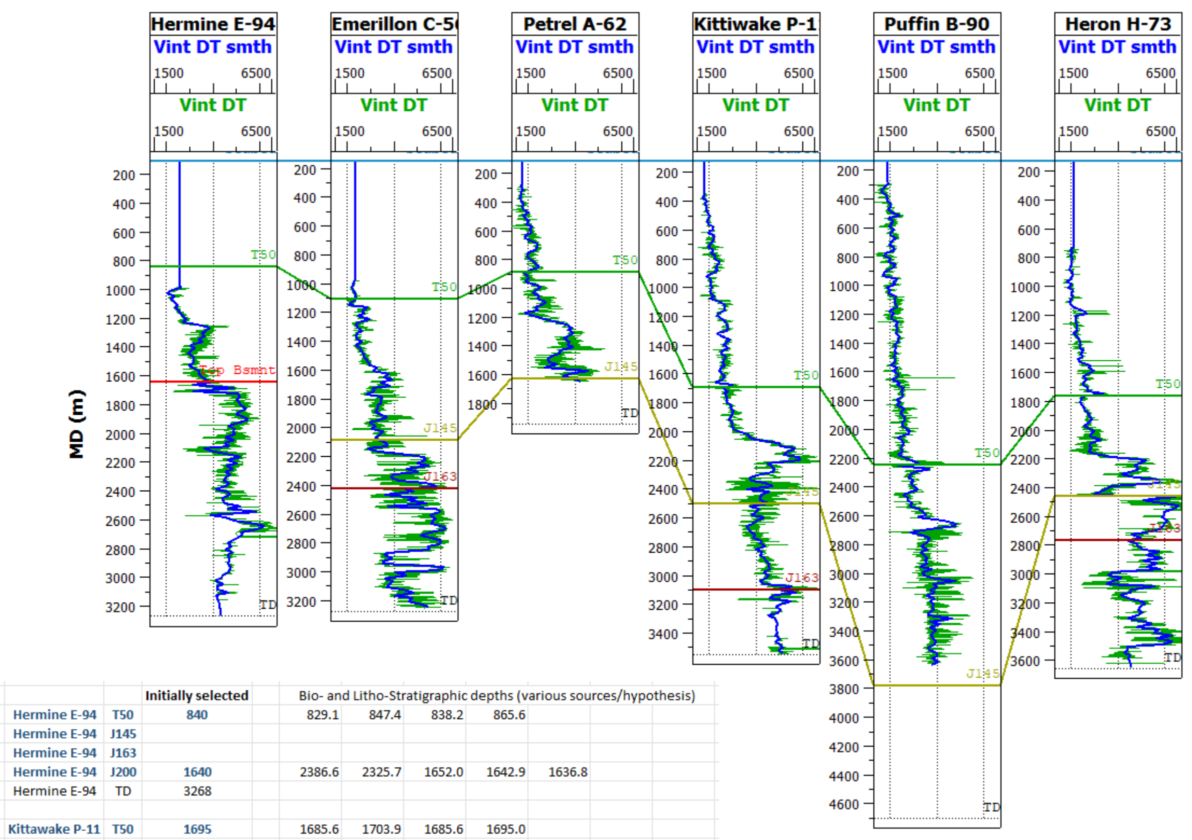

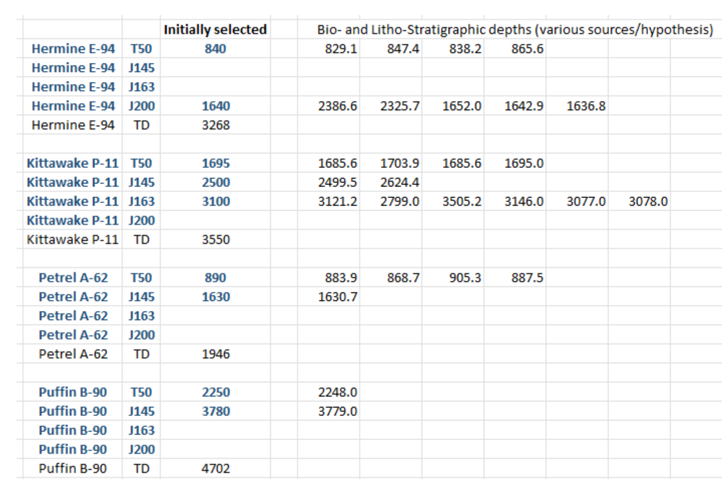

Figure 4: Marker depths selected for the 4 wells without geological markers

The calibration is done along a "test 'n try" process:

- A velocity at the Seafloor is estimated for a first trial (V0) extrapolated/evaluated from the first defined log point (V1). It defines a static time shift of zero ms
- The velocity is linearly interpolated between the Seabed and the first V1 sonic point (italic red values in Figure 5)
- TWT values are thus computed all along the well path
- When the intersection of the well path with the main horizons will suggest a static shift value for the TZ law (an average or chosen value), the V0 value will be modified so that shift(V0) be equal to that value
- The calibration will provide final TZ relationships and calibrated V_{int} logs
- The calibration is done along a "test 'n try" process:

PL. 2.3 and -.4 detail the calibration results.

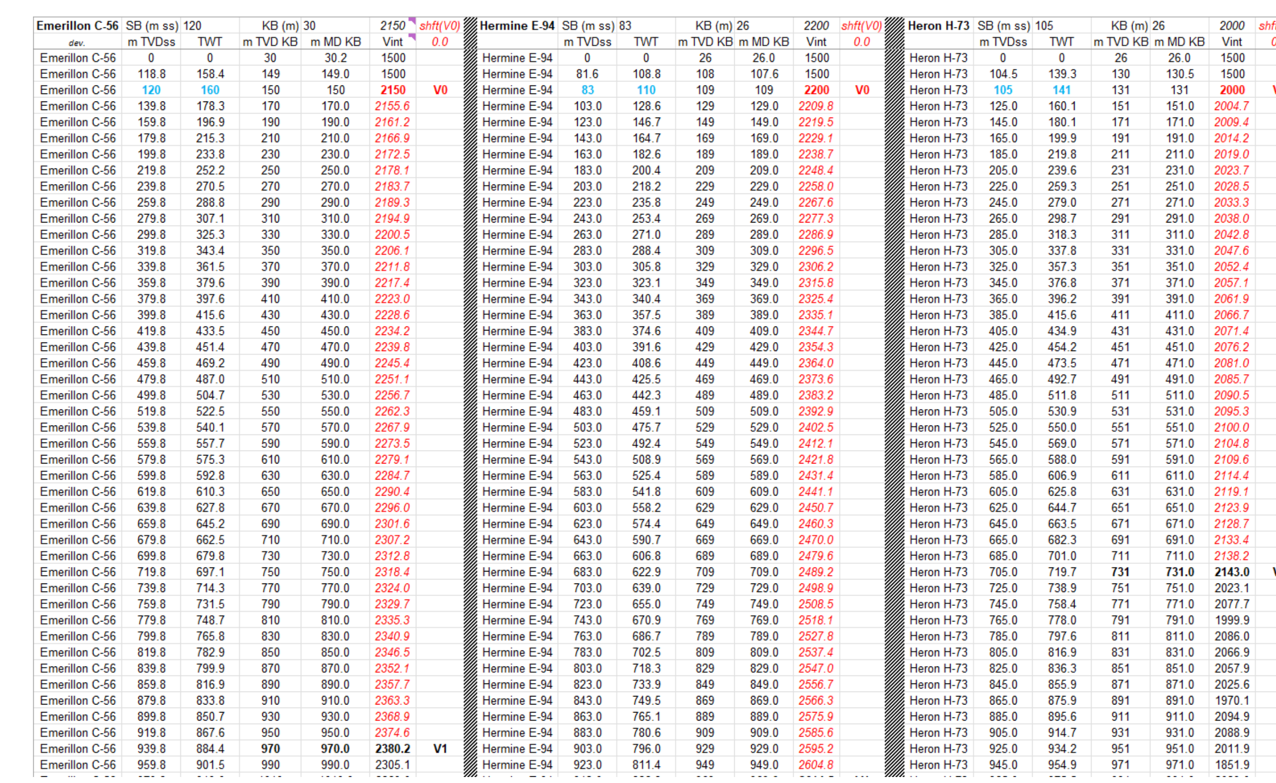

Figure 5: Example of computation sheet for the time calibration

Wells with checksot data

23 wells have checkshot data that enable to convert the wells in time with good enough accuracy and use the resulting interval velocities as hard velocity data. (see Figure 6 and 7)

A calibration step is nevertheless necessary as any calibration with checkshots (explained to the right side). PL. 2.3 and -.4 detail the calibration results.

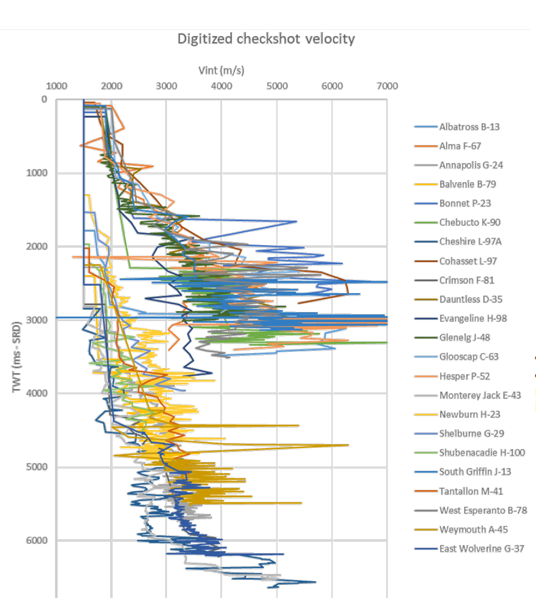

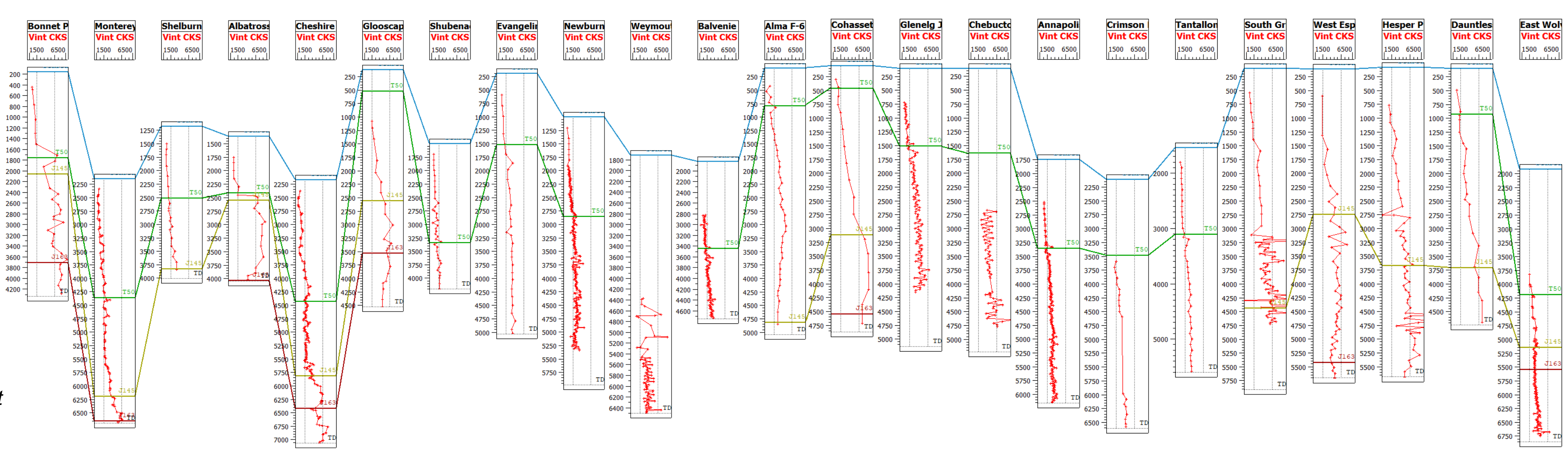

Figure 6 and 7: V_{int} from checkshot data (in TWT and TVD KB)

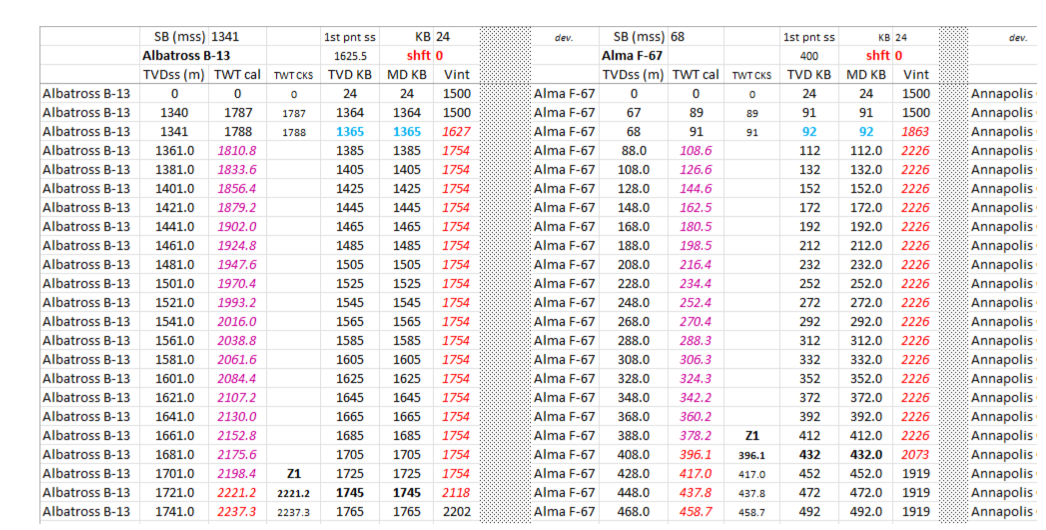

- The checkshot (Zss-TWT) is resampled every 20 m from Z1 (first checkshot point) to TD
- When the intersection of the well path with the main horizons will suggest a static shift value for the TZ law (an average or chosen value), the entered time shift value will:
  - statically shift the (red) TWT below Z1 ("TWT cal" column)
  - stretch the TWT values between Seabed and Z1 (purple values), giving a new constant (red) V_{int} value in this first layer
- Such calibration will thus provide TZ and V_{int} logs

Time shift determination

The original horizons are used to test the TZ conversion and find the best time shift (for wells with checkshot) or the shallower velocities given the best time shift (for wells with sonic) that globally adjust the converted markers with the TWT horizon intersections.

NB: concerning the checkshot calibration, it is not recommended to apply dynamical shifts (i.e. modify the whole TZ relationship to adjust all the horizon-marker correlations), only a constant static shift is searched to calibrate at best all the relevant markers. Concerning the wells with sonic, the TZ relationship computed from those sonic logs will first left as is, without any dynamic deformation, to check the degree of reliability/error in a first calibration step.

The following graphs represent the TWT error (in ms) between the well marker converted with the current TZ law and the TWT horizon intersection corresponding to that marker: error = $TWT_{marker} - TWT_{horizon}$. The wells are displayed from West (left) to East (right). The tested horizons are the original ones without editing; one must keep in mind that they are not necessarily well calibrated to their corresponding marker: they already represent merging of independent horizon grids, and the original synthetic calibrations are not available to check their geological reliability.

The number below the bars represents the selected time shift in ms (positive = downwards), which is the average on the "relevant" errors. Some markers are indeed not selected, as Seabed (SB) that will not be adjusted (error at Seabed means that the corresponding time horizon does not perfectly follow it; also the sea velocity uncertainty – set at 1500 m/s to convert the depth marker into TWT – may also add contribute to its "error"), as markers without checkshot data at their level (green cross). Some strong discrepancies are also not taken into account for the average computing (red cross) as such high value, not correctable, is probably related to horizon interpretation issues: thus, in those cases, a TWT section window comes with the bar graph to visualize the unfitting degree between the markers and the horizons.

TZ from checkshot

not taken into account (probably horizon interpretation problem)

checkshot data not existing at this level

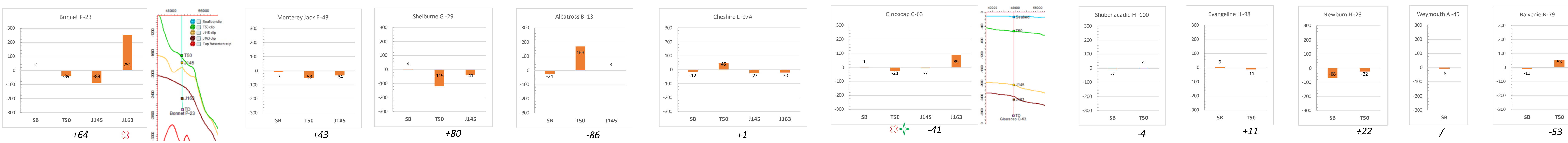

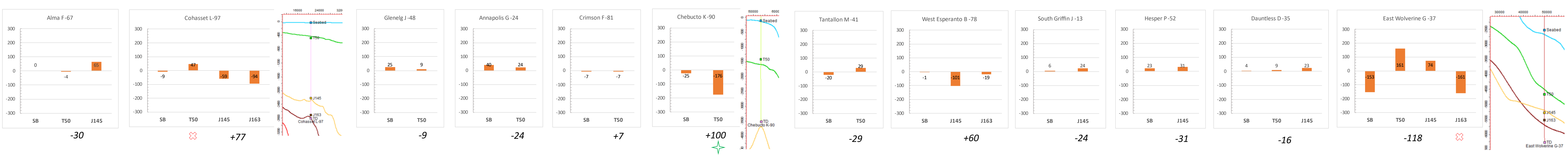

TZ from sonic log

4 wells (with bars in green), located to the East in the Laurentian sub-basin, have markers that were not validated and are very uncertain. The attempt of calibration can make them change (like with Hermine E-94). A strong unfitting – due to marker definition, horizon problems or both – prevents to use those markers for any TZ/velocity adjustment (violet cross): therefore most of these 6 wells with sonic log could not be differently calibrated than they are currently (with the first V0 estimation – see previous Plate).

green: markers from bio-lithostratigraphy

orange: geological markers

removed (probably marker problem)

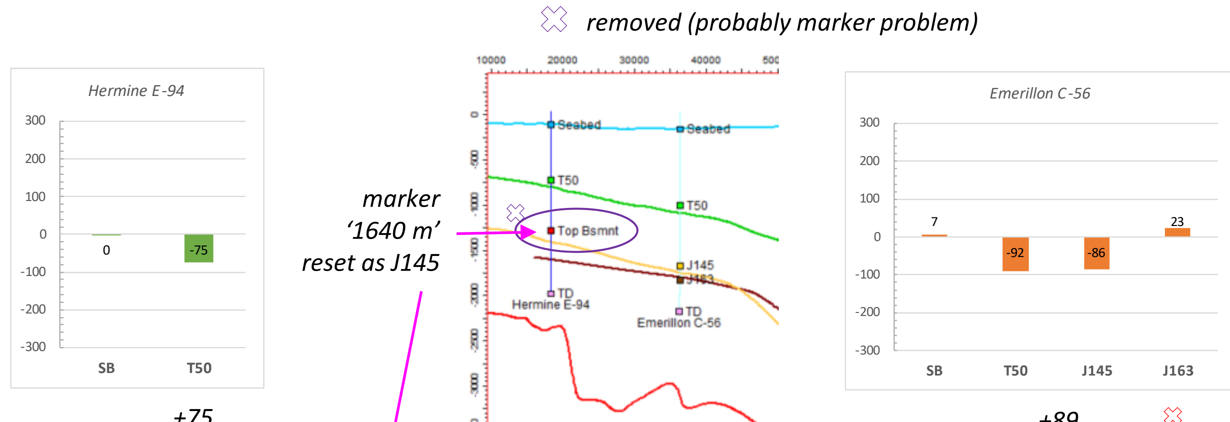

		Initially selected		Bio- and Litho-Stratigraphic depths (various sources/hypothesis)					
Hermine E-94	T50	840		829.1	847.4	838.2	865.6		
Hermine E-94	J145								
Hermine E-94	J163								
Hermine E-94	J200	1640		2386.6	2325.7	1652.0	1642.9	1636.8	
Hermine E-94	TD	3268							

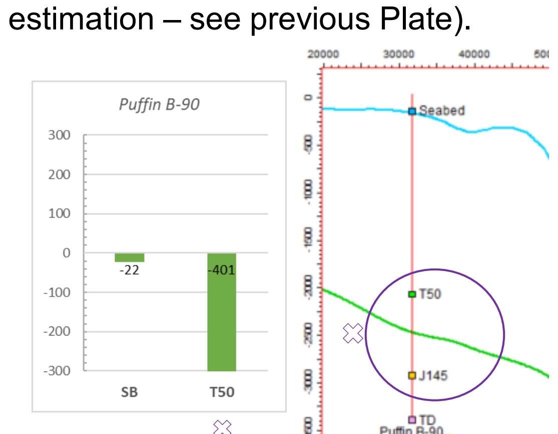

impossible to modify the missing V_{int} values so as to get a 400-ms shift
→ markers will not be not considered

Puffin B-90	SB (m ss)	107	KB (m)	30	1800	shft(V0)
	m TVDss	TWT	m TVD KB	m MD KB	Vint	0.0
Puffin B-90	0	0	30	30.0	1500	
Puffin B-90	105.7	140.9	136	135.7	1500	
Puffin B-90	107	142	137	137	1800	V0
Puffin B-90	127.0	164.7	157	157.0	1817.9	
Puffin B-90	147.0	186.6	177	177.0	1835.6	
Puffin B-90	167.0	208.3	197	197.0	1853.2	
Puffin B-90	187.0	229.8	217	217.0	1870.8	
Puffin B-90	207.0	251.1	237	237.0	1888.5	
Puffin B-90	227.0	272.1	**257**	**257.0**	**1906.1**	**V1**
Puffin B-90	247.0	293.1	277	277.0	1905.7	
Puffin B-90	267.0	313.9	297	297.0	1938.9	
Puffin B-90	287.0	335.2	317	317.0	1826.5	

markers of both wells will be removed

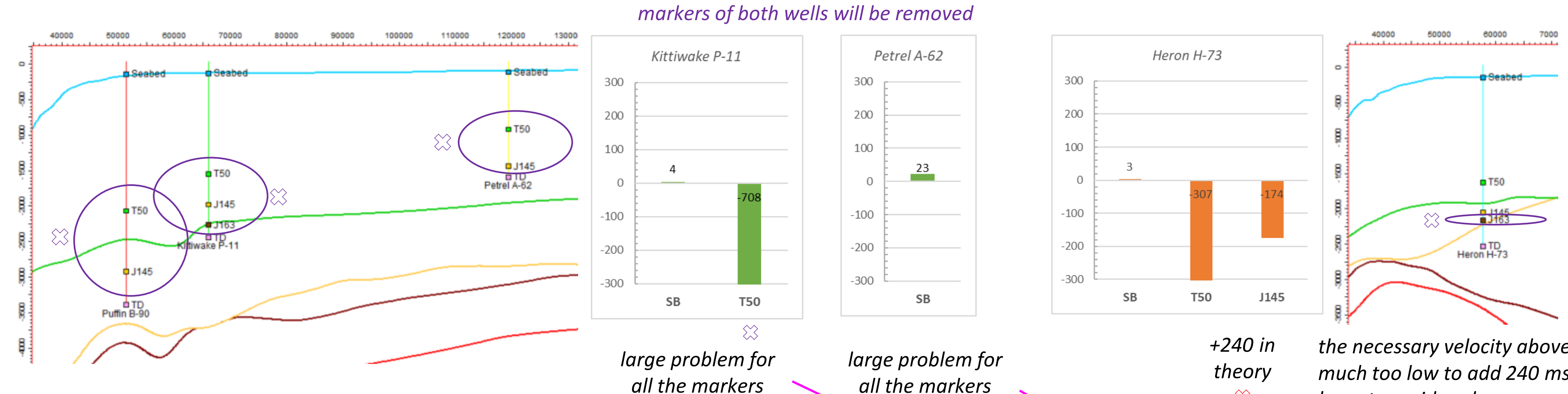

large problem for all the markers

large problem for all the markers

+240 in theory

the necessary velocity above first sonic point is much too low to add 240 ms → markers will not be considered

Heron H-73	SB (m ss)	105	KB (m)	26	2000	shft(V0)
	m TVDss	TWT	m TVD KB	m MD KB	Vint	240.0
Heron H-73	0	0	26	26.0	1500	
Heron H-73	104.5	139.3	130	130.5	1500	
Heron H-73	105	141	131	131	946	V0
Heron H-73	125.0	181.1	151	151.0	985.0	
Heron H-73	145.0	220.9	171	171.0	1024.9	
Heron H-73	165.0	259.2	191	191.0	1064.9	
Heron H-73	185.0	296.0	211	211.0	1104.8	
Heron H-73	205.0	331.6	231	231.0	1144.7	
Heron H-73	225.0	366.0	251	251.0	1184.7	
Heron H-73	245.0	399.2	271	271.0	1224.6	
Heron H-73	265.0	431.3	291	291.0	1264.5	
Heron H-73	285.0	462.4	311	311.0	1304.4	
Heron H-73	305.0	492.6	331	331.0	1344.4	
Heron H-73	325.0	522.0	351	351.0	1384.3	
Heron H-73	345.0	550.4	371	371.0	1424.2	
Heron H-73	365.0	578.1	391	391.0	1464.2	
Heron H-73	385.0	605.1	411	411.0	1504.1	
Heron H-73	405.0	631.3	431	431.0	1544.0	
Heron H-73	425.0	656.9	451	451.0	1584.0	
Heron H-73	445.0	681.9	471	471.0	1623.9	
Heron H-73	465.0	706.2	491	491.0	1663.8	
Heron H-73	485.0	729.9	511	511.0	1703.7	
Heron H-73	505.0	753.1	531	531.0	1743.7	
Heron H-73	525.0	775.8	551	551.0	1783.6	
Heron H-73	545.0	798.0	571	571.0	1823.5	
Heron H-73	565.0	819.7	591	591.0	1863.5	
Heron H-73	585.0	840.9	611	611.0	1903.4	
Heron H-73	605.0	861.7	631	631.0	1943.3	
Heron H-73	625.0	882.1	651	651.0	1983.2	
Heron H-73	645.0	902.1	671	671.0	2023.2	
Heron H-73	665.0	921.7	691	691.0	2063.1	
Heron H-73	685.0	940.9	711	711.0	2103.0	
Heron H-73	705.0	959.7	**731**	**731.0**	**2143.0**	**V1**
Heron H-73	725.0	978.9	751	751.0	2023.1	
Heron H-73	745.0	998.4	771	771.0	2077.7	

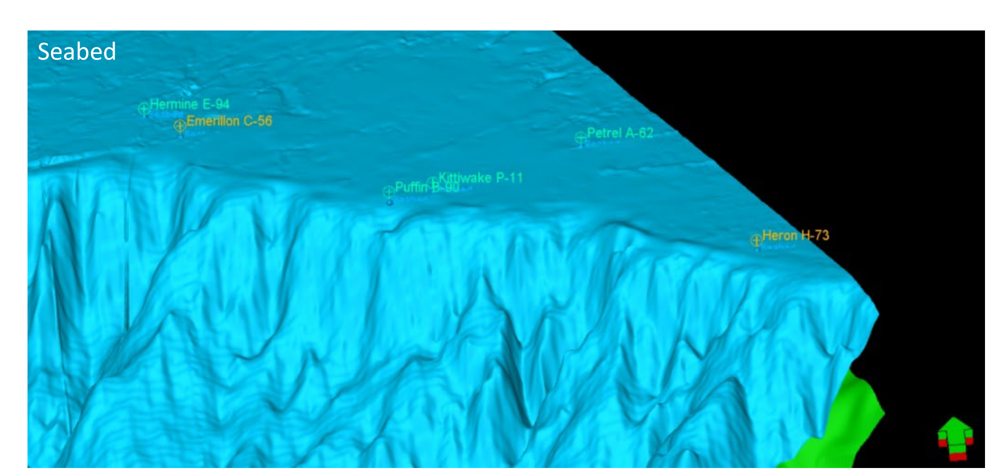

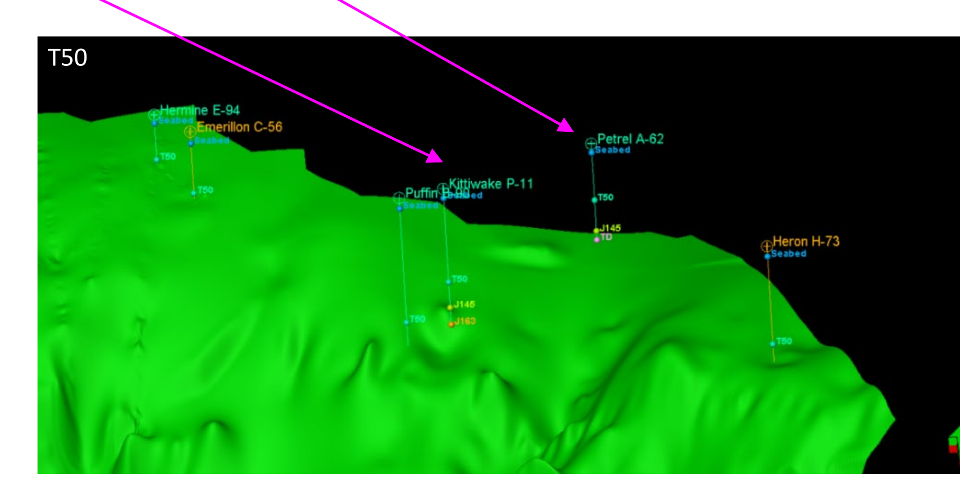

Time shift residuals

The following graphs show what will be the expected mismatch in ms after the calibration done on:

- the wells with TZ ruled by checkshot. As no deformation of the checkshot times is possible, the final calibration is focused on the minimization of the errors on the selected/relevant markers
- the wells with recorded sonic log. Only 2 wells out of the 6 could be calibrated with the help of their markers: Hermine E-94 and Emerillon C-56. The other 4 wells could not be modified: their TZ was kept unchanged, their velocity information (sonic log) will be used in the global interpolation in the current vertical position

TZ from checkshot

not taken into account (probably horizon interpretation problem)

checkshot data not existing at this level

TZ from sonic log

2 wells were recalibrated in TWT (here below).

The 6 sonic logs that will be used are vertically positioned as displayed in the Figure on the right.

green: markers from bio-lithostratigraphy

orange: geological markers

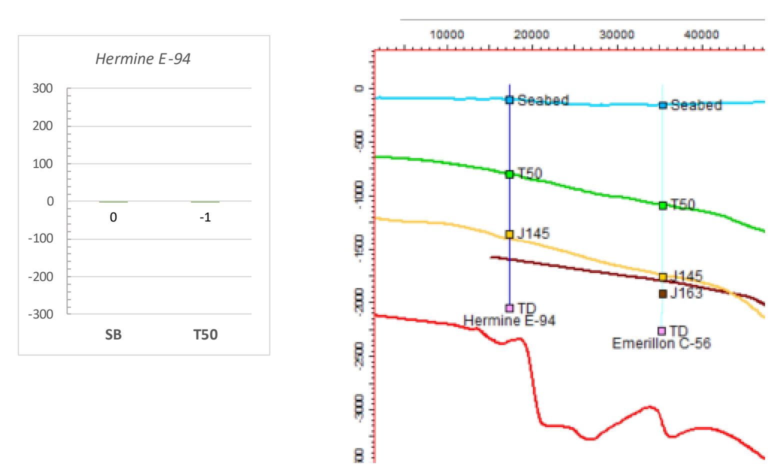

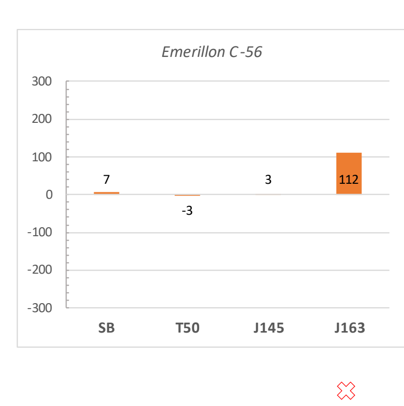

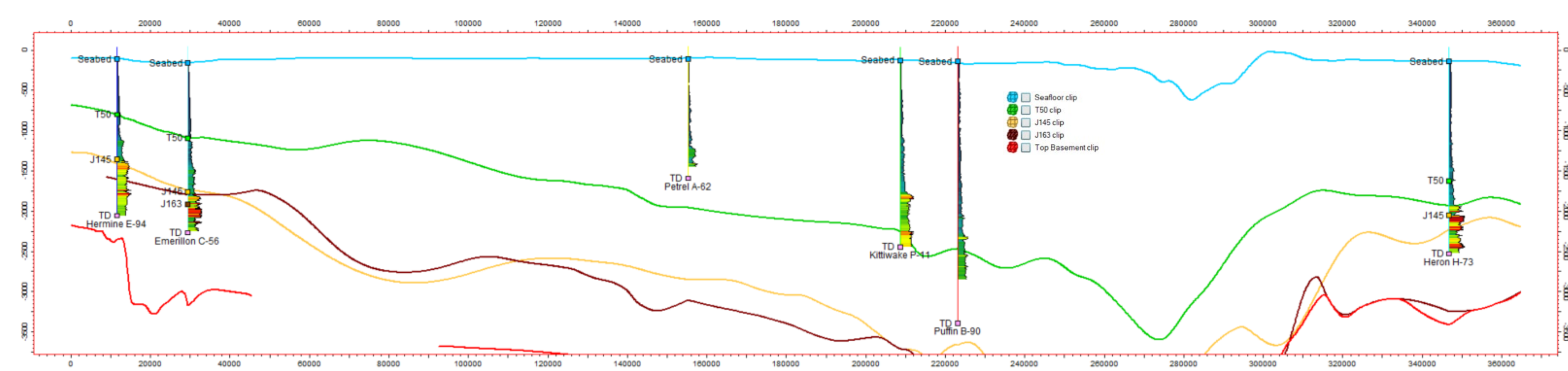

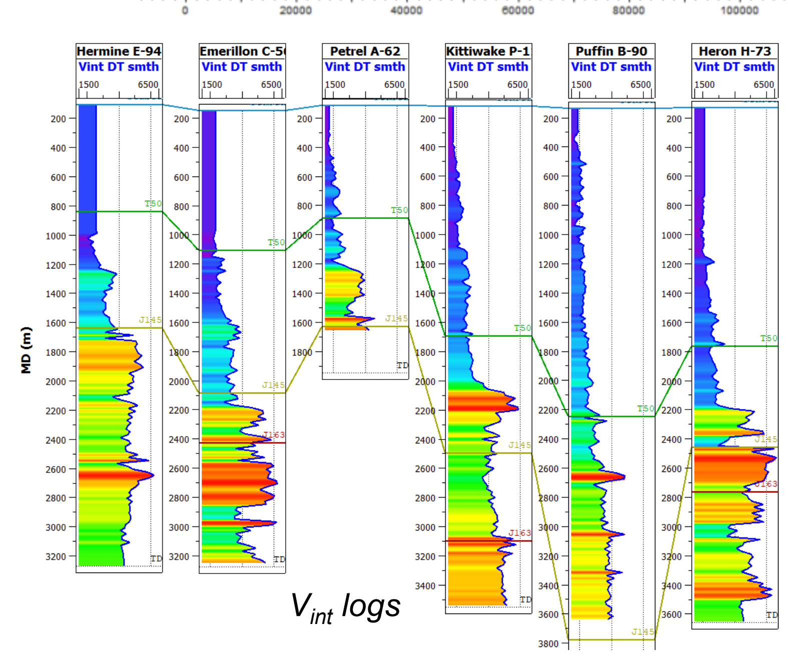

V_{int} logs

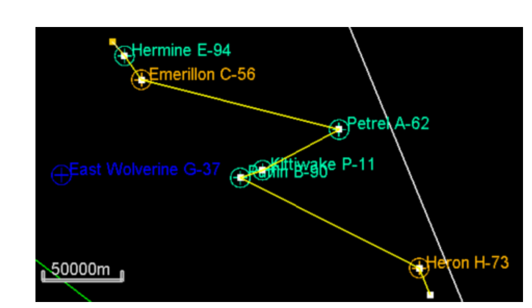

NB: Velocity at Petrel A-62 seems to be higher than its neighbours, but no element suggests wrong velocities, nor TZ conversion (sonic log begins very close to the Seabed)

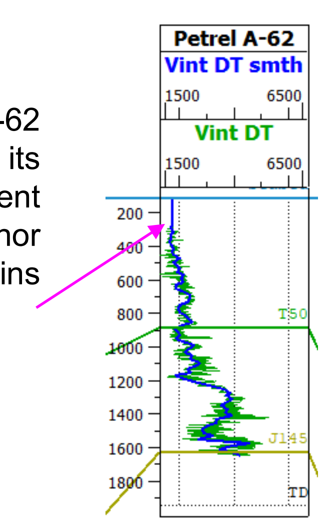

V_{int} log at Petrel A-62

Well – Time to Depth relationships (TZ) – TWT residuals after calibration

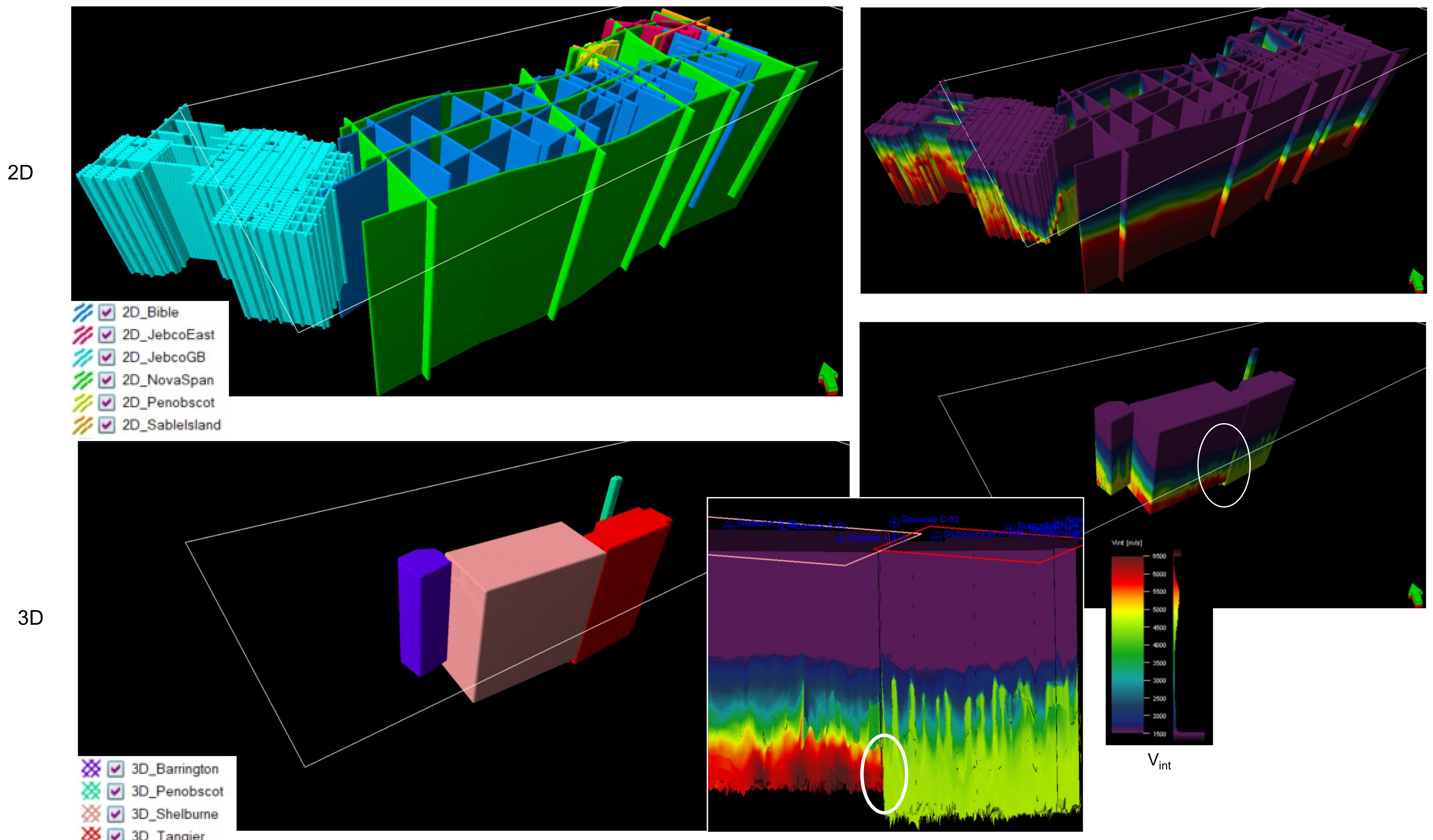

Figure 1: 2D and 3D seismic velocities and discrepancies between Shelburne and Tangier

Shelburne

Ratio was computed with 2D velocities (Bible and Nova Span lines) and show no strong differences from 8 s to very deep levels (arrow in Figure 2). Ratio was also done with the crossing wells (to increase the number of points, the neighbouring well Albatross B-13 was laterally shifted – less than 3 km off – to get 3 intersecting wells); it gave a factor that was eventually smoothed to be held within ± 15% maximum (Figure 3).

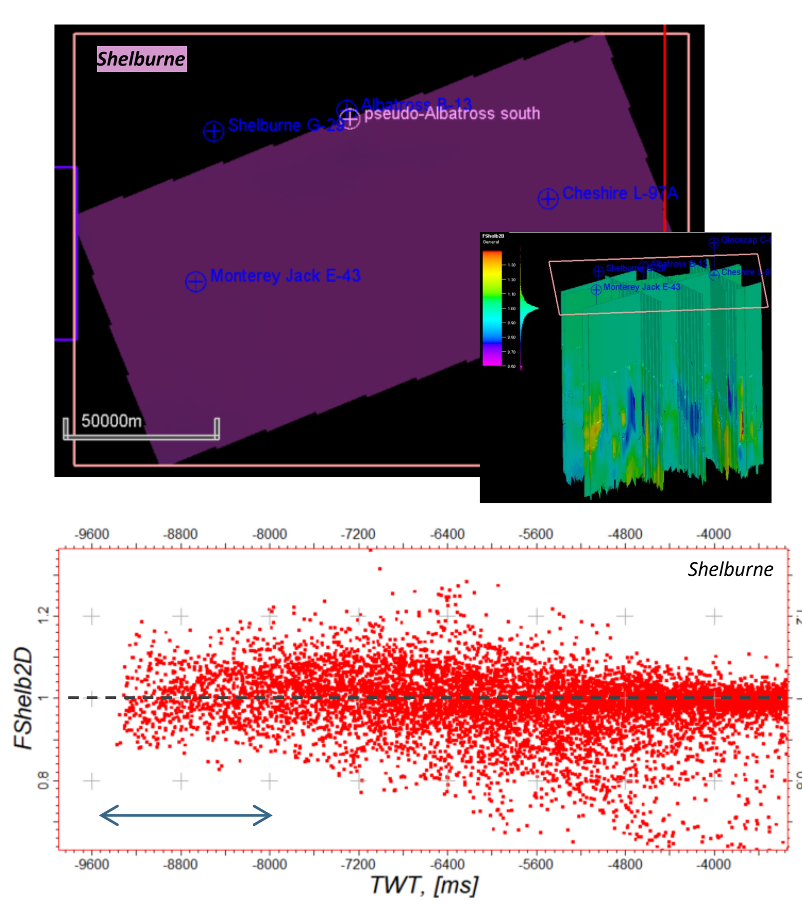

Figure 2: $F_{3D/2D}$ for Shelburne

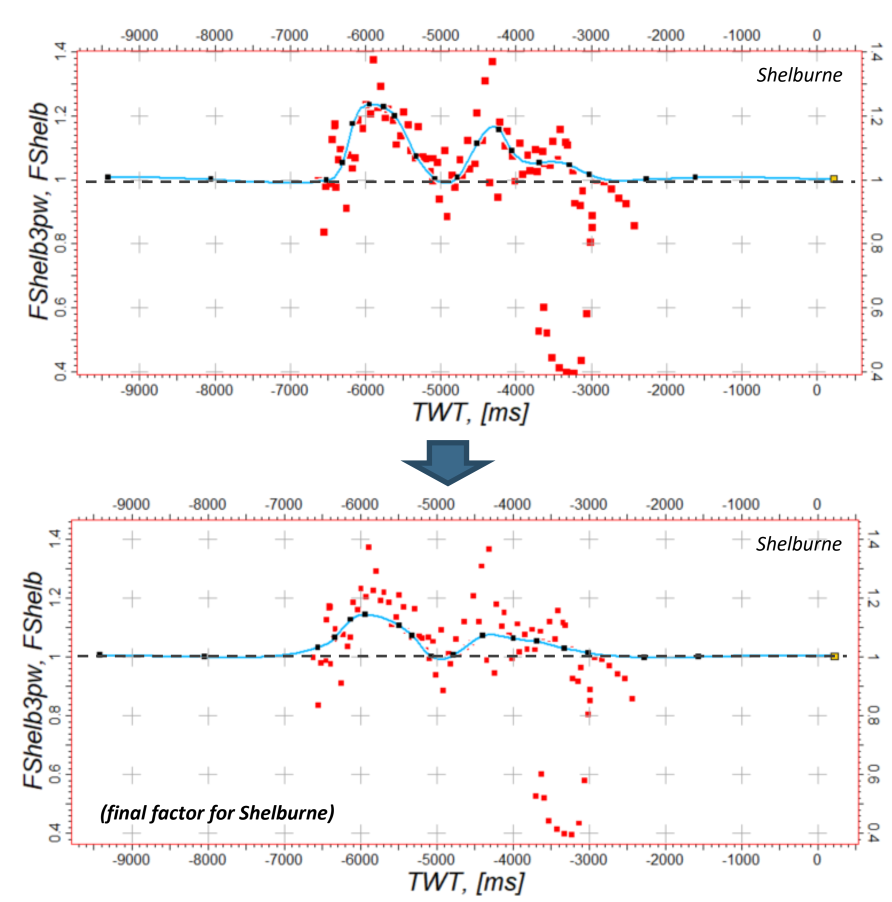

Figure 3: $F_{S/W}$ for Shelburne

Discrepancy in the seismic (processing) velocity values

Once the seismic velocities are converted in regular V_{int}, some discrepancies appear between adjacent sources:

- between adjacent 3Ds (see white ovals at Shelburne vs. Tangier area in Figure 1)
- at 2D vs. 3D junctions

Several adjustment phases were iteratively carried out using velocity ratios (functions of TWT):

- between seismic (2D or 3D) vs. well interval velocities: $F_{S/W} = V_{Seis} / V_{Well}$
- between 3D vs. 2D interval velocities: $F_{3D/2D} = V_{3D} / V_{2D}$
- between two 3D interval velocities fields: $F_{A/B} = V_{3D\_A} / V_{3D\_B}$

Tangier

Ratio was computed with 3 wells (1 original and two laterally shifted 1.3 and 7.7 km off) but gave no clear shape (Figure 4). The comparison with 2D lines (Figure 5) show that deep Tangier velocities (> 8 s) are too slow, both analysis were used to redraw the factor considering the shallow (wells) and deep (2D) ratios.

In parallel, a ratio between Tangier and Shelburne ratios could be computed after a small lateral displacement (~2 km): the deep levels show a discrepancy of 20% (Figure 6). All the three ratios were combined to get a final ratio factor.

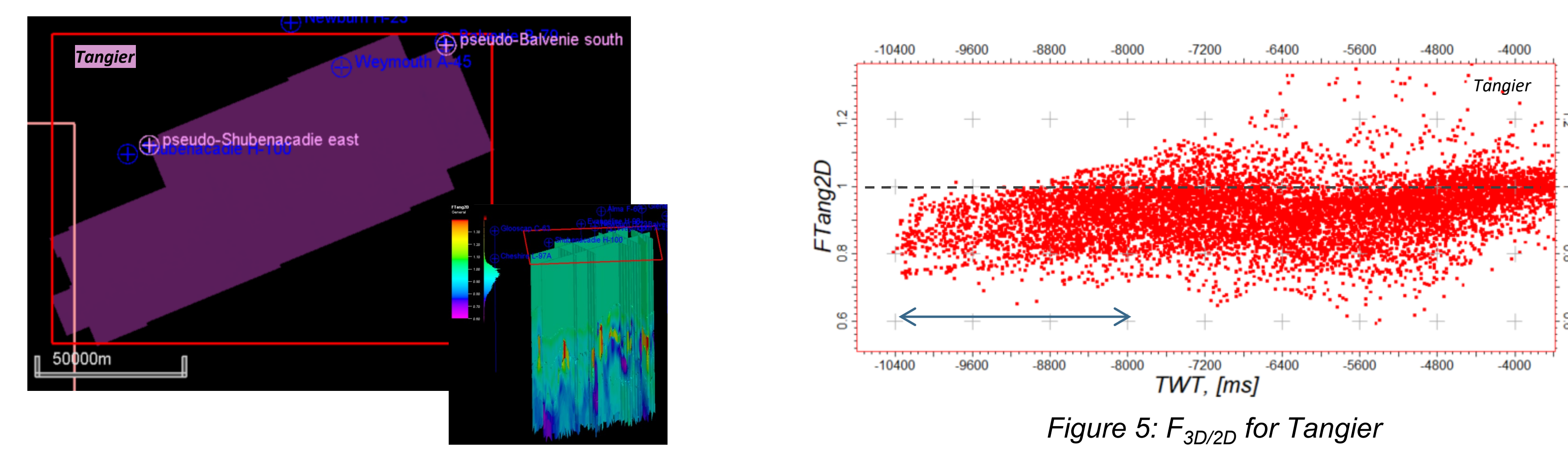

Figure 5: $F_{3D/2D}$ for Tangier

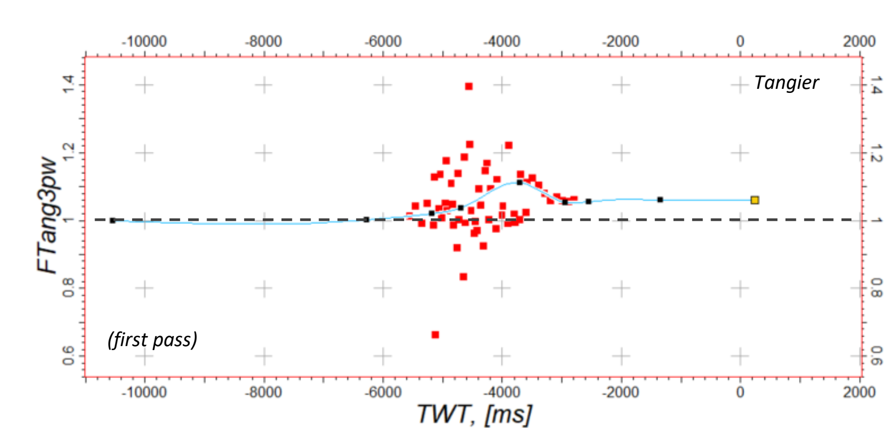

Figure 4: $F_{S/W}$ for Tangier

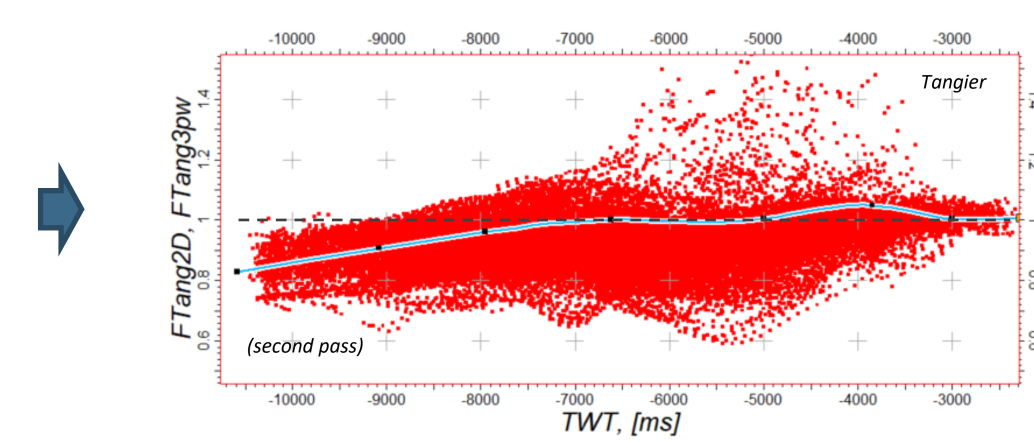

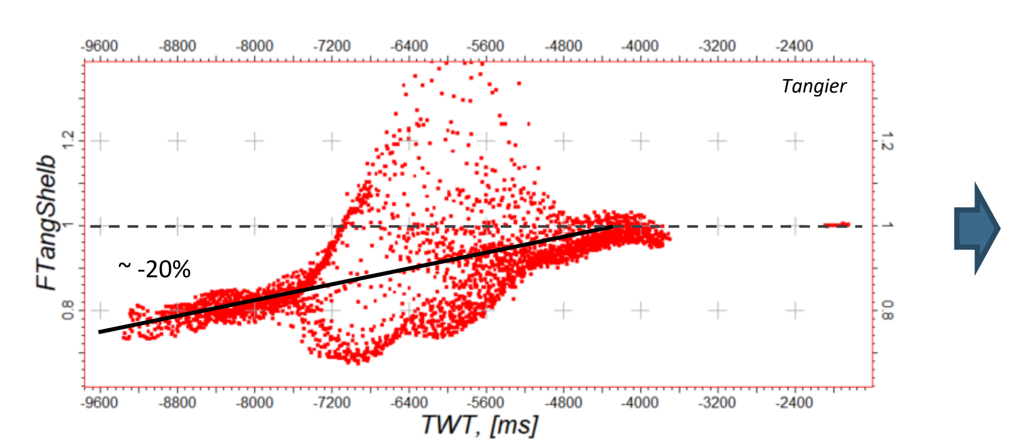

Figure 6: $F_{Tang/Shelb}$

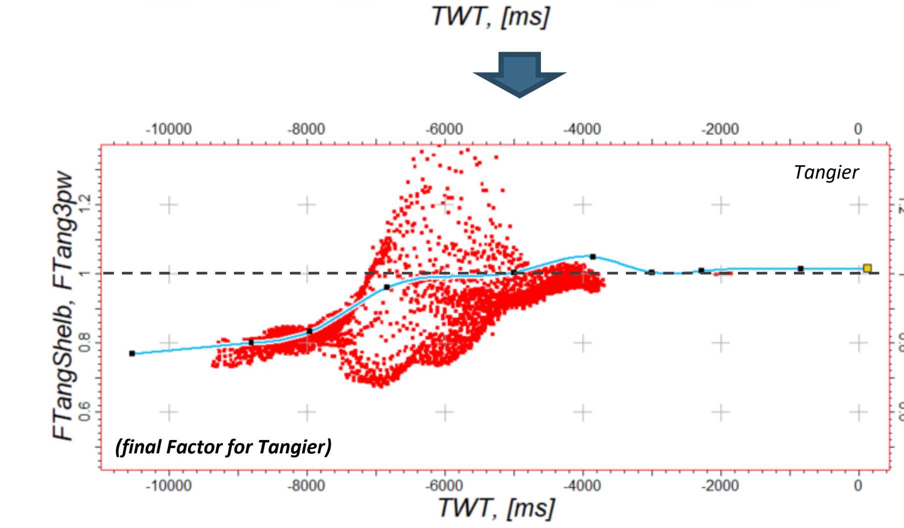

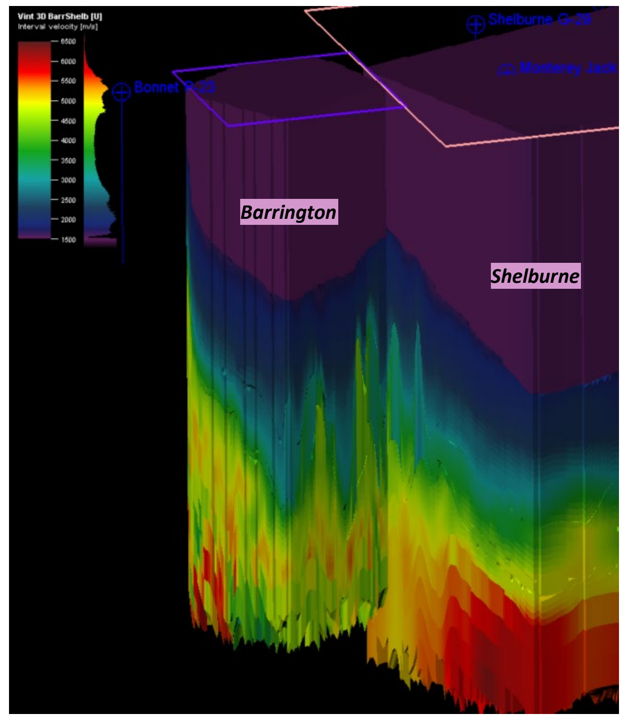

Figure 1: Discrepancies between Barrington and Shelburne cube velocities

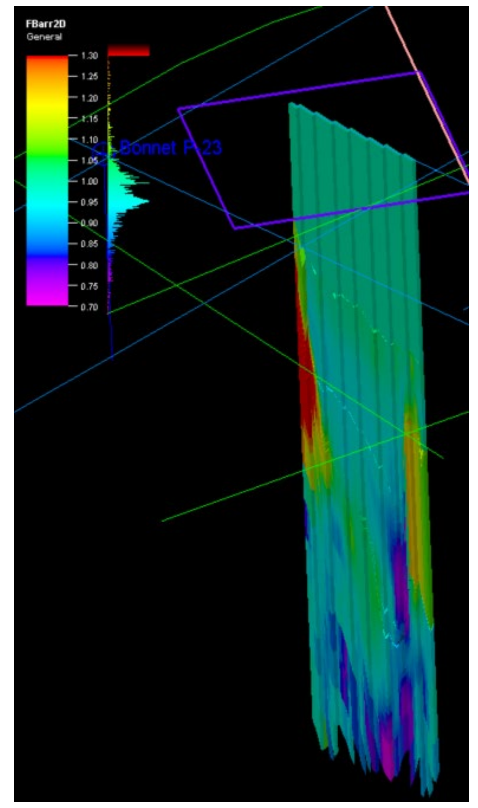

Figure 2: $F_{3D/2D}$ in Barrington

Barrington

No well crosses Barrington seismic traces. Visual comparisons show small discrepancies with adjacent Shelburne velocities (Figure 1). Only one 2D lines is common with the 3D cube; a ratio factor was computed (Figure 2), showing velocities quite lower in the 3D data for the deep parts (Figure 3).

After small lateral displacement to make them overlie, a ratio was computed between both adjacent cubes (Figure 4). The ratio factor was eventually drawn to match a common shape suitable for both analysis.

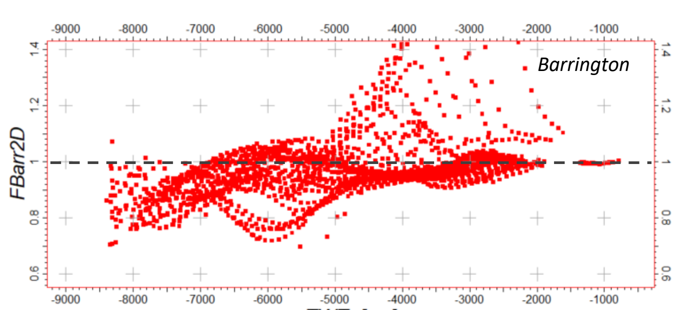

Figure 3: $F_{3D/2D}$ for Barrington

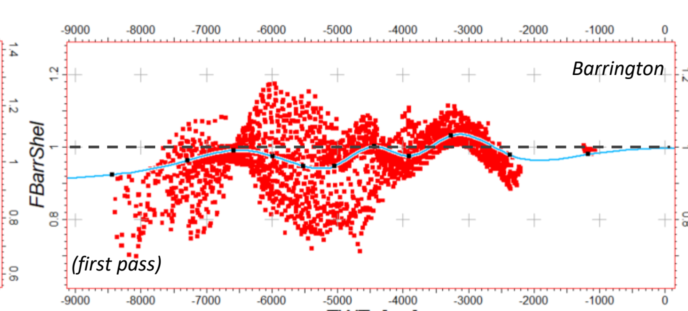

Figure 4: $F_{Barr/Shelb\_adj}$

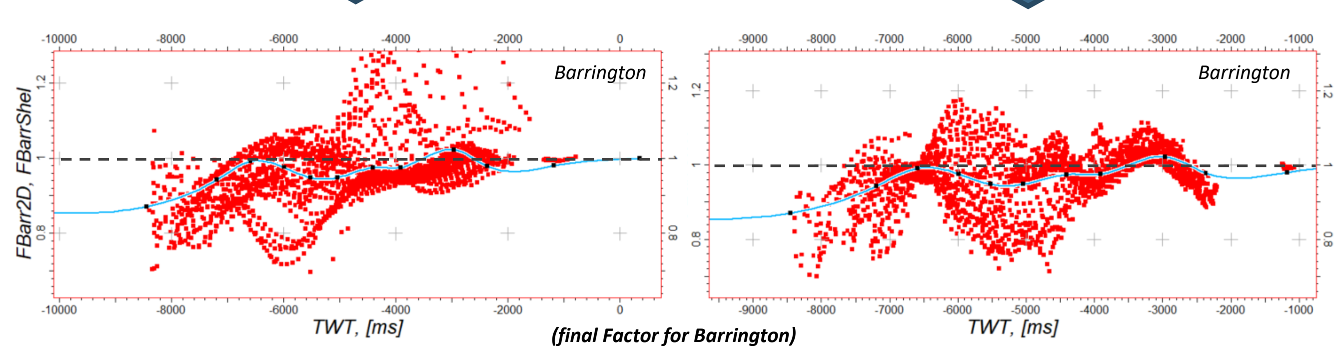

Penobscot

No well crosses Penobscot seismic traces, nor the 2D lines encompassing the 3D survey. A ratio was computed between both seismic sources (Figure 5), showing a big lowering trend in the deep parts (up to -20% - see here below).

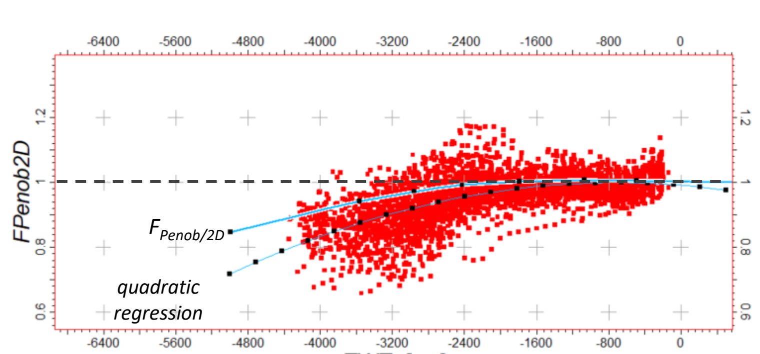

As no other information can be extracted, the ratio factor was taken as the middle curve between the quadratic regression and the constant '1' line (see on the left).

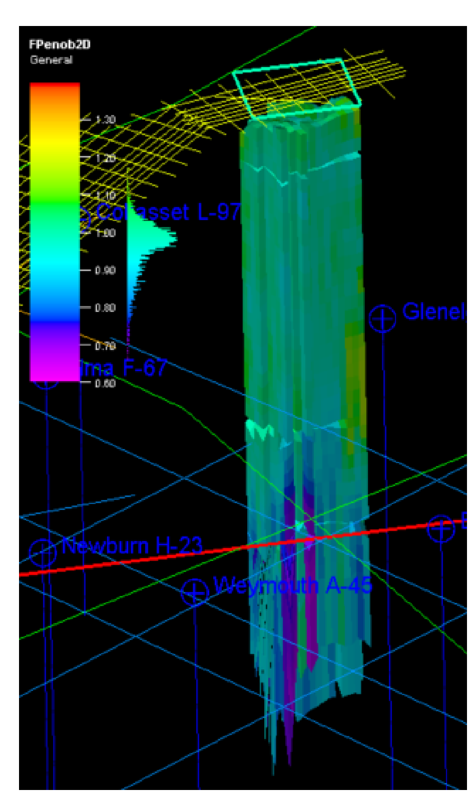

Figure 5: $F_{3D/2D}$ for Penobscot

Wells crossing Bible lines

Bonnet P-23*
Shelburne G-29
Albatross B-13
Glooscap C-63
Shubenacadie H-100*
Evangeline H-98
Newburn H-23*
Weymouth A-45
Crimson F-81*
Tantallon M-41

** small shift of the well*

Wells crossing Nova Span lines

Cheshire L-97A*
Shubenacadie H-100*
Annapolis G-24
West Esperanto B-78
Dauntless D-35

Wells crossing Jebco East lines

West Esperanto B-78
Hesper P-52
South Griffin J-13

$F_{S/W} = V_{Seis2D}/V_{Well}$

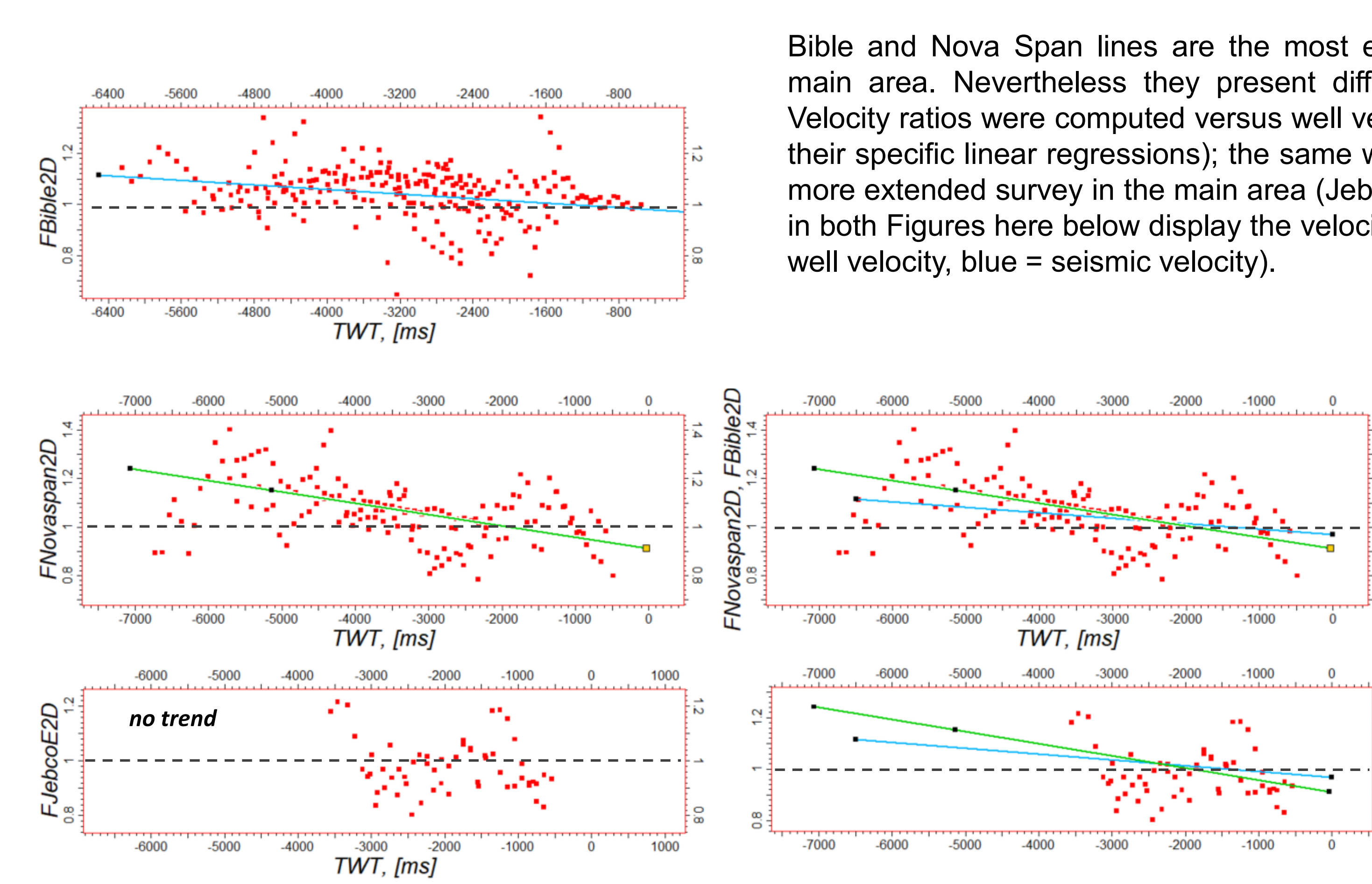

Bible vs. Nova Span velocities

Bible and Nova Span lines are the most extended ones covering the main area. Nevertheless they present differences at their crossings. Velocity ratios were computed versus well velocities (see on the left with their specific linear regressions); the same work was done with the third more extended survey in the main area (Jebco East). The vertical traces in both Figures here below display the velocity traces at each well (red = well velocity, blue = seismic velocity).

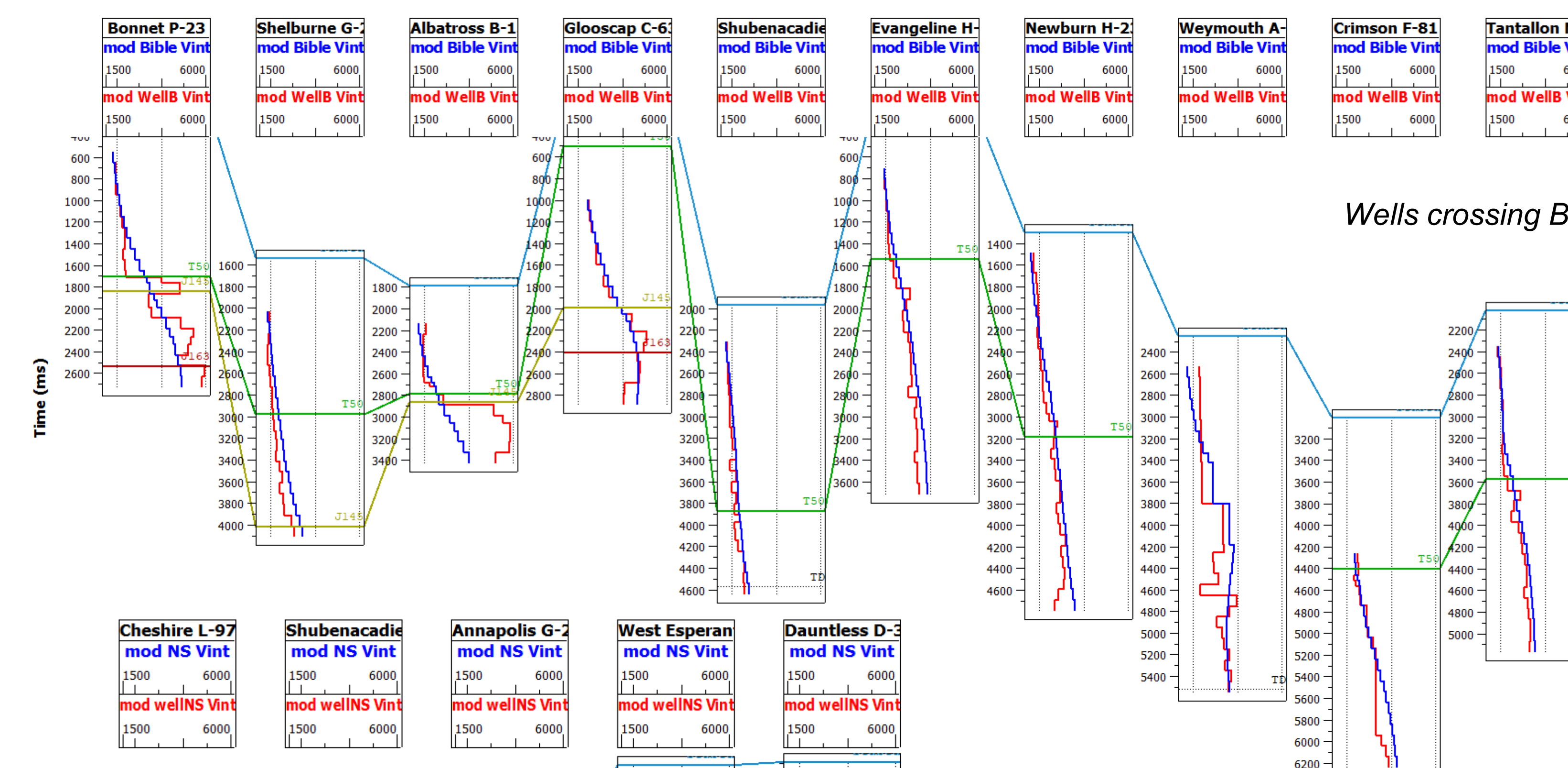

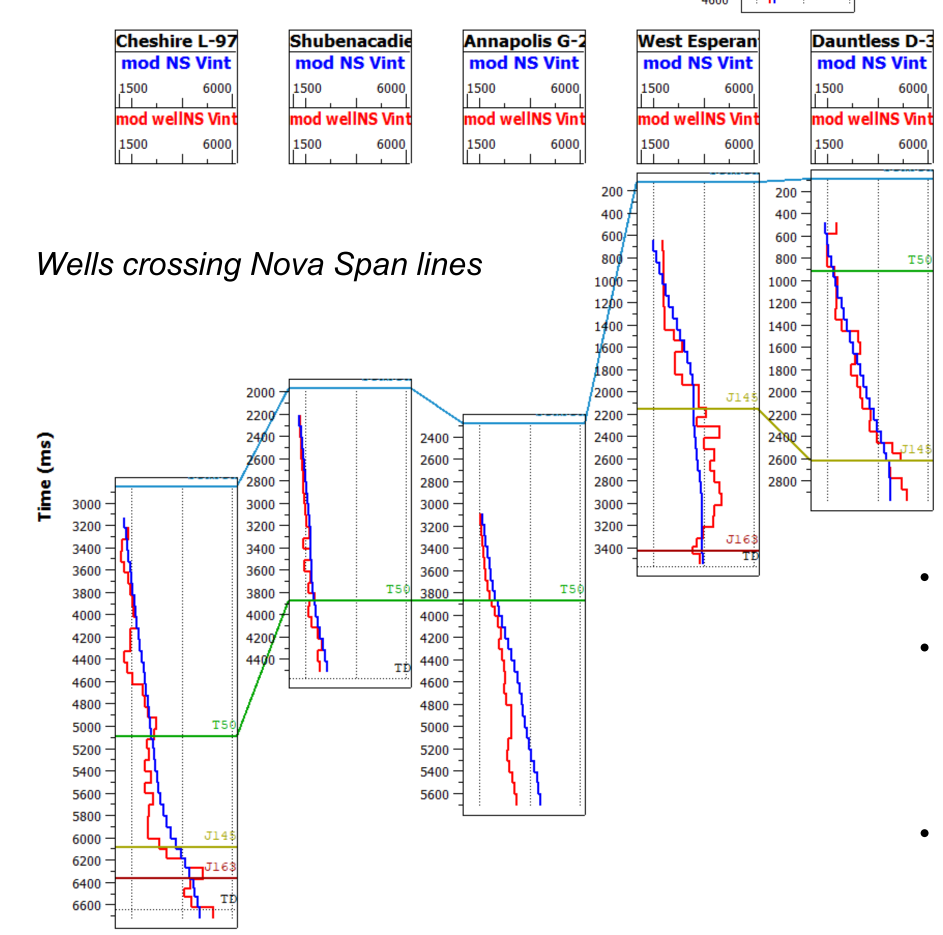

- Globally the seismic velocities are always higher than well velocities
- In the deep parts, Nova Span velocities seems to have slightly higher velocities than for Bible ones (which are higher in average than well velocities) → favour Bible lines than Nova Span ones when both are subparallel
- It is not possible to assess whether Bible or Nova Span velocities will be better in the Jurassic layers and below

Seismic velocities – Adjustments (2)

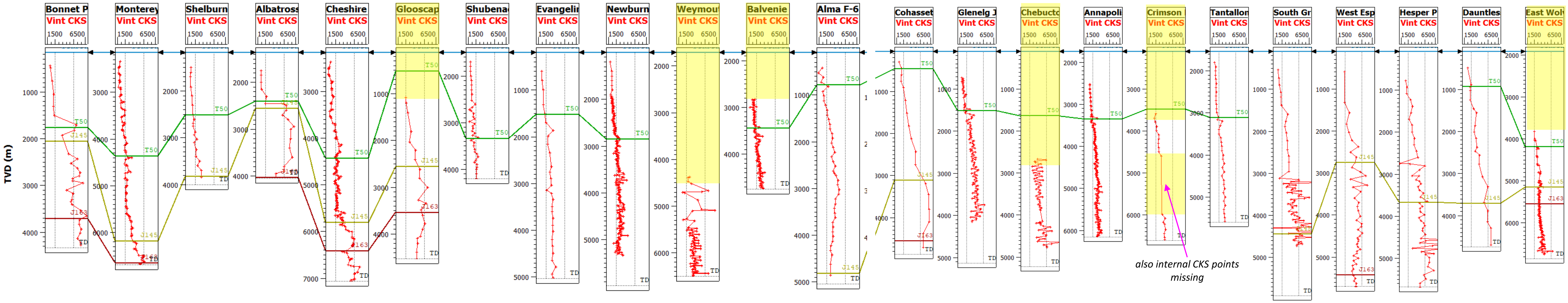

Figure 1: Wells with checkshot velocities

Well velocities adjustment – Second pass

Some wells with checkshot have no data in the shallow layers (Figure 1): for Weymouth A-45 there is a gap of 2600 m between Seabed and first checkshot point. The process described in PL.2.2, is sufficiently accurate for most of the wells with checkshot (that creates constant velocity in that interval without data). The real velocity variation (~ seen by seismic velocities) would not be considered: any interpolation/co-kriging with seismic velocities would not modify it. To keep/control these shallow well velocity values (that calibrate the well in absolute) before any interpolation/co-kriging, shallow velocity points were added in these wells to follow the general seismic velocity variations. A methodology was thought to add those new [TVD; V_{int}] couples without modifying the time-depth relationships present in the original checkshot.

6 wells were identified (see yellow parts in Figure 1). Their velocities were compared with adjacent seismic velocities, available for 4 wells among themselves (Chebucto K-90 and East Wolverine G-37 are too far from any seismic data).

The process is illustrated in Figure 2 with Weymouth A-45 example (steps in the alphabetical index 'a to c' order).

Figure 3 displays the results for the three other wells (new checkshot velocity = ocher color).

NB: all the new checkshot points are added to follow the seismic trend, and above all so that the first constant V_{int} layer below Seabed respects a geological velocity value (higher than water velocity and lower than the following V_{int} interval). In Crimson F-81, the interval velocity was linearized in the missing lower part of the checkshot data (see arrow in Figure 3).

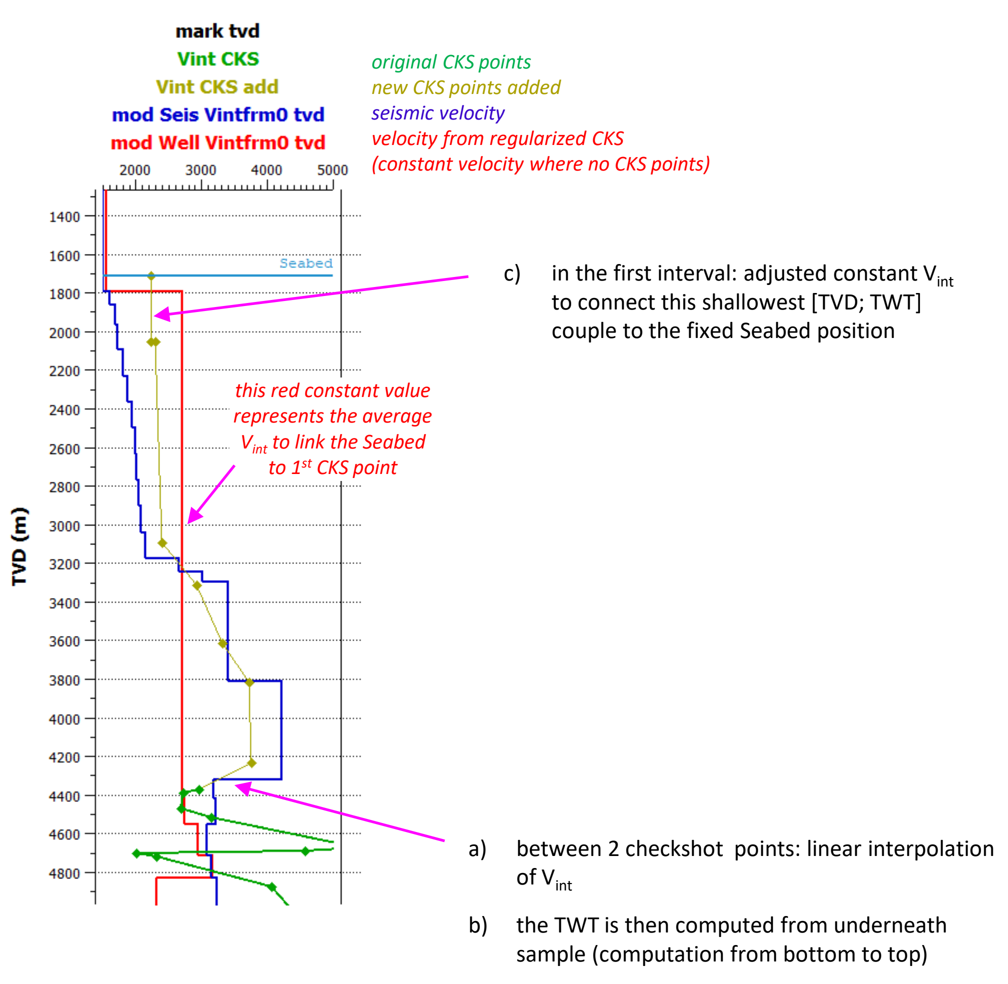

Figure 2: Methodology illustrated with Weymouth A-45

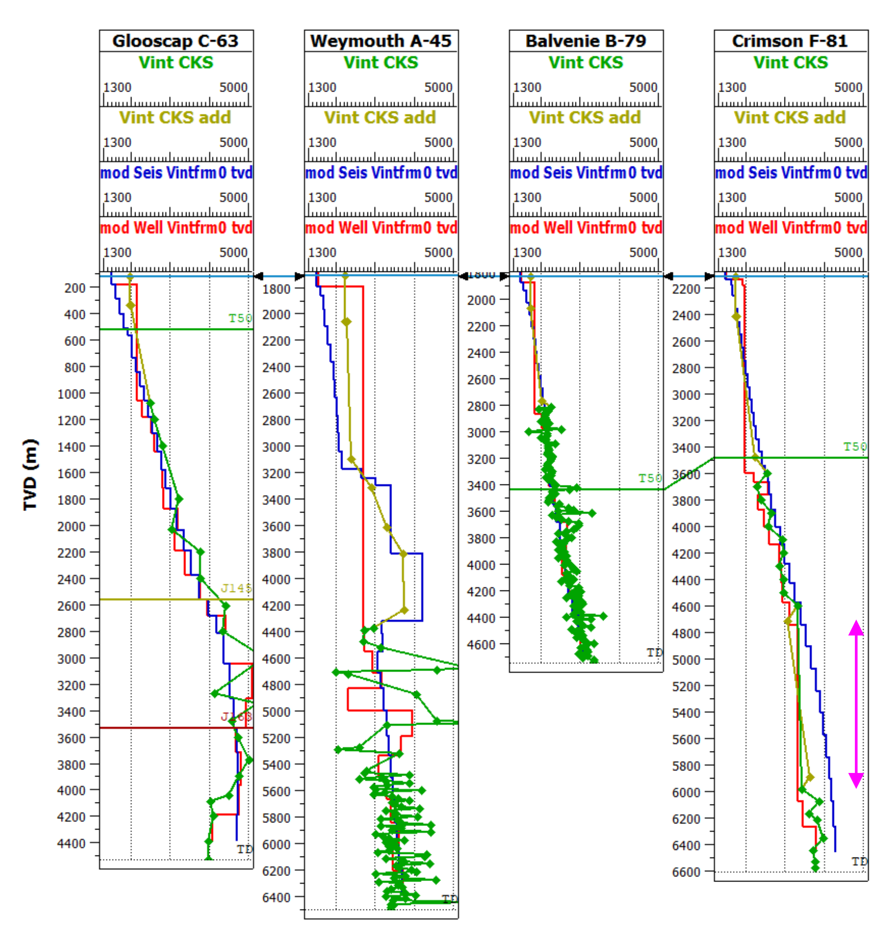

Figure 3: Completed checkshot velocities

Velocities adjustment before gridding

Different editing was done on seismic velocities before an overall gridding:

- The adjusted 3D data were slightly cut (no overlying between different 3D)
- 2D data were cut inside 3D surveys limits (slightly extended to prevent sharp transitions)
- At 2D intersections, the lowest quality data is cut. This objective quality was defined according to their sections in PL.1.7; the order is presented in the list here below
- When Nova Span line is subparallel to Bible one, the former is erased
- To control the extrapolation of seismic velocities eastwards (nothing in eastern third of the AOI), a pseudo seismic velocity trace is added at East Wolverine G-37, based on the well smoothed velocities (upwards, a linear extrapolation of missing velocities is applied). The resulting velocity is presented in Figure 4

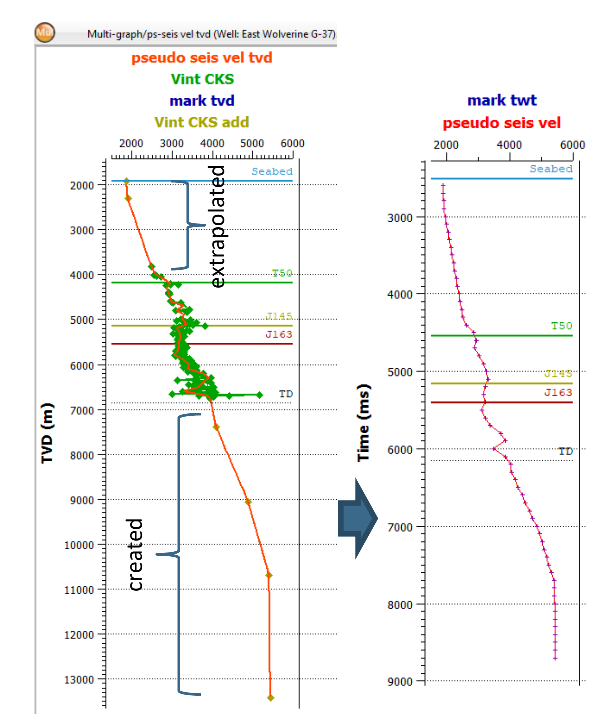

Figure 4: Pseudo seismic velocity at East Wolverine G-37

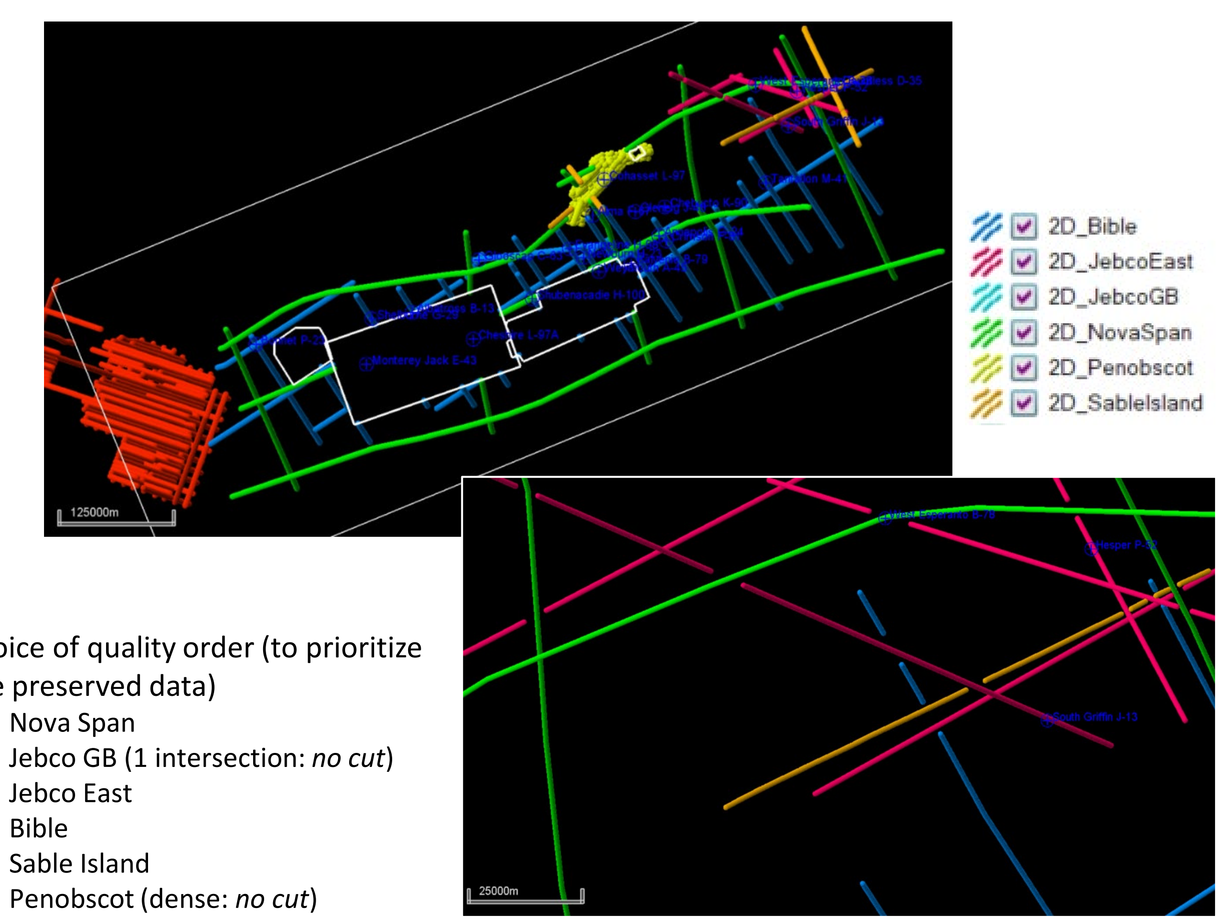

choice of quality order (to prioritize the preserved data)

1. Nova Span
2. Jebco GB (1 intersection: *no cut*)
3. Jebco East
4. Bible
5. Sable Island
6. Penobscot (dense: *no cut*)

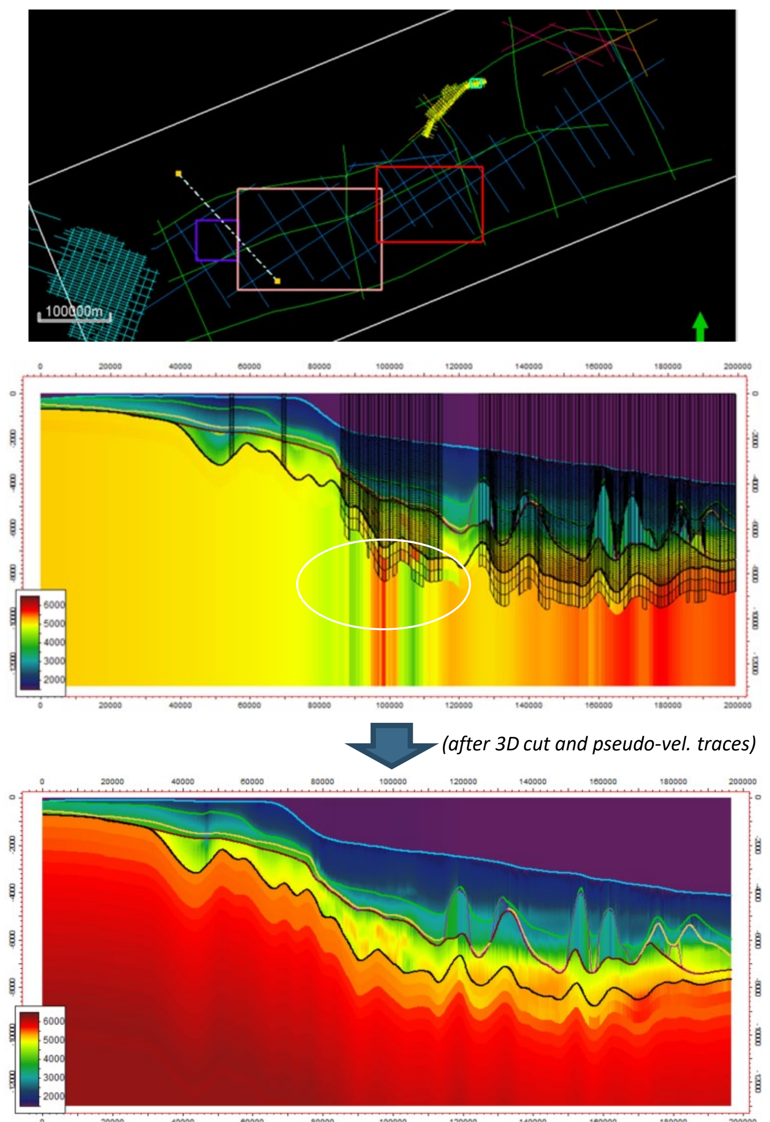

Figure 1: Barrington velocity cut below top Basement

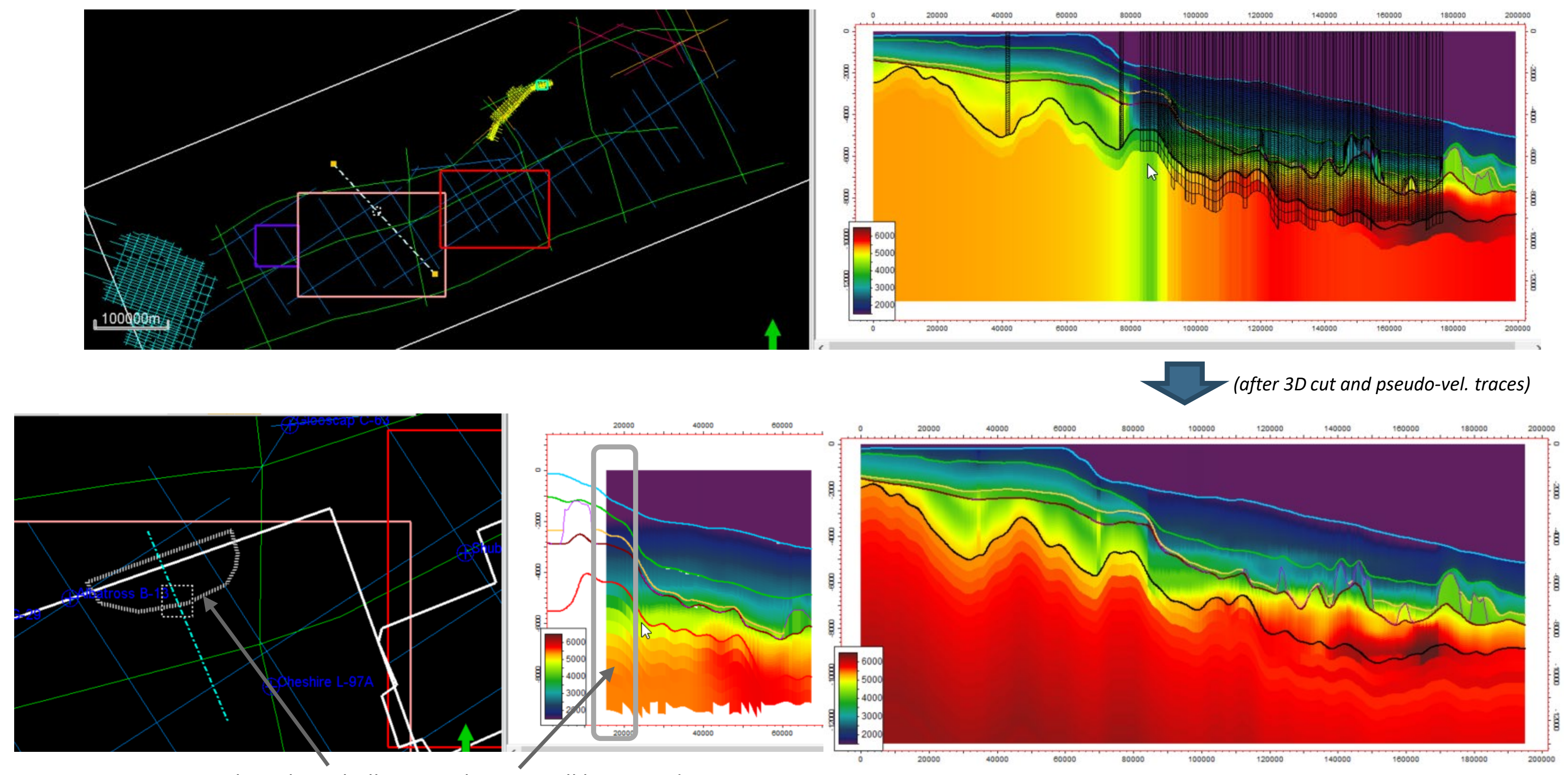

Figure 2: Shelburne velocity cut in a northern area

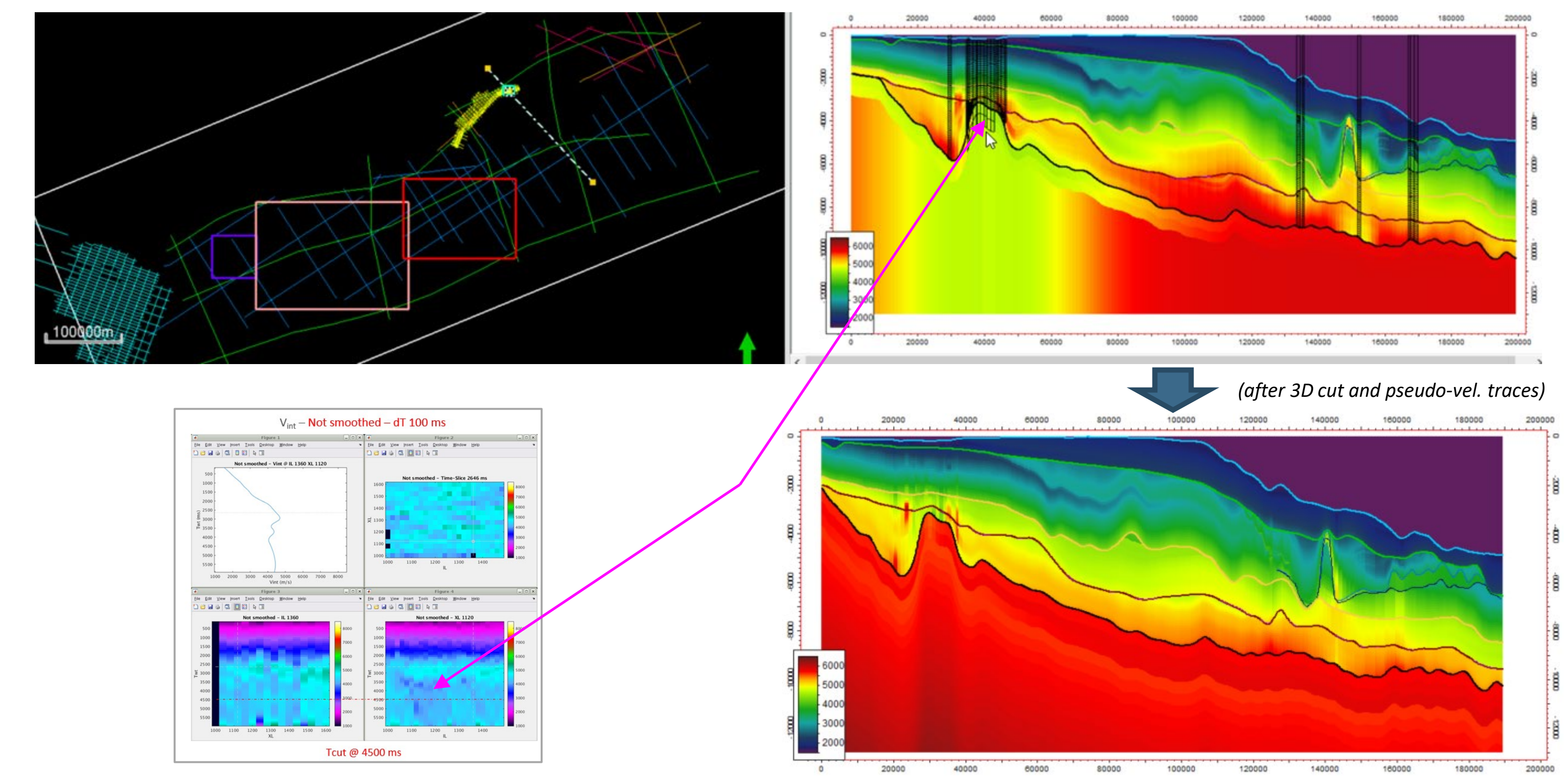

Figure 3: Penobscot low velocities cut below top Basement

Methodology

Many tests were performed to get the best available interpolator in *Petrel*^{TM}. The one selected was a Moving Average with quadrupled inversed distance weighting. "Test 'n try" runs show that supplementary editing passes on the seismic velocity sources were needed. They are summed up hereafter:

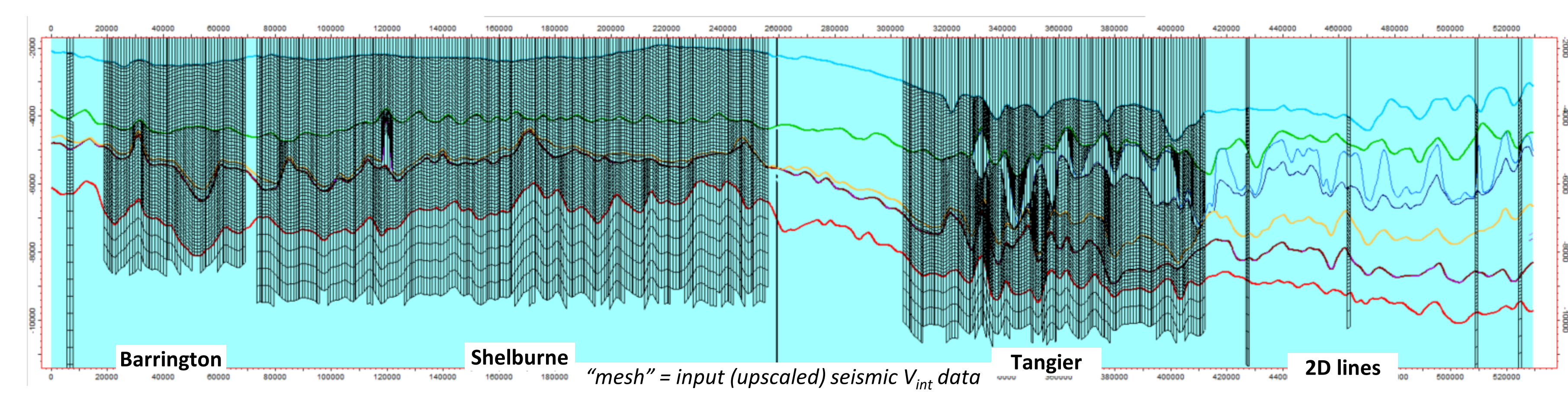

Figure 5: Random line crossing the 3 main 3D surveys and some 2D lines

- All 2D data were cut below top Basement (i.e. for the incompatible Bible and Nova Span lines)
- In [top Basement; 13 s] interval, Barrington velocities are too 'chaotic' (Figure 1), which creates wrong 3D extrapolations → velocity cut below top Basement
- Some northern Shelburne traces have low velocities (Figure 2). In this northern part, the variation of the seismic velocities field seems only horizontal: velocities can be erased without important loss of information → velocity cut below top Basement
- Penobscot velocities in [top Basement; 13 s] are manifestly too low (Figure 3); vertical sections show indeed a velocity lowering in depth → velocity cut below top Basement
- After this 3D erasing, supplementary pseudo seismic traces were added in [top Basement; 13 s] interval to help the extrapolations in the whole AOI (Figure 4): in Jebco GB survey, in the northern editing area at Shelburne, at Penobscot survey.
- After interpolation, a slight lateral smoothing filter was applied (see results in Figure 5 and 6 along a random line)
- As no well penetrates in [top Basement; 13 s] interval, no weighting adjustment could be done during a co-kriging between the secondary variable (seismic traces) and the hard data (wells). As this last interval will be defined by only seismic data, a pure assignment can be done without a well to seismic weighting. The ratio factor in Shelburne determined an average increase of 5% of the seismic velocities in the common time zone seismic vs. wells (Figure 7). Such factor of -5% was therefore applied to the seismic velocities below top Basement (see final seismic velocities in Figure 8).

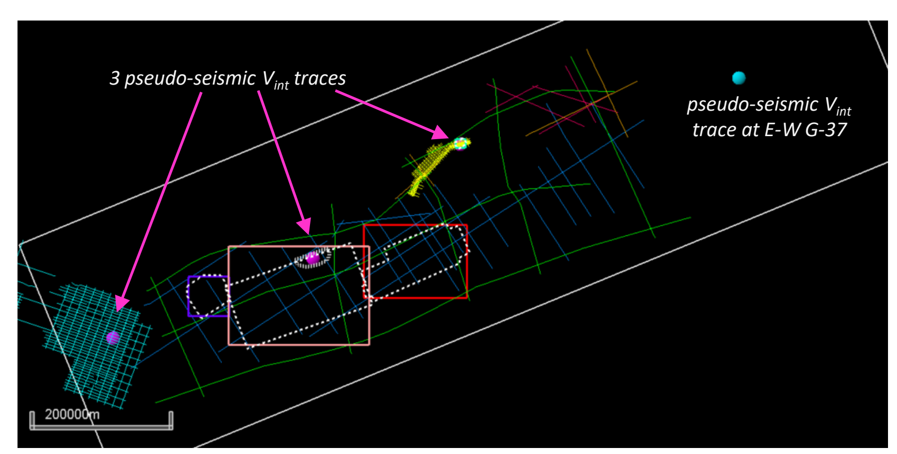

Figure 4: Pseudo seismic traces

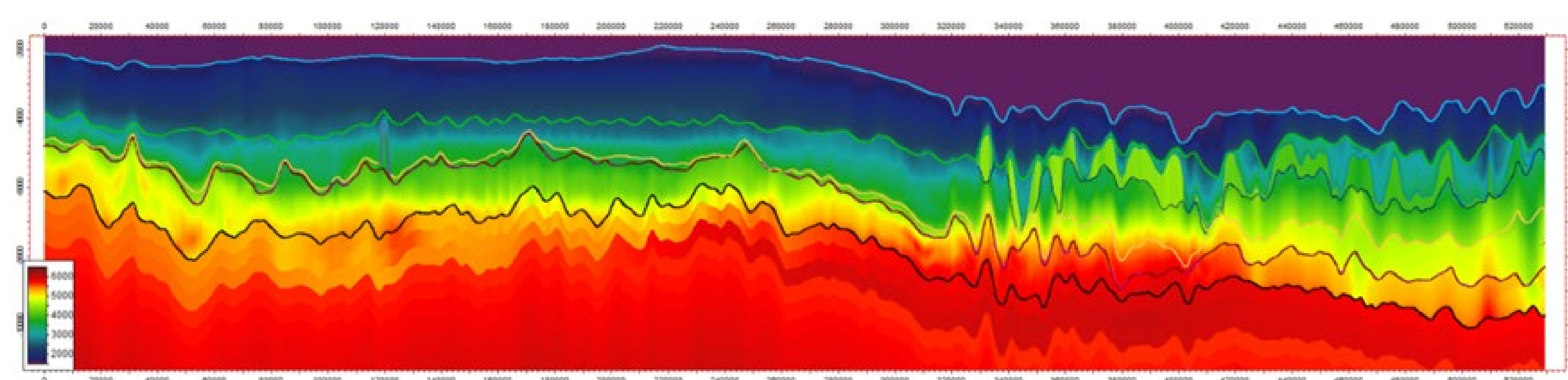

Figure 6: Seismic velocity interpolation after editing and smoothing

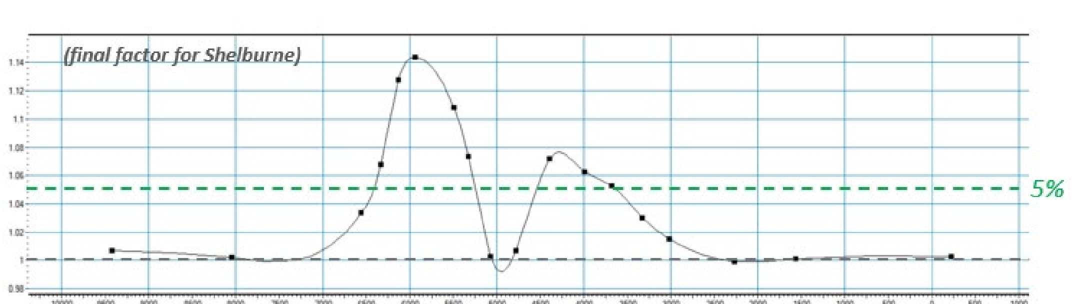

Figure 7: $F_{S/W}$ for Shelburne

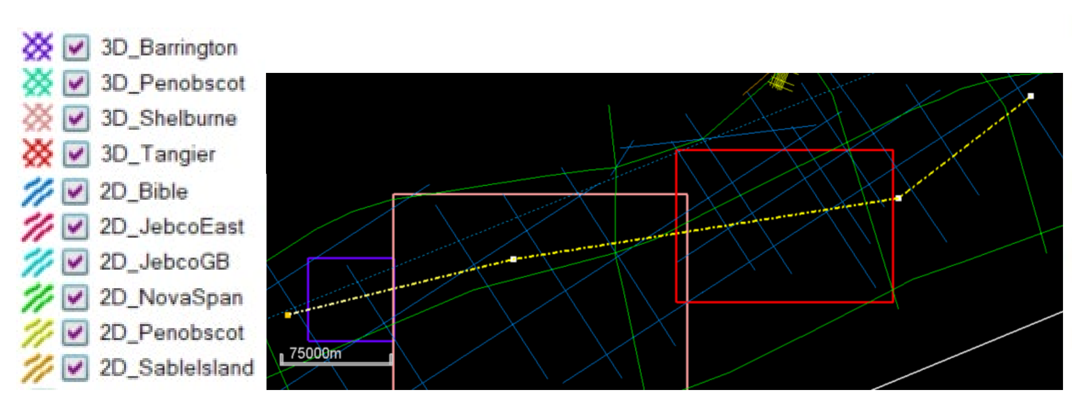

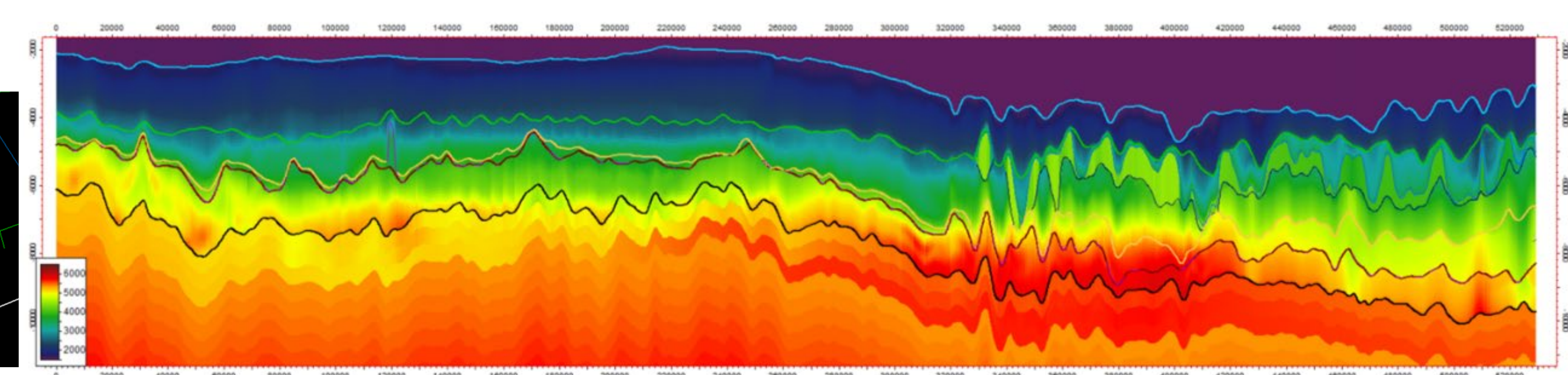

Figure 8: Final seismic velocity interpolation (after Basement velocities lowering)

Seismic processing velocities interpolation

Experimental variogram from well data

An experimental variogram from well data was computed in all the layers (parameters here below). The main results show:

- The dip direction (~N160) – set as the major one – gives a close range at about 25 km
- There is no real stationarity in the strike direction
- The vertical variogram is totally un-stationary (the velocity increases with depth)

Consequently, the kriging will be done with an isotropic variogram (spherical per default) with a range of 25 km.

Experimental variogram computation ☑ Search only inside zone

Direction	Azimuth	Dip	Number lags	Lag distance	Search radius	Band width	Tolerance angle	Lag tolerance	Thickness
Vertical	NA	90	10	100	1000	113.6	45	50	NA
Major	158	0	9	8000	72000	25000	45	50	0.001
Minor	68	0	9	8000	72000	25000	45	50	0.001

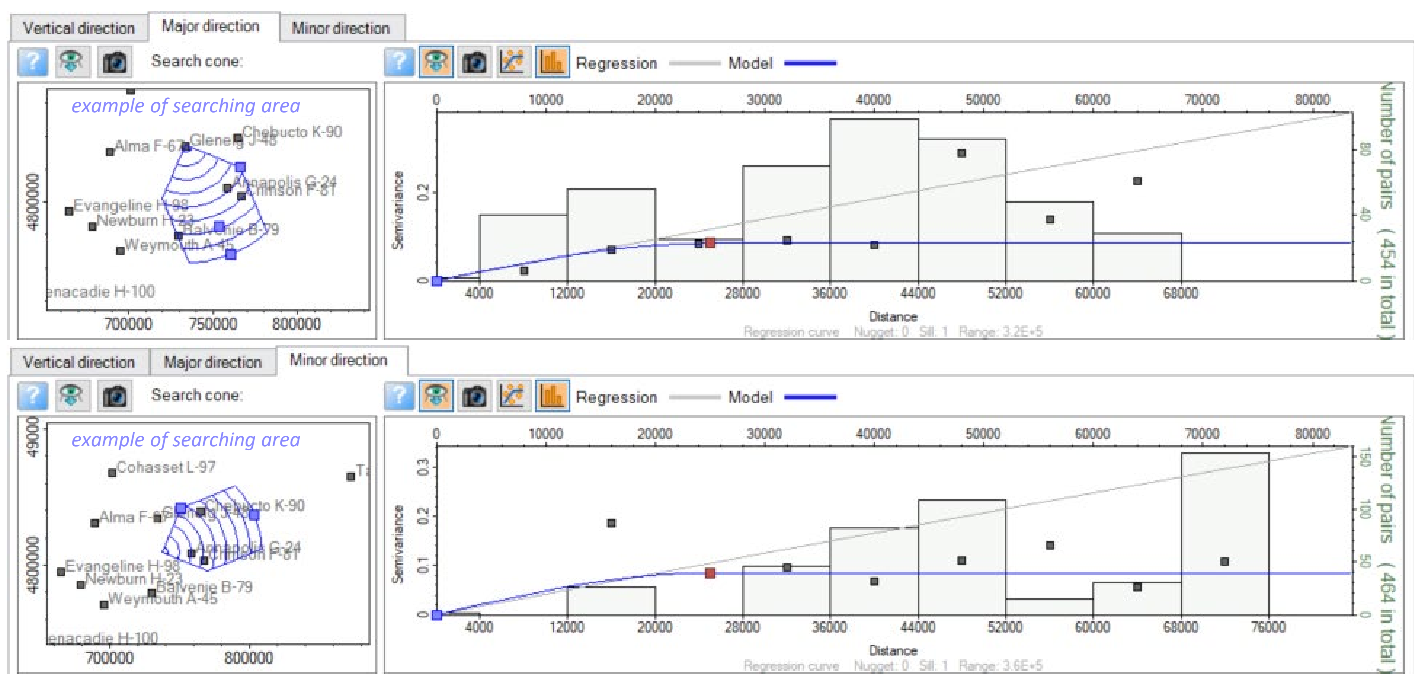

Co-kriging

The calibrated well velocities, whether checkshot (23) or sonic velocities (6), are co-kriged with the seismic velocities as secondary variable. Some parameters are added in the following:

- No well enters [Top Basement; 13000 ms] interval, which prevents the whole Co-Kriging → East-Wolverine G-37 is extended to upper Basement. Nevertheless, this layer was not filled with the co-kriging results, but with the seismic velocities lowered by 5% (see previous Plate)
- The salt zones are set at 4300 m/s
- The vertical variogram is totally un-stationary (the velocity increases with depth)

A first co-kriging pass was carried out (figures presented on the right):

- Basemap showing the 3 sections (2 sections cross wells without TZ that will be incorporated furthermore)
- Sections with the all the horizons
- Result of the co-kriging

Information of the 11 remaining wells (wells without own TZ information) can be used in a second co-kriging pass: their geological markers will be converted from Depth to Time using the resulting velocities of the first pass, and those velocities will be adjusted to get a better calibration before lopping them in a last co-kriging pass.

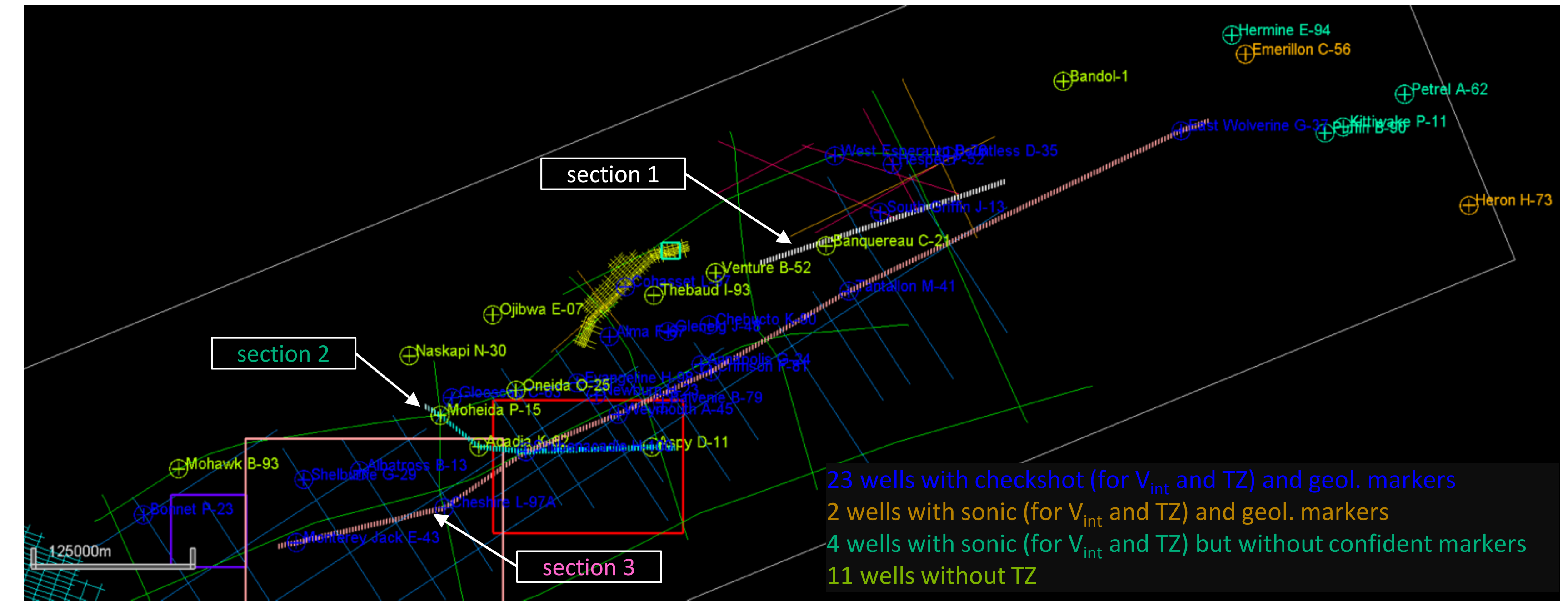

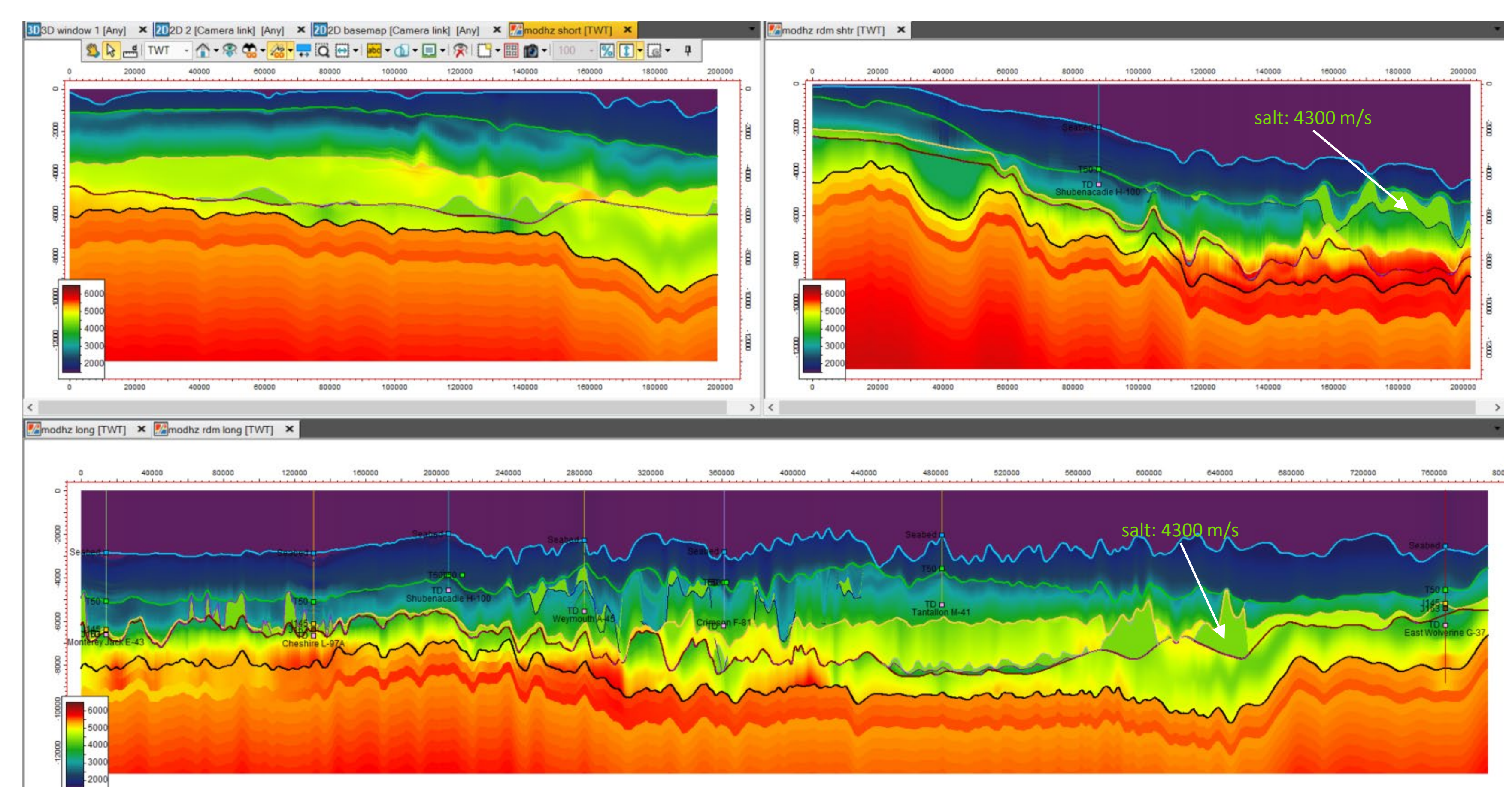

CHAPTER 3

DOMAIN CONVERSION

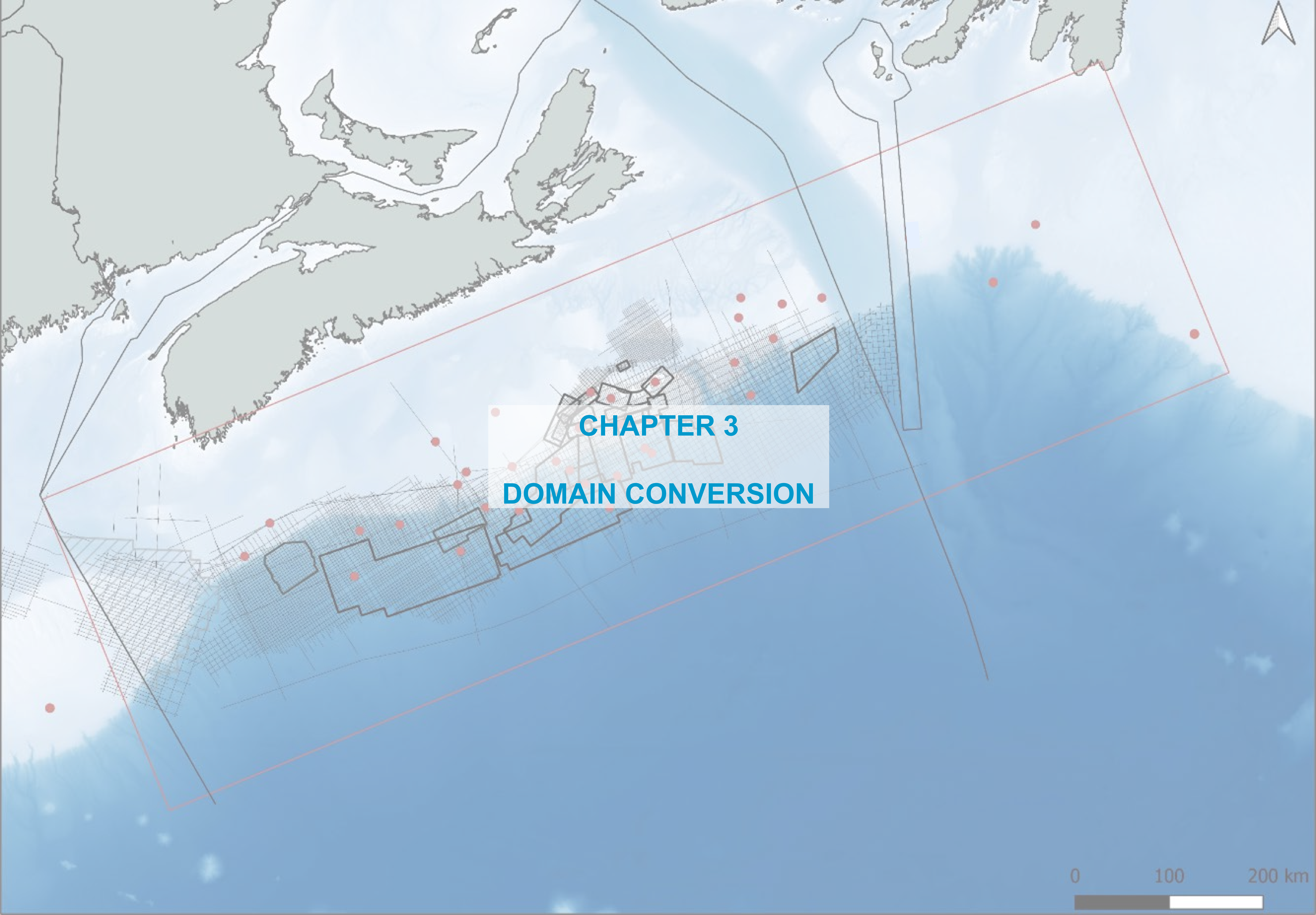

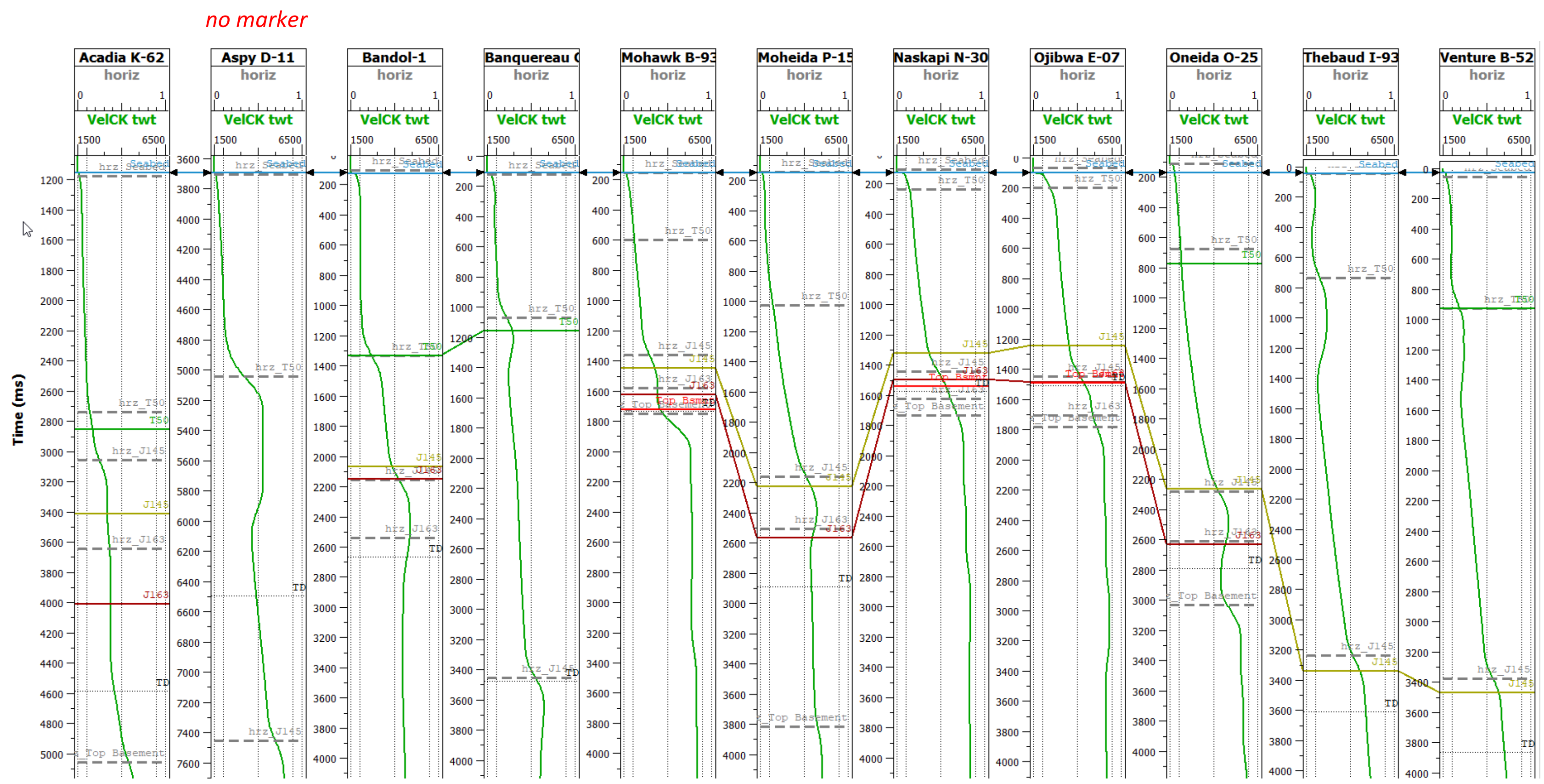

Figure 1: Velocity traces extracted at the 11 wells without own TZ

Incorporation of wells without own TZ

After the first pass of co-kriging, the resulting velocities were extracted along the 11 remaining wells still not used (see Figure 1). These velocities were differentiated to get Depth to Time laws to convert the geological markers into TWT (markers in colors in Figure 1). The marker vertical positions can be compared with the intersections of the related TWT horizons (color in grey).

The velocities were "stretch and squeezed" in some intervals between two horizons to better fit the markers and horizons, but without necessarily reaching a "perfect match" through strongly deformed velocities from the first co-kriging results (see Figure 2). Indeed, the horizons may also be incorrect (see PL. 2.3), forcing a perfect fit through non-geological velocities is often unsuitable.

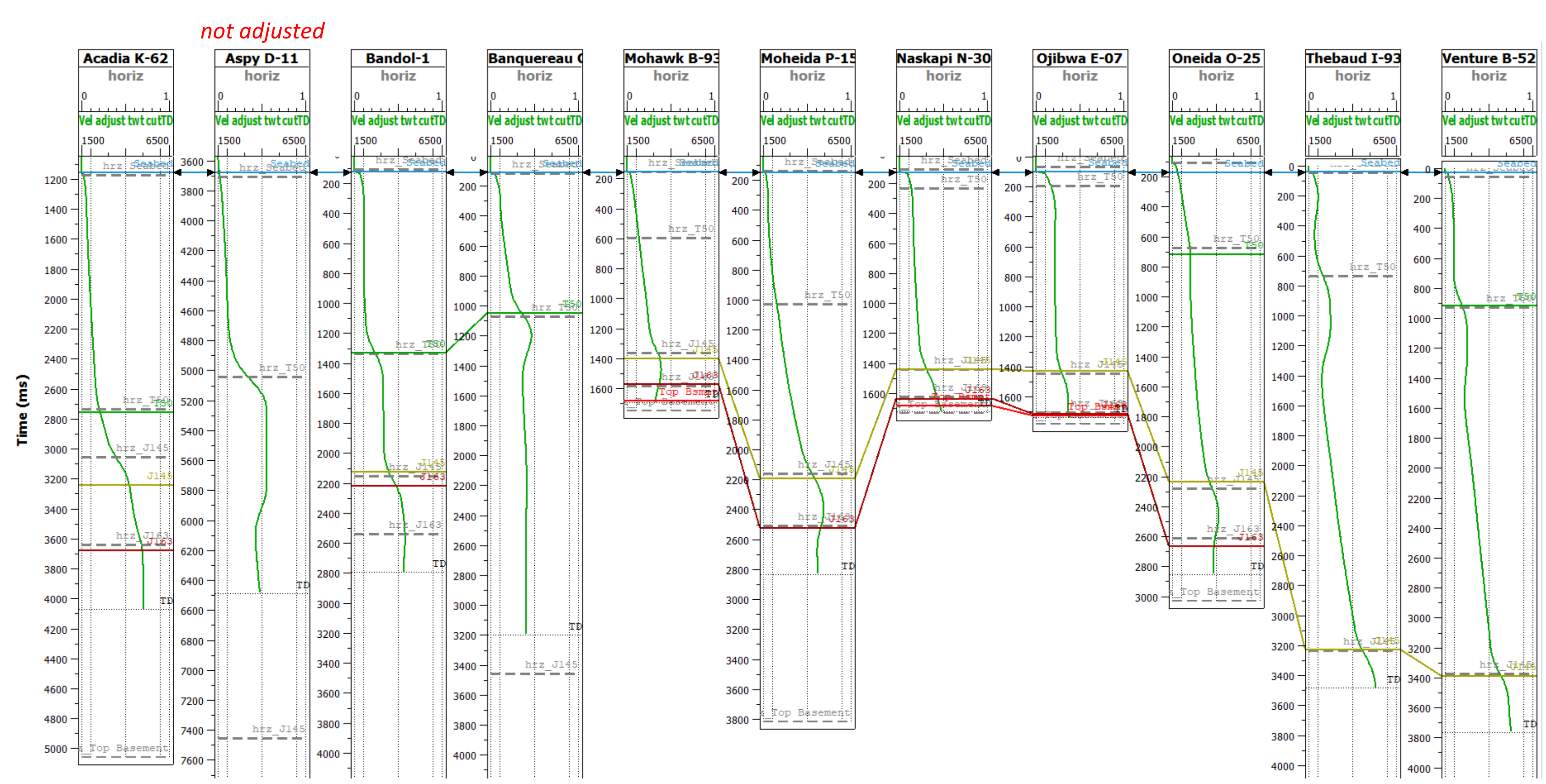

Figure 1: Velocity traces extracted at the 11 wells without own TZ

Co-kriging with all the wells

The second and final co-kriging pass was run with these 11 new wells and their adjusted velocity traces (except for Aspy D-11 without marker). The figures are presented on the right:

- Basemap showing the 3 sections
- Final V_{int} co-kriging (some new wells without own TZ appear now on the sections)
- Conversion of V_{int} to Average Velocity (V_{avg})

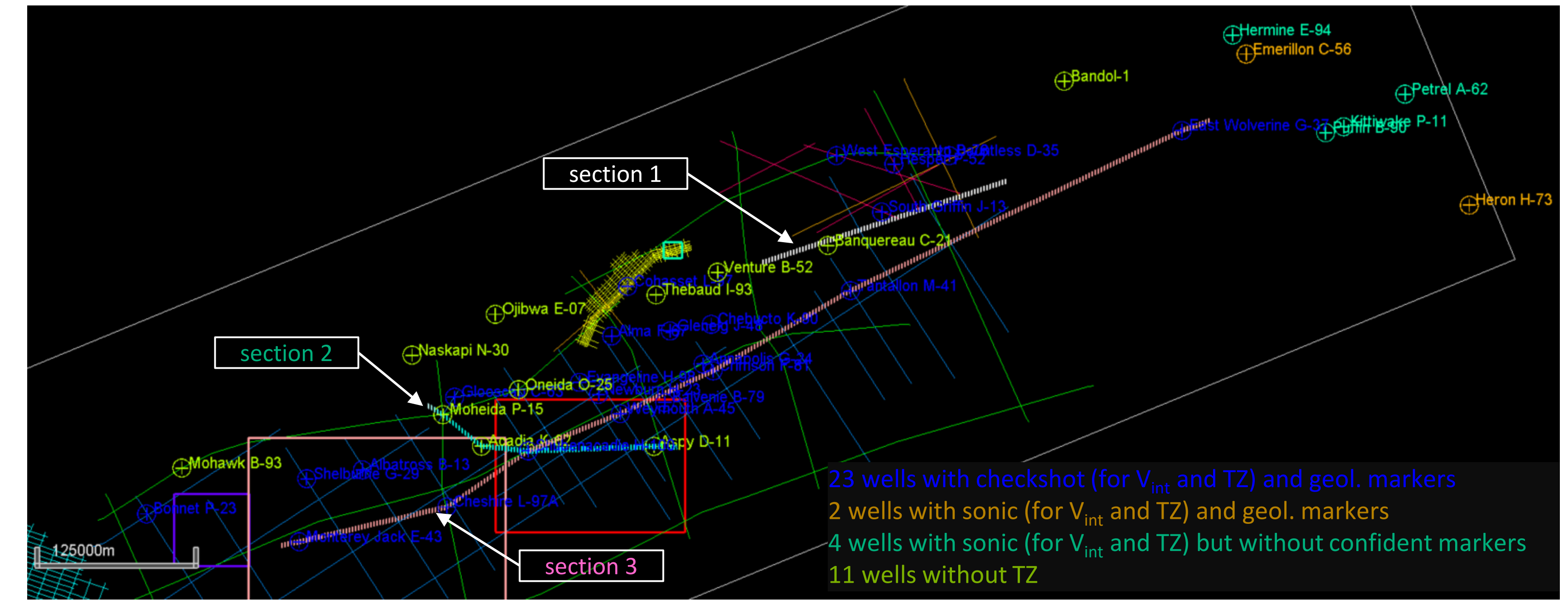

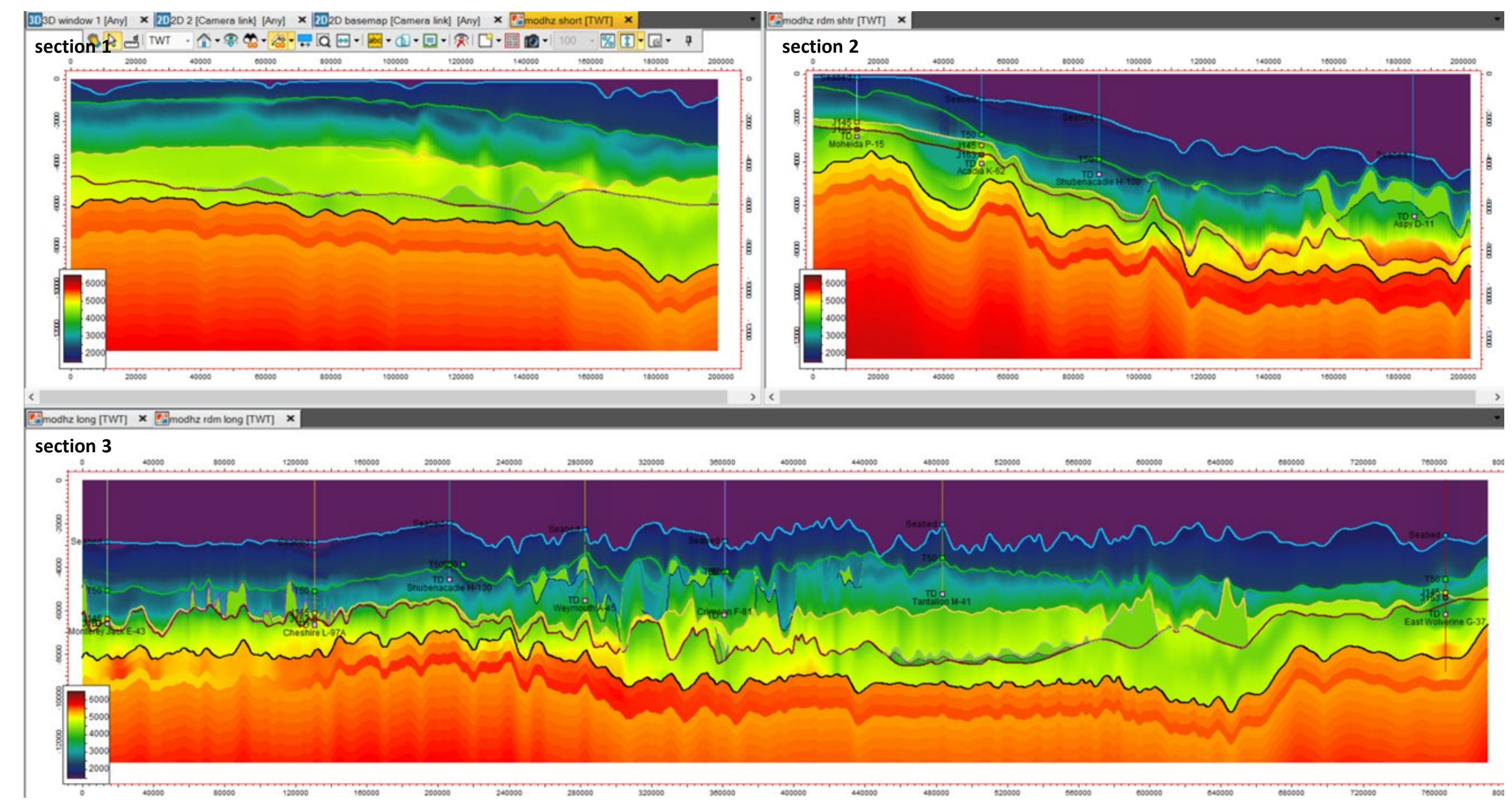

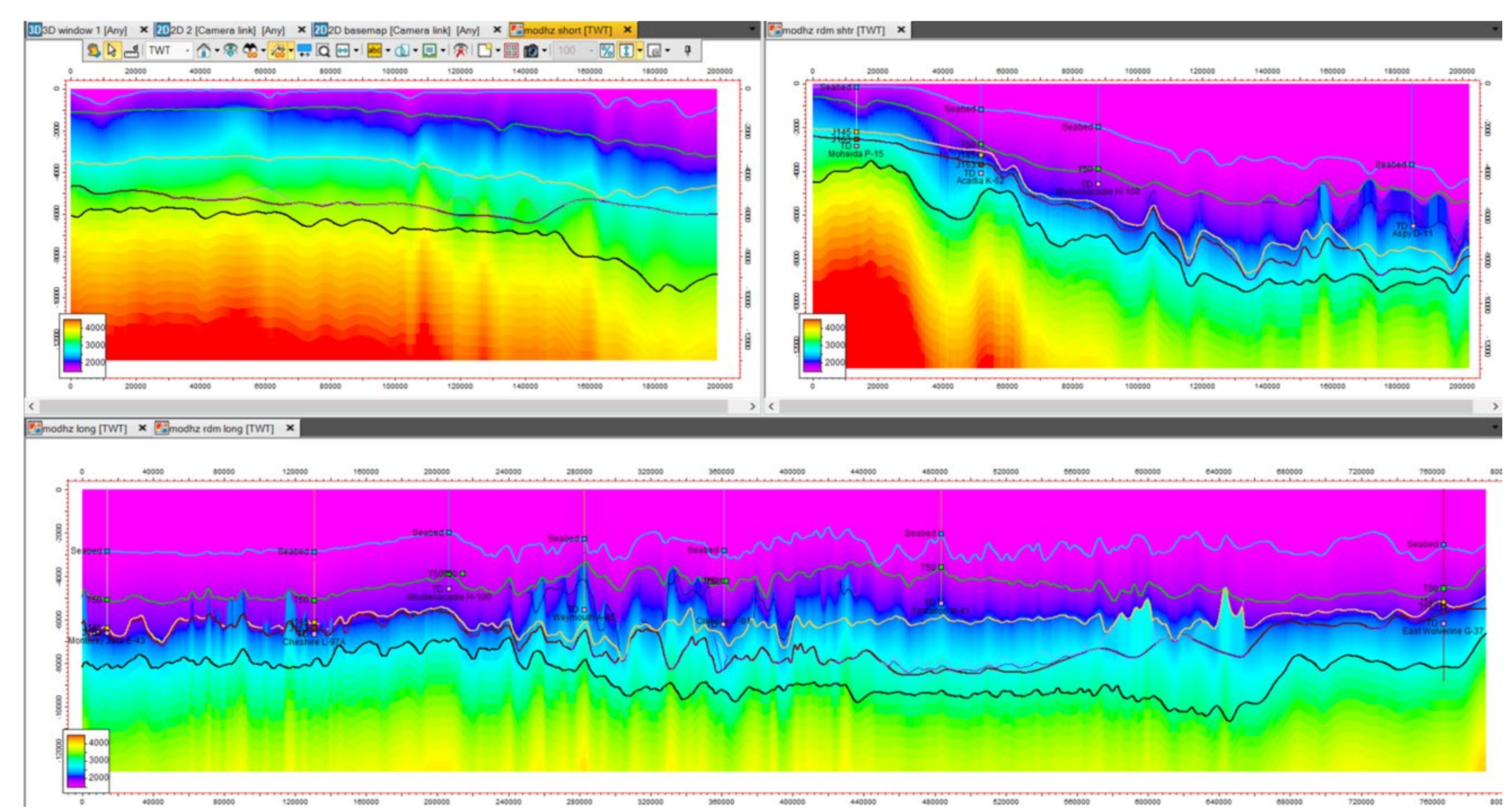

Horizon conversion

Once the Average Velocity property was implemented into *Petrel™* Velocity Model, any TWT geological object can be converted in Time or Depth domain. The TWT horizons were converted into Depth, and their intersection compared with the related geological markers. The horizons are the original ones without editing; one must keep in mind that they are not necessarily well calibrated to their corresponding marker: they already represent merging of independent horizon grids, and the original synthetic calibrations are not available to check their geological reliability. Besides Seabed (SB) is not adjusted (discrepancy at Seabed means that its time horizon does not perfectly follow it; also the sea velocity uncertainty – set at 1500 m/s to convert the depth marker into TWT – may also add contribute to its "discrepancy").

The following graphs show what is the depth mismatch in m after conversion: residual = $Zss_{converted\_horizon}$ - Zss_{marker}. The wells are displayed from West (left) to East (right) and gathered in 3 groups:

- the wells with TZ ruled by checkshot. As no deformation of the checkshot times is possible, all the horizons cannot be fitted. The strongest residuals are illustrated and commented with a TWT section
- the wells with sonic log. Plate 2.3 and -4 showed that only Hermine E-94 and Emerillon C-56 have markers coherent their related horizons (or vice versa). The depth residuals in the 4 remaining wells cannot be appraised with reliability
- the wells without any TZ recorded. As explained in the previous Plate, their fitting cannot be perfect

Wells with checkshot

not taken into account (probably horizon interpretation problem)

checkshot data not existing at this level

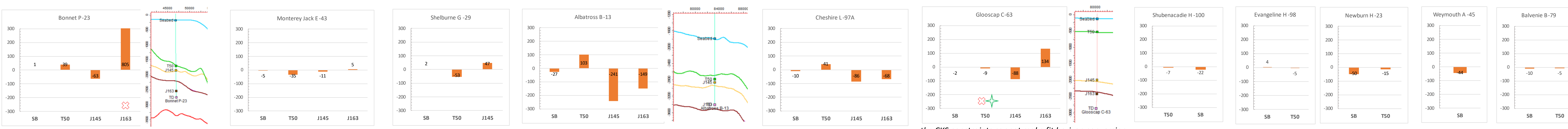

the CKS constraints cannot make fit horizon conversion with such J163 marker (→ horizon problem?)

the CKS constraints cannot make fit horizon conversion with such T50-J145 marker nearness (→ horizon problem)

the CKS constraints cannot make fit horizon conversion with such J145-J163 marker position (→ horizon problem)

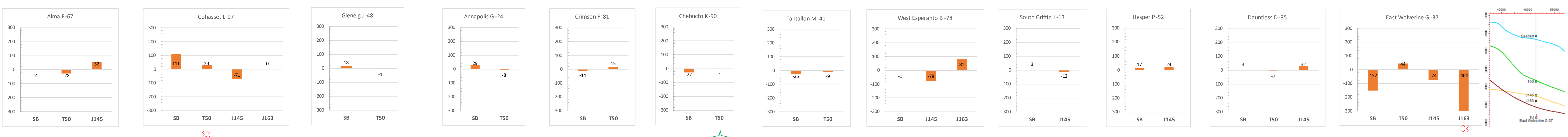

the CKS constraints cannot make fit horizon conversion with such J163 marker (→ horizon problem)

Wells with sonic log

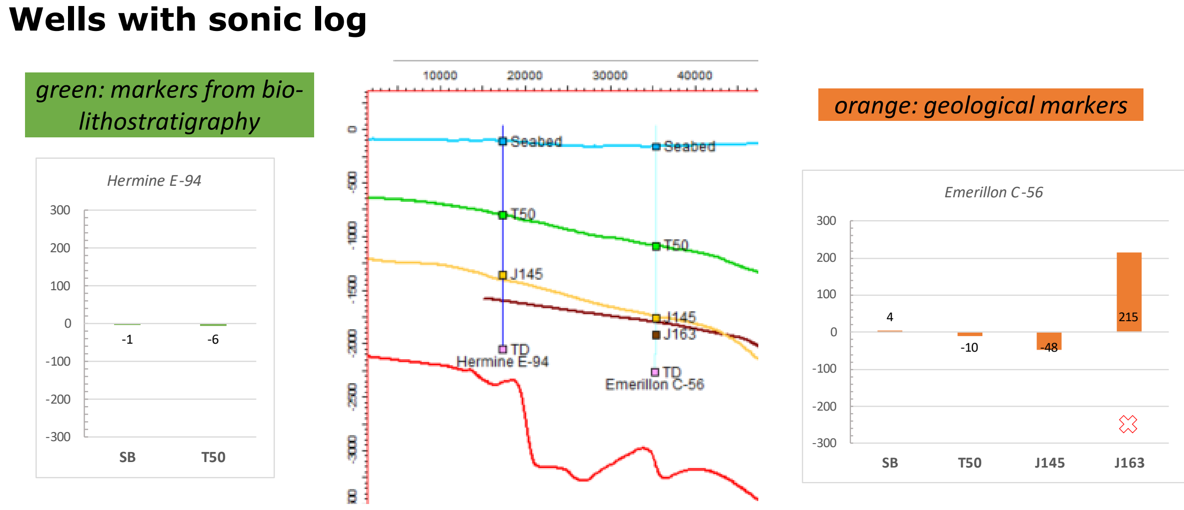

geological velocities constraints cannot make fit horizon conversion with such J145-J163 horizon nearness (→ horizon problem)

NB: the 4 remaining wells have too large discrepancies between horizons and roughly estimated markers to get significant depth residuals.

Wells without own TZ

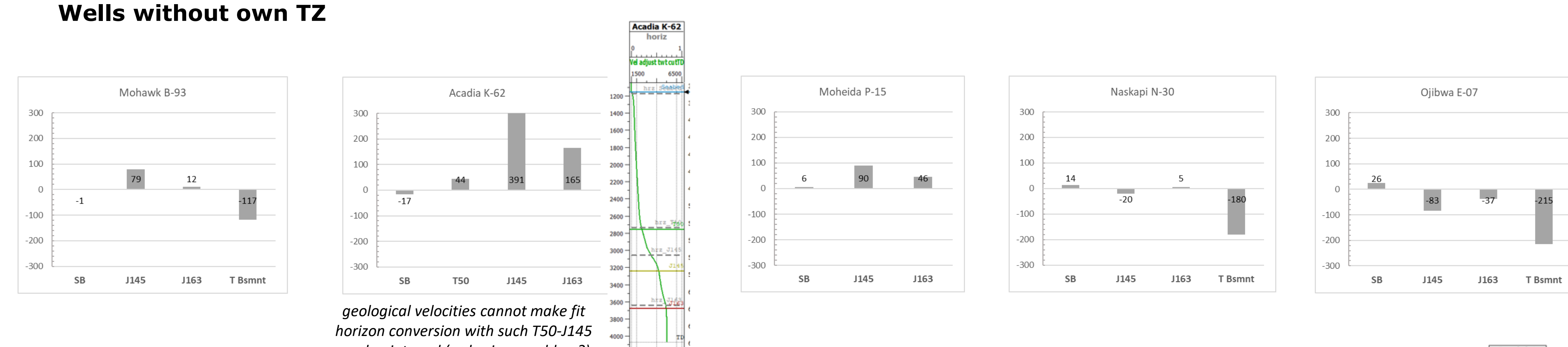

geological velocities cannot make fit horizon conversion with such T50-J145 marker interval (→ horizon problem?)

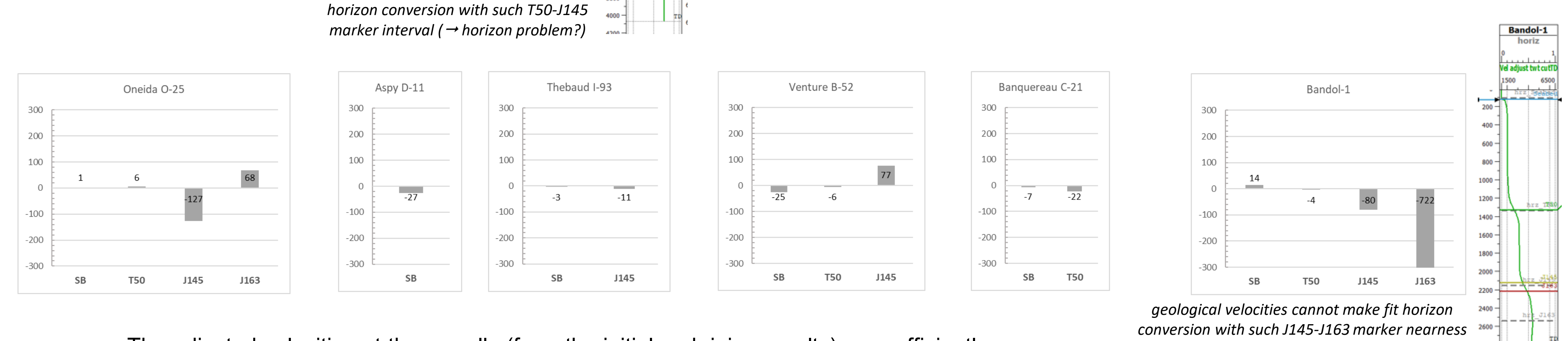

geological velocities cannot make fit horizon conversion with such J145-J163 marker nearness (→ horizon problem?)

The adjusted velocities at these wells (from the initial co-kriging results) are sufficiently fitted: their residuals are in the same range as for wells with recorded checkshot.